Alzawia University

Faculty Of Engineering

Electrical and Electronic Engineering Department

M. sc. THESIS

ON

The Effect of Electromagnetic Field of High voltage Transmission Line on Human

By

MAWLOUD JUMMAH ALBAKOUSH

Supervisor:

Dr. SALAH MOUSA

May2021

بسم الله الرحمن الرحيم

﴿يَرْفَعِ اللَّهُ الَّذِينَ آمَنُوا مِنكُمْ وَالَّذِينَ أُوتُوا الْعِلْمَ دَرَجَاتٍ﴾

سورة المجادلة: (آية 11)

Dedication

To the one whose brow was tired of sweat... and the days were cracked by him.... To the one whose name was associated with my name... **My dear father**

To whom her supplication is the secret of my success... To the tender heart..... **my beloved mother**

To my support in life after God Almighty....

My dear brothers and sisters

To whom I live the most beautiful days of my life...

To all those from whom I have gleaned knowledge and knowledge.... **Dear professors**

To everyone who helped me ...

my relatives - my loved ones - my friends

to my country

I dedicate this humble work

Thanks and appreciation

Praise be to God alone, and prayers and peace be upon the one after whom there is no prophet.

I thank God Almighty for having enabled me to complete this research. In the end, I can only express my heartfelt thanks and great gratitude to whom I had all the appreciation and respect, the esteemed **Professor Dr. Salah Mohammed Moussa**, who gave me his time, effort and knowledge without fail in order to show this work in the best way and who has the honor Any person working with him or under his guidance, and I ask God to guide him and reward him on my behalf with the best reward. I also extend my thanks, appreciation and gratitude to the **Engineer/ Suad Al-Orabi.** I also extend my sincere thanks and appreciation to the faculty members of the Faculty of Engineering Al-Zawiya and the Faculty of Engineering in Sabratha.

In conclusion, I thank everyone who supported me and helped me, whether through work or prayer.

Researcher

ABSTRACT

This thesis illustrates the effect of magnetic and electric fields on human body due to the pollution caused by 400 kV high voltage power lines in Sabratha province in Libya. An experimental work was carried out in aforementioned area, a variations in electric fields and magnetic fields were noticed based on the distances from the center of the tower, since small values of electric fields were noticed close to the tower could be due to parasitic capacitances, a higher values in the mid distance between the towers were also observed.

As far as for the magnetic fields, an ELF Field Strength Measurement System (Hi 3604) meter was used, similar results were found since the magnetic field intensity increase or decrease based on the distance from zero point (tower center). The achieved results are useful as a measure for the impact of the magnetic and electric fields densities on the human body at the ground level under or in the vicinity of the high voltage transmission line and under the safety limits recommendations of international committee. Finally, the measurement results were compared with computer simulation using the mat lab.

In this research, the concentration of radon gas in the soil in the city of Sabratha was also measured, using the technique of counting the effects .of alpha particles emitted by gas Radon in the nuclear ether detector (39-CR).

الملخص

توضح هذه الرسالة تأثير المجالات المغناطيسية والكهربائية على جسم الإنسان نتيجة التلوث الناتج عن خطوط الجهد العالي 400 ك.ف بمدينة صبراتة بليبيا. تم إجراء عمل تجريبي في المنطقة المذكورة أعلاه، ولوحظت اختلافات في المجالات الكهربائية والمجالات المغناطيسية بناءً على المسافات من مركز البرج، حيث لوحظت قيم صغيرة للحقول الكهربائية بالقرب من البرج يمكن أن تكون بسبب السعات الطفيلية، كما لوحظت قيم أعلى في منتصف المسافة بين الأبراج.

فيما يتعلق بالمجالات المغناطيسية، تم استخدام مقياس نظام قياس شدة المجال ذي التردد المنخفض (Hi 3604)، تم العثور على نتائج مماثلة منذ زيادة أو نقصان شدة المجال المغناطيسي بناءً على المسافة من نقطة الصفر (مركز البرج). أخيرًا، تمت مقارنة نتائج القياس بمحاكاة الكمبيوتر باستخدام ماتلاب.

في هذا البحث تم أيضا قياس تركيز غاز الرادون في التربة في مدينة صبراتة بالقرب من أبراج الضغط العالي وبعيداً عن أبراج الضغط العالي باستخدام تقنية حساب آثار جسيمات ألفا المنبعثة من غاز الرادون في كاشف الأثير النووي. (CR-39).

Publication

Dr. SALAH MOUSA, E. MAWLOUD ALBAKOUSH, I. ISMAIL ANAGEEM and Dr. ASHRAF ELDIEB, "Experimental Investigation of the Effect of Magnetic and Electric Fields of High Voltage Transmission Line on Human Body", The second conference on Engineering & Science and Technology, October, 29-31, 2019 , college of Engineering sabratha University , sabratha .

Contents

List of Figures

List of Tables

List of Abbreviations

Abbreviations	Expansion
AC	Alternating Current
ACSR	Aluminum Conductor Steel Reinforced
DC	Direct Current
DOF	Degree Of Freedom
EMF	Electro Magnetic Field
ELF	Extremely Low Frequency
FEM	Finite Element Method
HV	High Voltage
IEEE	Institute of Electrical & Electronics Engineers
IRPA	International Radiation Protection Association
LT	Low Tension
MRI	Magnetic Resonance Imaging
UK	United Kingdom
UNEP	United Nations Environment Programmed
WHO	World Health Organization
E	Electric filed intensity
D	Electric flux density
H	Magnetic field intensity
B	Magnetic flux density
J	Electric current density
M	Magnetic charge density
Q_e	Electric charge density
Q_m	Magnetic charge density
emf	Electromagnetic force
Q_{te}	Total electric charge
Q_{tm}	Total magnetic charge

Abbreviations	Expansion
ε_0	Permittivity of free space
ε_r	Relative permittivity of the medium
μ_o	Permeability of free space
μ_r	Relative permeability of the medium
σ	Conductivity of the medium
DC	Direct current
AC	Alternate current
ρ_e	Resistivity
t_0	Time instance
T_0	Time period
ω_0	Angular frequency
$\emptyset_i$	Current phase angle
$\emptyset_y$	Voltage phase angle
GECOL	General Electrical company of Libya
μT	Micro Tesla
mG	Mille Gauss
MATLAB	Matrix Laboratory
ICNIRP	International Commission on Non-Ionizing Radiation

List of Symbols

Symbols	Expansion
A	Ampere
B	Magnetic Flux density
C	Coulomb
E	Electric Field
H	Magnetic Field
Hz	Hertz
KV	Kilovolt
V	Volt
M	Meter
mA	Mile ampere
mT	mile tesla
μ	Magnetic Permeability
ω	Angular Frequency
σ	Conductivity
ε	Relative permittivity
SAR	Specific absorption rate

Names and units of the electric and magnetic quantities in the International system (in the order in which they appear in the text)

Symbol	Name	Unit	Abbreviation
v	Velocity	Meter/second	m/s
F	Force	newton	N
Q	Charge	coulomb	C
r, R	Distance	meter	M
ϵ_0, ϵ	Permittivity	farad/meter	F/m
E	Electric field intensity	volt/meter	V/m
ρ_V	Volume charge density	coulomb/meter^3	C/m^3
v	Volume	meter^3	m^3
ρ_L	Linear charge density	coulomb/meter	C/m
ρ_S	Surface charge density	coulomb/meter^2	C/m^2
Ψ	Electric flux	coulomb	C
D	Electric flux density	coulomb/meter^2	C/m^2
S	Area	coulomb^2	m^2
W	Work, energy	joule	J
L	Length	meter	M
V	Potential	volt	V
ρ	Dipole moment	coulomb-meter	C.m
I	Current	ampere	A
J	Current density	ampere/meter^2	A/m^2
μ_e, μ_h	Mobility	meter^2/volt-second	m^2/V.s
e	Electronic charge	coulomb	C
σ	Conductivity	Siemens/meter	S/m
R	Resistance	ohm	Ω
P	Polarization	coulomb/meter^2	C/m^2

Symbol	Name	Unit	Abbreviation
$\chi_{e,m}$	Susceptibility		
C	Capacitance	farad	F
R_s	Sheet resistance	ohm per square	Ω
H	Magnetic field intensity	ampere/meter	A/m
K	Surface current density	ampere/meter	A/m
B	Magnetic flux density	tesla (or weber/meter^2)	T (or Wb/m^2)
μ_0, μ	Permeability	henry/meter	H/m
Φ	Magnetic flux	weber	Wb
V_m	Magnetic scalar potential	ampere	A
A	Vector magnetic potential	weber/meter	Wb/m
T	Torque	newton-meter	N.m
m	Magnetic moment	ampere-meter^2	A.m^2
M	Magnetization	ampere/meter	A/m
R	Reluctance	ampere-turn/weber	A.t/Mb

Physical constants

Quantity	Value
Electron charge	$e = (1.60217733 \pm 0.0000046) \times 10^{-19} C$
Electron mass	$m = (9.1093897 \pm 0.0000054) \times 10^{-31} kg$
Permittivity of free space	$\epsilon_0 = 8.854187817 \times 10^{-12} F/m$
Permittivity of free space	$\mu_0 = 4\pi 10^{-7} H/m$
Velocity of light	$c = 2.99792458 \times 10^{8}\ m/s$

Chapter 1

Introduction of Electromagnetic field

1.1 The concept Electromagnetic Field

Earlier human being experienced naturally generating electric and magnetic fields which are by and large harmless. But in the last 50 years due to technological advancement and population growth people's demand have increased. Today we are generating more power, transmitting it more and distributing more which led to rise of artificial, extremely low frequency (ELF) electromagnetic fields at frequencies of 50 and 60 Hz mainly. Nowadays artificially generated electric field have more magnitude than natural fields at 50 and 60 Hz. Physiological functions such as neuromuscular action, glandular secretion, cell membrane building, and improvement, growth and repair of tissue are affected by internal electric field . As health of human being get affected from increase in electric fields and currents in the body as told by Grandolfo et al. 1985[1], questions emerge concerning conceivable impacts of artificially created fields on biological system. To be able to sustainably live with advances in science and technology, time has come to fix a safe limit for exposure of ELF electromagnetic fields. So that future growth of technology is smoothly maintained.

With the inputs from Grandolfo and Vecchiaa, 1989, Regulatory and advisory committees have been set up in many countries to examine the possible harmful effects of ELF electromagnetic fields on human health [2].

Electromagnetic energy is generated through changes in the motion state of electrical charges. A change in state of motion will result in emission or absorption of energy. The wavelength of emitted or absorbed energy is inversely proportional to the magnitude of the energy change. An electromagnetic wave propagates in a direction which is oriented at right angle to the vibration directions of (B) and electric (E) oscillating field vectors, transporting energy from the radiation source to an undetermined final destination. The two oscillating energy fields are mutually perpendicular and vibrate in phase following the mathematical

form of a sine wave. Not only are the magnetic and electrical field vectors perpendicular to each other, but also they are perpendicular to the direction of wave propagation.

High voltage overhead lines has an electric and magnetic fields around them. These field increase with the increase in loading. In Libya the 400k.v overhead lines is the highest voltage in use. People who are living very close to the overhead lines could be harmed by the effect of its fields.

In this thesis experimental measure and simulation of the electromagnetic fields of high voltage overhead lines (400kv) that extended from Zawia to Tripoli-West stations (Sabratha), are conducted and evaluated if it is within the interactional standards and give recommendation based on the findings. Many papers have been investigated about the distribution of electromagnetic fields under high voltage transmission lines. For example: Daniel Greenan from Ireland found that overhead lines have a negative visual impact and health implications [3].

Dib Djalel et l. from Algeria Confirmation of non-standards compliance to the limits of human exposure to ELF fields in the case of the town of Tebessa and approving the aggression on human health.[4]

Nmk Abdel-Gawad had discussed in his paper which had polished in the open Environmental Engineering Journal (2009), the Investigation into field Management under power Transmission Lines using Delta Configurations.[5]

Adel Z.Eldein had discussed his paper about the Mitigation of magnetic field under Egyptian 500kv Overhead Transmission line during the seventh international Multi-Conference on systems, signals and devices. (2010),[6]

These papers have explained only the lateral profile of the electromagnetic field distribution on the ground.

In this thesis the magnetic fields around high voltage overhead lines, one meter height above the ground will be measured with appropriate measurement device.

To safeguard the human being's health from the seemingly harmful effects of exposure to magnetic fields and electric fields at frequencies of 50/60 Hz many research work have been conducted. Most of the studies were animal based on and extrapolated to human being. Few of reports have been performed on human. Recent diametric studies have provided the link for extrapolating the studies on animals to human being. Comparisons of exposure can be made by comparing development of internal current densities and field around body surfaces.

Protect human health from the obvious adverse effects of exposure of 50/60 Hz magnetic and electric fields have been the subject of much research. resulting in most studies are based on animals and are inferred to be human. Recent measurement studies provide links to inferential research about human beings . and compare exposure to internal current density and area around the body surface.

The objective of this work is to investigate how safe is the transmission corridor limits (±30m, ROW edges) set by the Libyan government and to account for public awareness.

The electromagnetic (EM) fields have two components as electric field and magnetic field. The intensity of the electric field's voltage per meter is measured with voltmeter, the unit of measurement of the magnetic field is -'Tesla'- or another unit is -'Gauss'-. The specifications of electronic and magnetic fields are different. Therefore, impacts on the biological structures of living of these areas is different. How these areas affect the people is not yet fully understood. But according to studies; the magnetic fields are more effective than electric field. On the other hand, magnetic fields does not know obstacle, except some specially manufactured substances. The electric field creates a weak current on the

surface of the human body. Magnetic fields lead to the formation of such weak flow in the internal organs by entering into the body. In fact, variable magnetic fields crate current in all conductive around them (human body can be considered as a conductor)[7].

Exposure to electromagnetic fields in not a new phenomenon. However, during the 20^{th} century, environmental exposure to man-made electromagnetic fields has been steadily increasing as growing electricity demeaned, ever-advancing technologies and changes in social behavior have created more and more artificial source. Everyone is exposed to a complex mix of weak electric and magnetic fields, both at home and at work, from the generation and transmission of electricity, domestic appliances and industrial equipment, to telecommunications and broadcasting. Tiny electrical currents exist in the human body due to the chemical reactions that occur as part of the normal bodily functions, even in the absence of external electric fields. For example, nerves relay signals by transmitting electric impulses. Most biochemical reactions from digestion to brain activities go along with the rearrangement of charged particles. Even the heart is electrically active. Low-frequency electric fields influence the human body just as they influence any other material made up of charged particles. When electric fields act on conductive materials, they influence the distribution of electric charges at their surface. They cause current to flow through the body. Low-frequency magnetic fields induce circulating currents within the human body.[8]

The strength of these currents depends on the intensity of the outside magnetic field.

If sufficiently large, these currents could cause stimulation of nerves and muscles of affect other biological processes. Fig (1-1) indicates the low frequency electric and magnetic fields induce weak currents in human body. The body has sophisticated mechanisms to adjust to the many and varied influences we encounter in our

environment. Ongoing change forms a normal part of our lives. But, of course, the body does not possess adequate compensation mechanisms for all biological effects. Changes that are irreversible and stress the system for long periods of time may constitute a health hazard. An adverse health effect causes detectable impairment of the health of the exposed individual or of his or her off spring, a biological effect, on the other hand, may or may not result in an adverse health effect.[8]

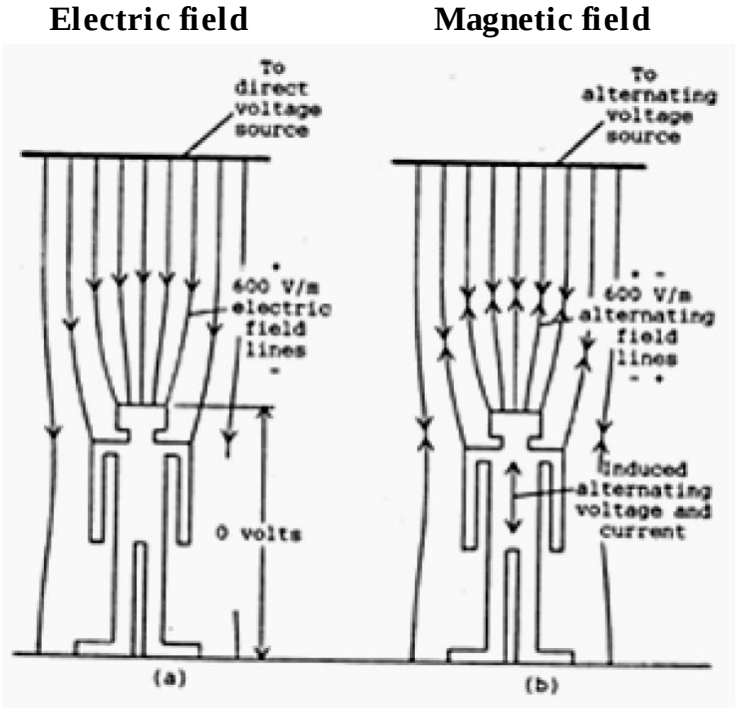

Fig (1.1): Low frequency electric and magnetic fields induce weak electric currents in humans body[8]

It is not disputed that electromagnetic fields above certain levels can trigger biological effects. Experiments with healthy volunteers indicate that short-term exposure at the levels present in the environment or in the home do not cause any apparent detrimental effects. Exposures to higher levels that might be harmful are restricted by national and international guidelines. In response to growing public health concerns over possible health effects from exposure to an ever increasing number and diversity of electromagnetic field sources, in 1996 the world Health Organization (WHO) launched a large, multidisciplinary research effort. The International EMF Project brings together current knowledge and

available resources of key international and national agencies and scientific institutions. In the area of biological effects and medical applications of non-ionizing radiation approximately 25,000 articles have been published over the past 30 years.[8]

There have been occasional reports of associations between health problems and presumed exposure to electromagnetic fields, such as reports of prematurity and low birth weight in children of workers in the electronics industry.[8]

A number of epidemiological studies suggest small increases in risk of childhood leukemia with exposure to low frequency magnetic fields in the home. However, scientists have not generally concluded that these results indicate a cause-effect relation between exposure to the fields and disease (as opposed to artifacts in the study or effects unrelated to field exposure). In part, this conclusion has been reached because animal and laboratory studies fail to demonstrate any reproducible effects that are consistent with the hypothesis that fields cause or promote cancer. Large-scale studies are currently underway in several countries and may help resolve these issues. Some individuals report "hypersensitivity" to electric or magnetic fields. They ask whether aches and pains, headaches, depression, lethargy, sleeping disorders, and even convulsions and epileptic seizures could be associated with electromagnetic field exposure. Recent Scandinavian studies found that individuals do not show consistent reactions under properly controlled conditions of electromagnetic filed exposure. Nor is there any accepted biological mechanism to explain hypersensitivity. Research on this subject is difficult because many other subjective responses may be involved, apart from direct effects of fields themselves. More studies are continuing on the subject. [8]

In Libya some people are living and still building houses right now under the power lines, Fig (1.2) shows that. The right of way (ROW) in not forced.

Fig (1.2) Building under overhead lines[8]

During measurements under vicinity of overhead transmission lines it`s found there are some Olive trees are drying, and those are not dry have their leaves nearly to being dry. It could be from H.V field effect, because the tree far from the lines are normal, as Fig (1.3) indicates.

Figure (1.3) Olive trees under overhead lines[8].

1.2 Thesis lay-out

This thesis deals with the following:

1-The application of theory of electromagnetic fields method.

2-The detailed discussion on performance of transmission line is presented and the parameters of transmission line is also included.

3-The effect of electromagnetic fields of 400kv high voltage transmission line on human was applied in two different ways:

a-Experiment method.

b-Simulation method.

4-The comparison between experiment measured and simulation using mat-lab program.

Chapter 2

Theory Of Electromagnetic Fields

2- Introduction

Electricity is such a basic element of modem life makes everybody exposed to ascertain degree of electromagnetic fields. The two fields associated with the use of electricity are electric fields which are produced by the voltage, and magnetic fields which are produced by the current. The two fields taken together are the electromagnetic fields (EMF).

Several developments have taken place in the design of the power lines in order to reduce the electromagnetic field, such as increasing the distance between the lines and the residences, decreasing the current, shielding, changing the geometry of the conductors through the compaction method, the phase splitting method as well as the current-phase rearrangement method. It is important to implement these techniques because many researchers still suspect the existence of an association between the EMF induced from power lines and health damages.

At the beginning of the 21st century, communities and individuals are still facing problems whenever a new overhead transmission power line has to be installed. The presumed effects of the electromagnetic fields on the individual health tend to scare people. Due to this fear protests usually tend to be issue in order to prevent the installation of these high voltage transmission lines.

High voltage (HV) transmission lines and electric equipment produce electric and magnetic field in their vicinity, which are likely to have harmful effects on plants, animals and human beings when their levels are beyond certain limits. Radiation from power transmission lines are inescapable. Magnetic field was measured under 400kv lines. Data from these studies and biological effects of electric and magnetic fields are discussed.

In recent years the living or working condition near high voltage transmission lines are subjected of many researches due to the harmful effects of electromagnetic field on human`s health. This subject is very popular and it is now the research aim of national scientific organizations, so that the world Health Organization (WHO) has offered useful advises for the maximum time of being under electromagnetic field. That kind of organizations which are working in this subject believe that applying such as time limitations are not reliable enough and is just a discretionary act, however regarding to all this condition all of this organizations believe that living near electrical installations is not safe. According to this and to better evaluate electromagnetic field around of the transmission lines, the simulation and also measurement of the magnetic field generated by 400kV lines will be done.[9]

One of the main characteristics which defines an electromagnetic field (EMF) is its frequency or its corresponding wavelength. Fields of different frequencies interact with the body in different ways. One can imagine electromagnetic waves as series of very regular waves that travel at, the speed of light.

Another important characteristic of electromagnetic fields: Electromagnetic waves are carried out by particles called quanta. Quanta of higher frequency (shorter wavelength) waves carry more energy than lower frequency (longer. wavelength) fields. Some electromagnetic waves carry so much energy per quantum that they have the ability to break bonds between molecules. In the electromagnetic spectrum, gamma rays given off by radioactive materials, cosmic rays and X-rays carry this property and are called 'ionizing radiation'. Fields whose quanta are insufficient to break molecular bonds are called 'non-ionizing radiation. Man-made sources of electromagnetic fields that form a major part of industrialized life- electricity, microwaves and radiofrequency fields are found at the relatively long wavelength and low frequency end of the spectrum and their quanta are unable to break chemical bonds. [10]

2.1- GAUSS'S LAW:

The results of Faraday's experiments with the concentric spheres could be summed up as an experimental law by stating that the electric flux passing through any imaginary spherical surface lying between the two conducting spheres is equal to the charge enclosed within that imaginary surface. This enclosed charge is distributed on the surface of the inner sphere, or it might be concentrated as a point charge at the center of the imaginary sphere. However, since one coulomb of electric flux is produced by one coulomb of charge, the inner conductor might just as well have been a cube or a brass door key and the total induced charge on the outer sphere would still be the same. Certainly the flux density would change from its previous symmetrical distribution to some unknown configuration, but + coulombs on any inner conductor would produce an induced charge of -Q coulombs on the surrounding sphere. Going one step further, we could now replace the two outer hemispheres by an empty (but completely closed) soup can. Q coulombs on the brass door key would produce v = Q lines of electric flux and would induce- Q coulombs on the tin can.[10]

These generalizations of Faraday's experiment lead to the following statement, which is known as Gauss's law:

The electric flux passing through any closed surface is equal to the total charge enclosed by that surface.

The contribution of Gauss, one of the greatest mathematicians the world has ever produced, was actually not in stating the law as we have, but in providing a mathematical form for this statement, which we shall now obtain.

Let us imagine a distribution of charge, shown as a cloud of point charges in Fig (2.1), surrounded by a closed surface of any shape. The closed surface may be the surface of some real material, but more

generally it is any closed surface we wish to visualize. If the total charge is Q, then Q coulombs of electric flux will pass through the enclosing surface. At every point on the surface the electric-flux-density vector D will have some value Ds, where the subscript S merely reminds us that D must be evaluated at the surface, and Ds will in general vary in magnitude and direction from one point on the surface to another

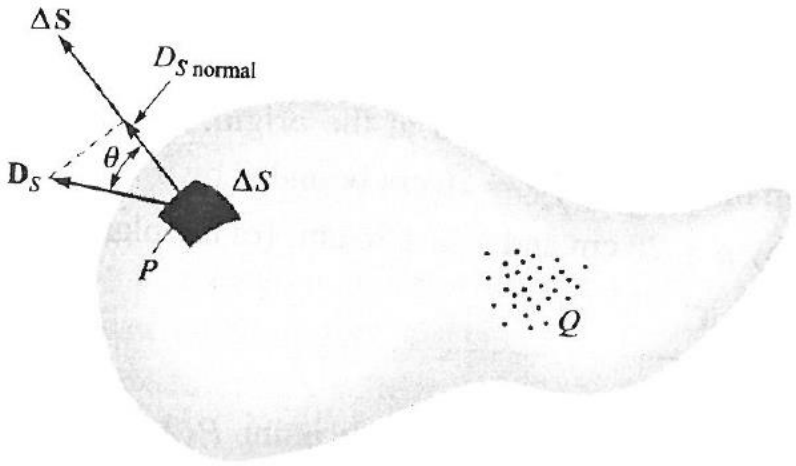

Fig. 2.1 The electric flux density Ds at P due to charge Q. The total flux passing through ΔS is Ds. ΔS.[10]

An incremental element of area Δs is very nearly a portion of this surface element requires not only a statement of its magnitude Δs but also of its orientation in space. In other words, the incremental surface element is a vector quantity. The only unique direction which may be associated with Δs is the direction of the normal to that plane which is tangent to the surface at the point in question. There are, of course, two such normal, and the ambiguity is removed by specifying the outward normal whenever the surface is closed and "outward" has a specific meaning.

At any point P consider an incremental element of surface Δs and let Ds make an angle θ with Δs, as shown in Fig (2.1). The flux crossing Δs is then the product of the normal component of Ds and Δs

$$\Delta s, \Delta \Psi = flux\ crossing\ \Delta S = D_{s,norm} \Delta s = D_s cos\theta \Delta s = Ds.\Delta s$$

The total flux passing through the closed surface is obtained by adding the differential contributions crossing each surface element Δs,

$$\Psi = \int d\Psi = \oint_{surface}^{closed} Ds.dS \qquad (2.1)$$

The resultant integral is a closed surface integral, and since the surface element ds always involves the differentials of two coordinates, such as $dx\,dy, \rho d\emptyset\,dp,$ or $r^2 \sin\theta\,d\theta\,d\emptyset$, the integral is a double integral. Usually only one integral sign Illustrations is used for brevity, and we shall always place an S below the integral sign to indicate a surface integral, although this is not actually necessary since the differential ds is automatically the signal for a surface integral. One last convention is to place a small circle on the integral sign itself to indicate that the integration is to be performed over a closed surface. Such a surface is often called a Gaussian surface. We then have the mathematical formulation of Gauss's law,

$$\Psi = \oint_s D_s.d\mathbf{S} = charge\ enclosed = Q \qquad (2.2)$$

The charge enclosed might be several point charges, in which case

$$Q = \sum Qn \qquad (2.3)$$

or a line charge,

$$Q = \int \rho L\,dL \qquad (2.4)$$

or a surface charge,

$$Q = \int_S \rho S\,dS\ (not\ necesarily\ a\ closed\ surface) \qquad (2.5)$$

or a volume charge distribution,

$$Q = \int_{\text{vol}} \rho v\,dv \qquad (2.6)$$

The last form is usually used, and we should agree now that it represents any or all of the other forms. With this understanding, Gauss's law may be written in terms of the charge distribution as

$$\oint_S \mathbf{D}s.d\mathbf{S} = \int_{vol} \rho_v dv \qquad (2.7)$$

a mathematical statement meaning simply that the total electric flux through any closed surface is equal to the charge enclosed.

To illustrate the application of Gauss's law, let us check the results of Faraday's experiment by placing a point charge Q at the origin of a spherical coordinate system Fig (2.2) and by choosing our closed surface as a sphere of radius a. The electric field intensity of the point charge has been found to be

$$E = \frac{Q}{4\pi\epsilon 0 r^2} a_r \qquad (2.8)$$

and since

$$D = \epsilon_0 E \qquad (2.9)$$

we have, as before,

$$D = \frac{Q}{4\pi r^2} a_r \qquad (2.10)$$

At the surface of the sphere,

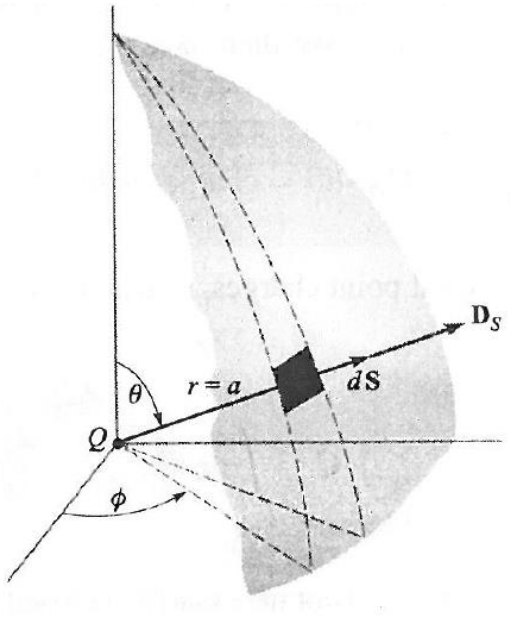

Fig. 2.2. The electric flux density D is everywhere normal to the spherical surface and has a constant magnitude at every point on it.[10]

The differential element of area on a spherical surface is, in spherical coordinates from:

$$dS = r^2 sin\,\theta\, d\theta\, d\emptyset = a^2 \sin\theta\, d\theta\, d\emptyset \qquad (2.11)$$

or

$$dS = a^2 sin\,\theta\, d\theta\, d\emptyset\, a_r \qquad (2.12)$$

The integrand is

$$D_s . dS = \frac{Q}{4\pi a^2} a^2 sin\,\theta d\theta\, d\emptyset a_r . a_r = \frac{Q}{4\pi} sin\,\theta\, d\theta\, d\emptyset \qquad (2.13)$$

leading to the closed surface integral

$$\int_{\emptyset=0}^{\emptyset=2\pi} \int_{\theta=\emptyset}^{\Theta=\pi} \frac{Q}{4\pi} sin\,\theta\, d\theta\, d\emptyset \qquad (2.14)$$

Where the limits on the integrals have been chosen on that the integration is carried over the entire surface of the sphere once.[10] Integrating gives

$$\int_0^{2\pi} \frac{Q}{4\pi}(-cos\,\theta)\Big|_0^{\pi} d\emptyset = \int_0^{2\pi} \frac{Q}{2\pi} d\emptyset = Q \qquad (2.15)$$

and we obtain a result showing that Q coulombs of electric flux are crossing the surface, as we should since the enclosed charge is Q coulombs.

The following section contains examples of the application of Gauss`s law to problems of a simple symmetrical geometry with the object of finding the electric field intensity[10].

2.2- The steady Magnetic field:

At this point the concept of a field should be a familiar one. Since we first accepted the experimental law of forces existing between two point charges and defined electric field intensity as the force per unit charge on a test charge in the presence of a second charge, we have discussed numerous fields. These fields possess no real physical basis, for physical measurements must always be in terms of the forces on the

charges in the detection equipment. Those charges which are the source cause measurable forces to be exerted on other charges, which we may think of as detector charges. The fact that we attribute a field to the source charges and then determine the effect of this field on the detector charges amounts merely to a division of the basic problem into two parts for convenience.

The relation of the steady magnetic field to its source is more complicated than is the relation of the electrostatic field to its source. We shall find it necessary to accept several laws temporarily on faith alone, relegating their proof to the (rather difficult) final section in this chapter. This section may well be omitted when studying magnetic fields for the first time. It is included to make acceptance of the laws a little easier; the proof of the laws does exist and is available for the disbelievers or the more advanced student.

2.3- BIOT-SAVART LAW

The source of the steady magnetic field may be a permanent magnet, an electric field changing linearly with time, or a direct current. We shall largely ignore the permanent magnet and save the time-varying electric field for a later discussion. Our present relationships will concern the magnetic field produced by a differential dc element in free space.

We may think of this differential current element as a vanishingly small section of a current carrying filamentary conductor, where a filamentary conductor is the limiting case of a cylindrical ion as the radius approaches zero. We assume a current I flowing in a differential vector length of the filament $d\mathbf{L}$. The law of Biot-Savart.[10] then states that at any point P the magnitude of the magnetic field intensity produced by the differential element is proportional to the product of the current, the magnitude of the differential length, and the sine of the angle lying

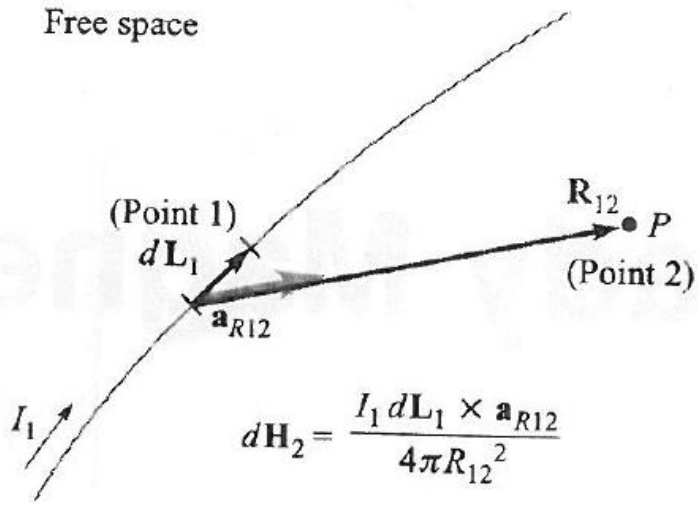

Fig. 2.3 The law of Biot-Savart expresses the magnetic field intensity dH_2 produced by a differential current element I_1 dL_1. [10].

between the filament and a line connecting the filament to the point P at which the field is desired; also, the magnitude of the magnetic field intensity is inversely proportional to the square of the distance from the differential element to the point P. The direction of the magnetic field intensity is normal to the plane containing the differential filament and the line drawn from the filament to the point P. Of the two possible normal, that one is to be chosen which is in the direction of progress of a right-handed screw turned from $d\mathbf{L}$ through the smaller angle to the line from the filament to P, the constant of proportionality is $1/4\pi$.

The Biot-Savart law, just described in some 150 words, may be written concisely using vector notation as

$$d\boldsymbol{H} = \frac{Id\boldsymbol{L} \times a_R}{4\pi R^2} = \frac{Id\boldsymbol{L} \times \boldsymbol{R}}{4\pi R^3} \qquad (2.16)$$

The units of the magnetic field intensity H are evidently amperes per meter (A/m). The geometry is illustrated in Fig (2.3). Subscripts may be used to indicate the point to which each of the quantities in (2.16) refers. If we locate the current element at point 1 and describe the point P at which the field is to be determined as point 2, then

$$d\boldsymbol{H}_2 = \frac{I_1 d\boldsymbol{L}_1 \times \boldsymbol{a}_{R12}}{4\pi R_{12}^2} \qquad (2.17)$$

The law of Biot-Savart is sometimes called Ampère's law for the current element, but we shall retain the former name because of possible confusion with Ampère's circuital law, to be discussed later.

In some aspects, the Biot-Savart law is reminiscent of Coulomb's law when that law is written for a differential element of charge,

$$dH_2 = \frac{dQ_1 a_{R12}}{4_{\pi\epsilon 0} R_{12}^2} \qquad (2.18)$$

Both show an inverse-square-law dependence on distance, and both show a linear relationship between source and field. The chief difference appears in the direction of the field[10].

It is impossible to check experimentally the law of Biot-Savart as expressed by (2.16) or (2.17) because the differential current element cannot be isolated. We have restricted our attention to direct currents only, so the charge density is not a function of time.

$$\nabla . J = \frac{\partial pv}{\partial t} \qquad (2.19)$$

Therefore shows that

$$V.J = 0 \qquad (2.20)$$

or upon applying the divergence theorem,

$$\oint_s J . ds = 0 \qquad (2.21)$$

The total current crossing any closed surface is zero, and this condition may be satisfied only by assuming a current flow around a closed path. It is this current flowing in a closed circuit which must be our experimental source, not the differential element.

It follows that only the integral form of the Biot-Savart law can be verified experimentally,

$$H = \oint \frac{Id\boldsymbol{L} \times a_R}{4\pi R^2} \qquad (2.22)$$

Equation (2.16) or (2.17), of course, leads directly to the integral form (2.22), but other differential expressions also yield the same integral formulation. Any term may be added to (2.16) whose integral around a closed path is zero. That is, any conservative field could be added to (2.16). The gradient of any scalar field always yields a conservative field, and we could therefore add a term VG to (2.16), where G is a general scalar field, without changing (2.21) in the slightest. This qualification on (2.16) or (2.17) is mentioned to show that if we later ask some foolish questions, not subject to any experimental check, concerning the force exerted by one differential current element on another, we should expect foolish answers.

The Biot-Savart law may also be expressed in terms of distributed sources, such as current density **J** and surface current density **K**. Surface current flows in a sheet of vanishingly small thickness, and the current density **J**, measured in amperes per square meter, is therefore infinite. Surface current density, however, is measured in amperes per meter width and designated by **K**. If the surface current density is uniform, the total current I in any width b is

$$I = Kb \qquad (2.23)$$

where we have assumed that the width b is measured perpendicularly to the direction in which the current is flowing. The geometry is illustrated by Fig (2.4). For a no uniform surface current density, integration is necessary:

$$I = \int KdN \qquad (2.24)$$

where *dN* is a differential element of the path across which the current is flowing. Thus the differential current element I d**L**, where dL is in the direction of the current, may be expressed in terms of surface current density **K** or current density **J**,

$$I\,d\mathbf{L} = \mathbf{K}\,dS = \mathbf{J}\,dv \qquad (2.25)$$

and alternate forms of the Biot-Savart law obtained ‹

$$\boldsymbol{H} = \int_s \frac{\boldsymbol{K} \times \boldsymbol{a}_R dS}{4\pi R^2} \qquad (2.26)$$

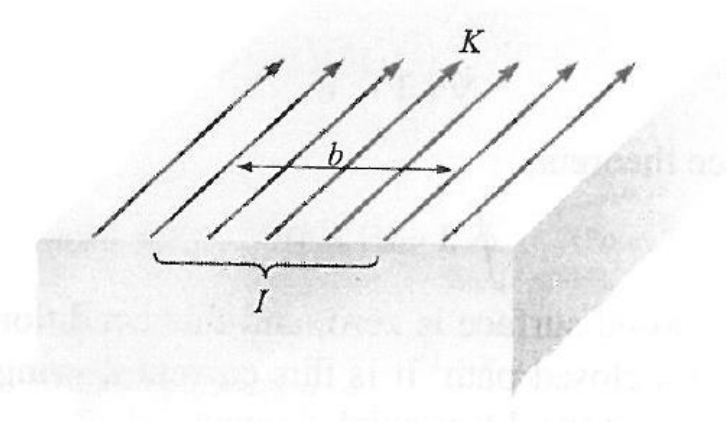

Fig. 2.4 The total current I within a transverse width b, in which there is a uniform surface current density K, is Kb.[10]

and

$$\mathbf{H} = \int_{vol} \frac{\mathbf{J} \times \mathbf{a}_R dv}{4\pi R^2} \qquad (2.27)$$

We may illustrate the application of the Biot-Savart law by considering an infinitely long straight filament. We shall apply (2.16) first and then integrate. This, of course, is the same as using the integral form (2.17) in the first place.[10]

Referring to Fig (2.5), we should recognize the symmetry of this field. No variation with z or with ∅ can exist. Point 2, at which we shall determine the field, is therefore chosen in the z=0 plane. The field point r is therefore r = pa. The source point r' is given by r' = z'az, and therefore

$$R_{12} = r - r` = \rho a_\rho - z` a_z \qquad (2.28)$$

so the

$$aR_{12} = \frac{\rho a_\rho - z` a_z}{\sqrt{\rho^2 + z`^2}} \qquad (2.29)$$

We take dL = dz'az and (1.3) becomes

$$dH_2 = \frac{I dz` a_z \times \left(\rho a_\rho - z` a_z\right)}{4\pi(\rho^2 + z`^2)^{3/2}} \qquad (2.30)$$

Since the current is directed toward increasing values of Z', the limits are - integral, and we have

$$H_2 = \int_{-\infty}^{\infty} \frac{I\, dz` a_z \times \left(\rho a_\rho - z` a_z\right)}{4\pi(\rho^2 + z`^2)^{3/2}} = \frac{I}{4\pi} \int_{-\infty}^{\infty} \frac{\rho dz` a_\emptyset}{(\rho^2 + z`^2)^{3/2}} \qquad (2.31)$$

At this point the unit vector $a_\emptyset$ under the integral sign should be investigated, for it is not always a constant, as are the unit vectors of the rectangular coordinate system. A vector is constant when its magnitude and direction are both constant. The unit vector Illustrations certainly has constant magnitude, but its direction may change. Here ap changes with the coordinate $\emptyset$ but not with p or z. Fortunately, the integration here is with respect to z', and $a_\emptyset$ is

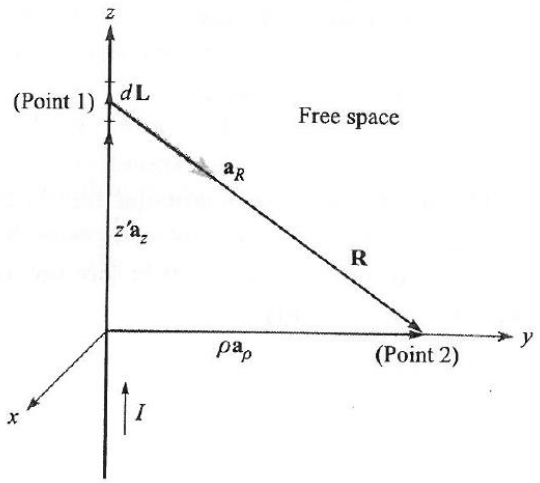

Fig. 2.5 An infinitely long straight filament carrying a direct current I. The field at point 2 is $\boldsymbol{H} = \left(\frac{I}{2\pi\rho}\right)\boldsymbol{a}_\emptyset[\mathbf{10}]$.

a constant and may be removed from under the integral sign,

$$\mathbf{H}_2 = \frac{I\rho a_\emptyset}{4\pi}\int_{-\infty}^{\infty}\frac{dz`}{(\rho^2+z`^2)^{3/2}} = \frac{I\rho a_\emptyset}{4\pi}\frac{z`}{\rho^2\sqrt{\rho^2+z`2}}\Big|_{-\infty}^{\infty} \qquad (2.32)$$

and

$$\mathbf{H}_2 = \frac{I}{2\pi\rho}\mathbf{a}_\emptyset \qquad (2.33)$$

The magnitude of the field is not a function of or (2.3), and it varies inversely with the distance from the filament. The direction of the magnetic-field-intensity vector is circumferential. The streamlines are therefore circles about the filament, and the field may be mapped in cross section as in Fig (2.6).

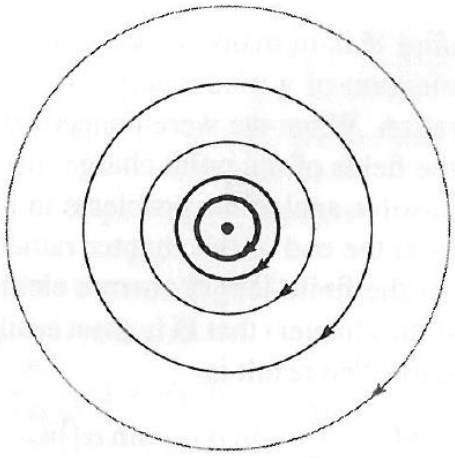

Fig. 2.6 The streamlines of the magnetic field intensity about an infinitely long straight filament carrying a direct current I.[10]

The separation of the streamlines is proportional to the radius, or inversely proportional to the magnitude of H. To be specific, the streamlines have been drawn with curvilinear squares in mind. As yet we have no name for the family of lines[10] which are perpendicular to these circular streamlines, but the spacing of the streamlines has been adjusted so that addition of this second set of lines will produce an array of curvilinear squares.

A comparison of Fig (2.7) with the map of the *electric* field about an infinite line charge shows that the streamlines of the magnetic field correspond exactly to the equipotential of the electric field, and the unnamed (and undrawn) perpendicular family of lines in the magnetic field corresponds to the streamlines of the electric field. This correspondence in not an accident, but there are several other concepts which must be mastered before the analogy between electric and magnetic fields can be explored more thoroughly.

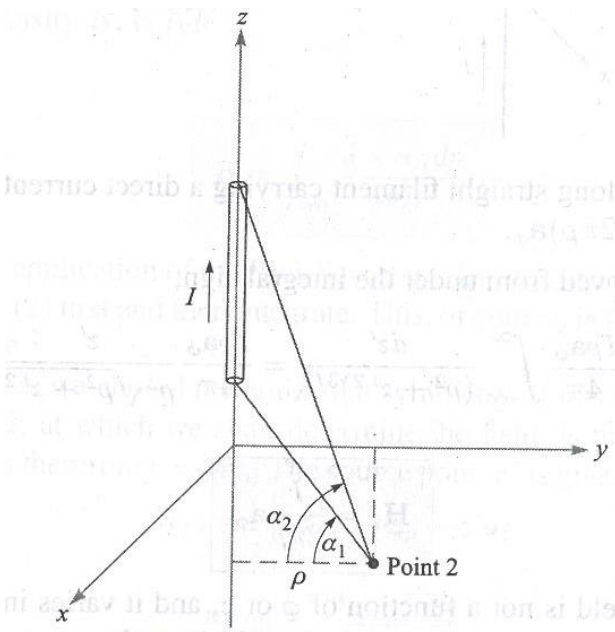

Fig 2.7 The magnetic field intensity caused by a finite-length current filament on the z axis is $(I/4\pi\rho)(\sin a_2 - \sin a_1)a\emptyset$.[10]

Using the Biot-Savart law to find **H** is in many respects similar to the use of coulomb`s law to find **E**. Each requires the determination of a moderately complicated integrand containing vector quantities, followed by an integration. When we were concerned with Coulomb`s law we solved as number of examples, including the fields of the point charge, line charge, and sheet of charge. The law of Biot-Savart can be used to solve analogous problems in magnetic fields, and some of these problems now appear as exercises at the end of the chapter rather than as examples here.

One useful result is the field of the finite-length current element, shown in Fig (2.7)

$$\mathbf{H} = \frac{I}{4\pi\rho}(sin\,\alpha_2 - sin\,\alpha_1)\mathbf{a}\emptyset \qquad (2.34)$$

If one or both ends are below point 2, then α_1, or both α_1 and α_2, are negative.

Equation (2.34) may be used to find the magnetic field intensity caused by current filaments arranged as a sequence of straight-line segments.

2.4- AMPERE`S CIRCUITAL LAW:

After solving a number of simple electrostatic problems with Coulomb`s law, we found that the same problems could be solved much more easily by using Gauss`s law whenever high degree of symmetry was present. Again, an analogous procedure exists in magnetic fields. Here, the law that helps us solve problems more easily is known as Ampere`s circuital law, sometimes called Ampere`s work law. This law may may be derived from the Biot-Savart law, For the present we might agree to accept Ampere`s circuital[10] law temporarily as another law capable of experimental proof. As is the case with Gauss`s law, its use will also require careful consideration of the symmetry of the problem to determine which variables and components are present[10].

Ampere`s circuital law states that the line integral of **H** about any closed path is exactly equal to the direct current enclosed by that path,

$$\oint H.d\mathbf{L} = I \qquad (2.35)$$

We define positive current as flowing in the direction of advance of a right-handed screw turned in the direction in which the closed path is traversed.

Referring to Fig (2.8), which shows a circular wire carrying a direct current I, the line integral of H about the closed paths lettered a and b results in an answer of l; the integral about the closed path c which passes through the conductor gives an answer less than I and is exactly that portion of the total current which is enclosed by the path c. Although paths a and b give the same answer, the integrands are, of course, different. The line integral directs us to multiply the component of H in the direction of the path by a small increment of path length at one point of the path, move along the path to the next incremental length, and repeat the process, continuing until the path is completely traversed. Since H will generally vary from point to point, and since paths a and b are not alike, the contributions to the integral made by, say, each micrometer of path length are quite different. Only the final answers are the same.

we shall use to represent the closed path. Some strange and formidable paths can be constructed by twisting and knotting the rubber band, but if neither the rubber band nor the conducting circuit is broken, the current enclosed by the path is that carried by the conductor. Now let us replace the rubber band by a circular ring of spring steel across which is stretched a rubber sheet. The steel loop forms the closed path, and the current-carrying conductor must pierce the rubber sheet if the current is to be enclosed by the path. Again, we may twist the steel loop, and we may also deform the rubber sheet by pushing our fist into it or folding it in any way we wish. A single current-carrying conductor still pierces the sheet once, and this is the true measure of the current enclosed by the path. If we should thread the conductor once through the sheet from front to back and once from back to front, the total current enclosed by the path is the algebraic sum, which is zero[10].

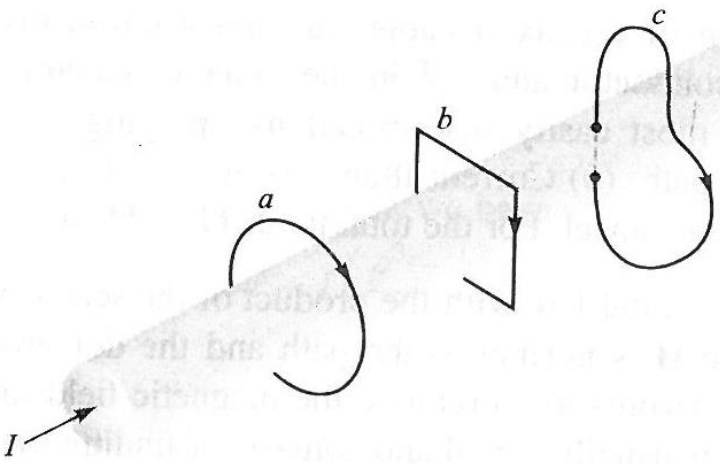

Fig. 2.8 A conductor has a total current I. The line integral of H about the closed paths a and b is equal to I, and the integral around path c is less than *I*, [10]

In more general language, given a closed path, we recognize this path as the perimeter of an infinite number of surfaces (not closed surfaces). Any current-carrying conductor enclosed by the path must pass through every one of these surfaces once. Certainly some of the surfaces may be chosen in such a way that the conductor pierces them twice in one direction and once in the other direction, but the algebraic total current is still the same.

The nature of the closed path is usually extremely simple and can be drawn on a plane. The simplest surface is, then, that portion of the plane enclosed by the path. We need merely find the total current passing through this region of the plane.

The application of Gauss's law involves finding the total charge enclosed by a closed surface; the application of Ampère's circuital law involves finding the total current enclosed by a closed path.

Let us again find the magnetic field intensity produced by an infinitely long filament carrying a current *I*. The filament lies on the z axis in free space (as in Fig (2.5), and the current flows in the direction given by az. Symmetry inspection comes first, showing that there is no variation with z or *0*. Next we determine which components of H are present by using the Biot-Savart law. Without specifically using the cross product, we may say that the direction of d**H** is perpendicular to the plane

containing d**L** and R and therefore is in the direction of ap. Hence the only component of His *Ho*, and it is a function only of *p*.

We therefore choose a path to any section of which H is either perpendicular or tangential and along which *H i*s constant. The first requirement (perpendicularity or tangency) allows us to replace

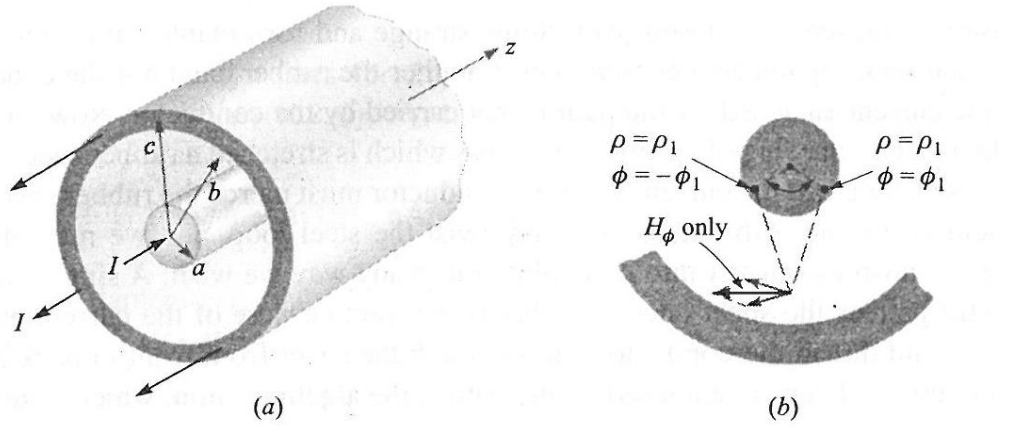

Fig. 2.9 (a) Cross section of a coaxial cable carrying a uniformly distributed current I in the inner conductor and -I in the outer conductor.. (b) Current filaments at $\boldsymbol{\rho = \rho_1, \emptyset = \pm\emptyset_1}$, produces $\boldsymbol{H_\rho}$, components which cancel. For the total field, $\boldsymbol{H = H_\emptyset ap}$[10].

the dot product of Ampère's circuital law with the product of the scalar magnitudes, except along that portion of the path where H is normal to the path and the dot product is zero; the second requirement (constancy) then permits us to remove the magnetic field intensity from the integral sign. The integration required is usually trivial and consists of finding the length of that portion of the path to which H is parallel.

In our example the path must be a circle of radius p, and Ampère's circuital law becomes

$$\oint H.dL = \int_0^{2\pi} H_\emptyset \rho d\emptyset = H_\emptyset \rho \int_0^{2\pi} d\emptyset = H_\emptyset 2\pi\rho = I \qquad (2.36)$$

or

$$H_\emptyset = \frac{I}{2\pi\rho} \qquad (2.37)$$

as before.

As a second example of the application of Ampère's circuital law, consider an infinitely long coaxial transmission line carrying a uniformly distributed total current I in the center conductor and -I in the outer conductor. The line is shown in Fig (2.9a). Symmetry shows that H is not a function of $\emptyset$ or *z*. In order to determine the components present, we may use the results of the previous example by considering the solid conductors as being composed of a large number of filaments. No filament has a *z* component of **H**. Furthermore, the H_ρ, component produced by $\emptyset = 0^0$, produced by one filament located at $\rho = \rho_1, \emptyset$, is canceled by the H_ρ, component produced by a symmetrically located filament at $\rho = \rho_1, \emptyset = -\emptyset_1$. This symmetry is illustrated by Figure 2.9b. Again we find only an $H_\emptyset$ component which varies with ρ.

A circular path of radius p, where p is larger than the radius of the inner conductor but less than the inner radius of the outer conductor, then leads immediately to

$$H_\emptyset = \frac{I}{2\pi\rho} \ (a < \rho < b) \qquad (2.38)$$

If we choose p smaller than the radius of the inner conductor, the current enclosed is

$$I_{encl} = I\frac{\rho^2}{\alpha^2} \qquad (2.39)$$

and

$$2\pi\rho H_\emptyset = I\frac{\rho^2}{\alpha^2} \qquad (2.40)$$

or

$$H_\emptyset = \frac{I\rho}{2\pi a^2} (\rho < a) \qquad (2.41)$$

If the radius p is larger than the outer radius of the outer conductor, no current is enclosed and

$$H_\emptyset = 0 \ (\rho > a) \qquad (2.42)$$

Finally, if the path lies within the outer conductor, we have

$$2\pi\rho H_{\emptyset} = I - I\left(\frac{\rho^2 - b^2}{c^2 - b^2}\right) \qquad (2.43)$$

$$H_{\emptyset} = \frac{I}{2\pi p}\frac{c^2 - p^2}{c^2 - b^2}\ (b < \rho < c) \qquad (2.44)$$

The magnetic-field-strength variation with radius is shown in Figure 2.10 for a coaxial cable in which b= 3a, c = 4a. It should be noted that the magnetic field intensity H is continuous at all the conductor boundaries. In other words, a slight increase in the radius of the closed path does not result in the enclosure of a tremendously different current. The value of *Ho* shows no sudden jumps.

The external field is zero. This, we see, results from equal positive and negative currents enclosed by the path. Each produces an external field of magnitude *1/2np*, but complete cancellation occurs Fig 2.10.

This is another example of "shielding"; such a coaxial cable carrying large currents would not produce any noticeable effect in an adjacent circuit[10].

As a final example, let us consider a sheet of current flowing in the positive *y* direction and located in the z = 0 plane. We may think of the return current as equally divided between two

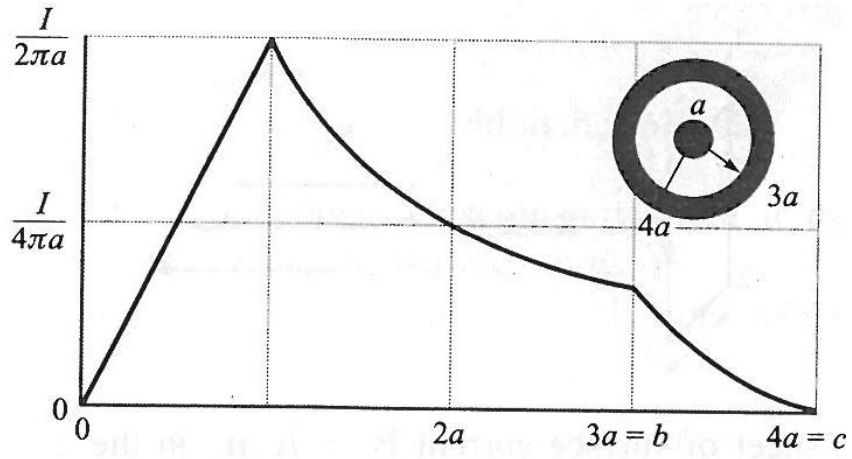

Fig. 2.10 The magnetic field intensity as a function of radius in an infinitely long coaxial transmission line with the dimensions [10].

distant sheets on either side of the sheet we are considering. A sheet of uniform surface current density K = Kyay is shown in Fig 2.11. H cannot vary with x or *y*. If the sheet is subdivided into a number of filaments, it is evident that no filament can produce an *Hy c*omponent. Moreover, the Biot-Savart law shows that the contributions to *H*, produced by a symmetrically located pair of filaments cancel. Thus, *H*, is zero also; only an *H*e component is present. We therefore choose the path 1-1'-2-2-1 composed of straight-line segments which are either parallel or perpendicular to *Hr*. Ampère's circuital law gives

$$H_{x1}L + H_{x2}(-L) = K_{\mathrm{y}}L \qquad (2.45)$$

or

$$H_{x1} - H_{x2} = K_{\mathrm{y}} \qquad (2.46)$$

If the path 3-3-2-2-3 is now chosen, the same current is enclosed, and

$$H_{x3} - H_{x2} = K_{\mathrm{y}} \qquad (2.47)$$

and therefore

$$H_{x3} = H_{x1} \qquad (2.48)$$

It follows that *He* is the same for all positive z. Similarly, *Hx* is the same for all negative z. Because of the symmetry, then, the magnetic field intensity on one side of the current sheet is the negative of that on the other. Above the sheet,

$$H_x = \frac{1}{2}K_y \ (z > 0) \qquad (2.49)$$

while below it

$$H_x = -\frac{1}{2}K_y \ (z < 0) \qquad (2.50)$$

Letting an be a unit vector normal (outward) to the current sheet, the result may be written in a form correct for all z as

$$\mathbf{H} = \frac{1}{2}\mathbf{K} \times \mathrm{a}_N \qquad (2.51)$$

If a second sheet of current flowing in the opposite direction, K=-K_y a_y, is placed at z = h, (2.13) shows that the field in the region between the current sheets is

$$\mathbf{H} = \mathbf{K} \times a_N (0 < z < h) \qquad (2.52)$$

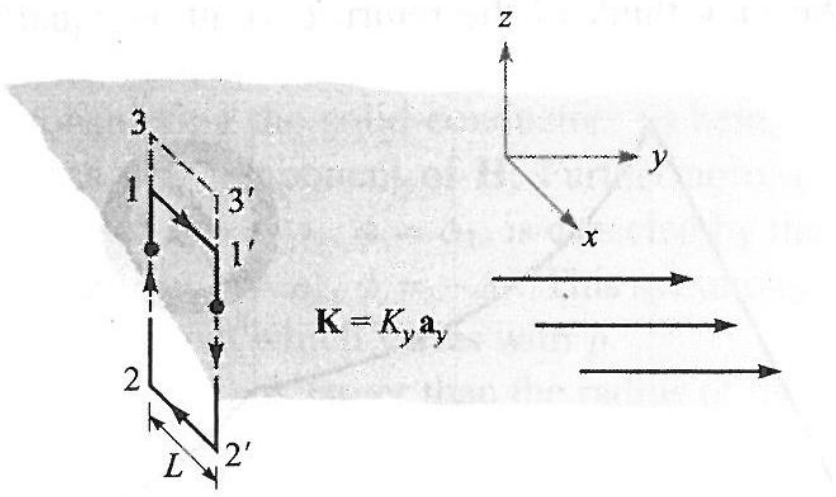

Fig. 2.11 A uniform sheet of surface current $K = K_y a_y$ in the z=0 plane. H may be found by applying Ampère's circuital law about the paths 1-1-2-2-1 and 3-3' 2′-2-3[10].

and is zero elsewhere,

$$\mathbf{H} = 0 \ (z < 0, z > h) \qquad (2.53)$$

The most difficult part of the application of Ampère's circuital law is the determination of the components of the field which are present. The surest method is the logical application of the Biot-Savart law and a knowledge of the magnetic fields of simple form. outlines the steps involved in applying Ampère's circuital law to an infinitely long solenoid of radius a and uniform current density Kaaϕ, as shown in Fig (2.12a). For reference, the result is

$$\mathbf{H} = K_a a_z \ (\rho < a) \qquad (2.54)$$

$$\mathbf{H} = 0 \quad (\rho > a) \qquad (2.55)$$

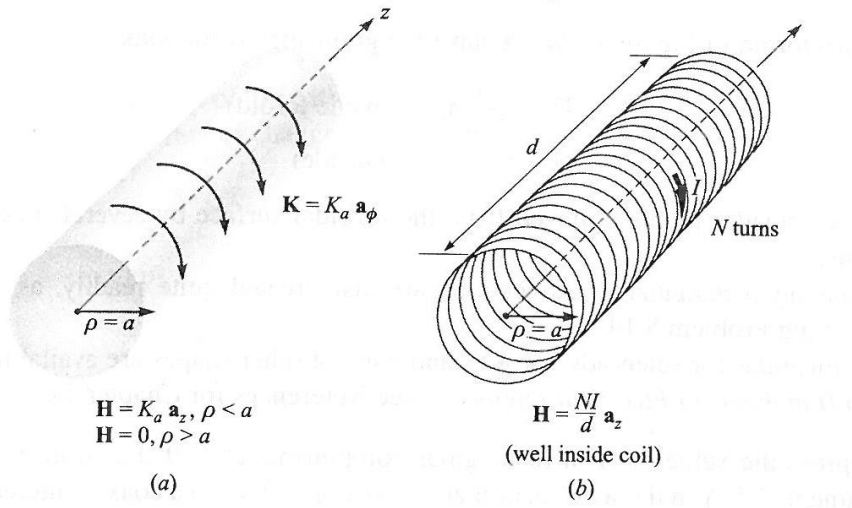

Fig. 2.12 ***(a)*** **An ideal solenoid of infinite length with a circular current sheet** $K = K_a \mathrm{a}_\emptyset$. ***(b)*** **An N-turn solenoid of finite length** ***d.[10]***

If the solenoid has a finite length d and consists of N closely wound turns of a filament that carries a current *I* (Fig 2.12b), then the field at points well within the solenoid is given closely

by

$$\mathbf{H} = \frac{NI}{d}\mathrm{a}_z \text{ (Well within the solenoid)} \qquad (2.56)$$

The approximation is useful it if is not applied closer than two radii to the open ends, nor closer to the solenoid surface than twice the separation between turns.

shown in Fig (2.13), it can be shown that the magnetic field intensity for the ideal case, Fig 2.13a, is

$$\mathbf{H} = K_a \frac{\rho_0 - a}{\rho}\mathrm{a}_\emptyset \text{ (inside toroid)} \qquad (2.57)$$

$$\mathbf{H} = 0 \qquad \text{(outside)} \qquad (2.58)$$

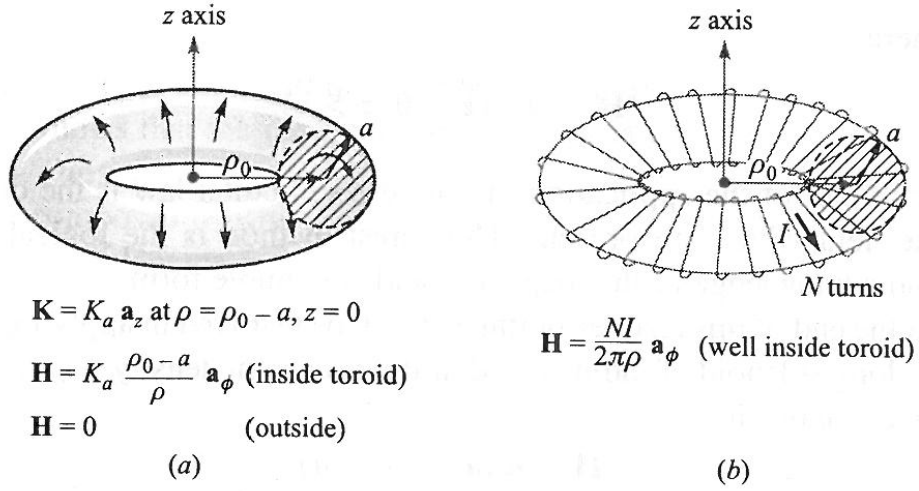

Fig. 2.13 *(a)* An ideal toroid carrying a surface current K in the direction shown. *(6)* An N-turn toroid carrying a filamentary current *I[10].*

For the N-turn toroid of Fig 2.13b, we have the good approximations,

$$\mathbf{H} = \frac{NI}{2\pi\rho} \mathrm{a}_\emptyset \text{ (inside toroid)} \qquad (2.59)$$

$$\mathbf{H} = 0 \qquad \text{(outside)}$$

as long as we consider points removed from the toroidal surface by several times the separation between turns.

2.5- MAGNETIC FLUX AND MAGNETIC FLUX DENSITY

In free space, let us define the *magnetic flux density* **B** as

$$\mathbf{B} = \mu_0 \mathbf{H} \qquad \text{(free space only)} \qquad (2.60)$$

where **B** is measured in webers per square meter (Wb/m^2) or in a newer unit adopted in the International System of Units, tesla (T). An older unit that is often used for magnetic flux density is the gauss (G), where 1 T or $1Wb/m^2$ is the same as 10000 G. The constant μ_0 is not dimensionless and has the defined value for space, in henrys per meter (H/m), of

$$\mu_0 = 4\pi \times 10^{-7} \text{ H/m} \qquad (2.61)$$

The name given to μ_0 is the permeability of free space.

We should note that since **H** is measured in amperes per meter, the weber is dimensionally equal to the product of henry and amperes. Considering the henry as a new unit, the weber is merely a convenient abbreviation for the product of henrys and amperes. When time-varying fields are introduced, it will be shown that a weber is also equivalent to the product of volts and seconds.

The magnetic-flux-density vector **B**, as the name weber per square meter implies, is a member of the flux-density family of vector fields. One of the possible analogies between electric and magnetic fields[10] compares the laws of Biot-Savart and Coulomb, thus establishing an analogy between **H** and **E**. The relations B = μ_0 H and D = ϵ_0 E then lead to an analogy between b and D. If B is measured in teslas or webers per square meter, then magnetic flux should be measured in webers. Let us represent magnetic flux by Φ and define Φ as the flux passing through any designated area,

$$\Phi = \int_S \boldsymbol{B}.d\boldsymbol{S}\ Wb \qquad (2.62)$$

Our analogy should now remind us of the electric flux Ψ, measured in coulombs, and of Gauss`s law, which states that the total flux passing through any closed surface is equal to the charge enclosed,

$$\Psi = \int_S \boldsymbol{D}.d\boldsymbol{S} = Q \qquad (2.63)$$

The charge Q is the source of the lines of electric flux and these lines begin and terminate on positive and negative charge, respectively.

No such source has ever been discovered for the lines of magnetic flux. In the example of the infinitely long straight filament carrying a direct current *I*, the H field formed concentric circles about the filament. Since $B = \mu_0$ H, the B field is of the same form. The magnetic flux lines are closed and do not terminate on a "magnetic charge". For this reason Gauss`s law for the magnetic field is

$$\int_S \boldsymbol{B}.d\boldsymbol{S} = 0 \qquad (2.64)$$

and application of the divergence theorem shows us that

$$\nabla.B = 0 \qquad (2.65)$$

We have not proved (2.64) or (2.65) but have only suggested the truth of these statements by considering the single field of the infinite filament. It is possible to show that (2.64) or (2.65) follows from the Biot-Savart law and the definition of **B**, $\boldsymbol{B} = \mu_0$ H

Equation (2.65) is the last of Maxwell`s four equations as they apply to static electric fields and steady magnetic fields. Collecting these equations, we then for static electric fields and steady magnetic fields.

$$\left.\begin{aligned} \nabla.\mathbf{D} &= \rho_v \\ \nabla \times \mathbf{E} &= 0 \\ \nabla \times \mathbf{H} &= \mathbf{J} \\ \nabla.\mathbf{B} &= 0 \end{aligned}\right\} \qquad (2.66)$$

To these equations we may add the two expressions relating **D** to **E** and **B** to **H** in free space,

$$\boldsymbol{D} = \epsilon_0 \boldsymbol{E} \qquad (2.67)$$

$$\boldsymbol{B} = \mu_0 \boldsymbol{H} \qquad (2.68)$$

We have also found it helpful to define an electrostatic potential,

$$\boldsymbol{E} = -\nabla V \qquad (2.69)$$

and we shall discuss a potential for the steady magnetic field in the following section. In addition, we have extended our coverage of electric fields to include conducting materials and dielectrics, and we have introduced the polarization P. A similar treatment will be applied to magnetic fields in the next chapter.

Returning to (2.66), it may be noted that these four equations specify the divergence and curl of an electric and a magnetic field. The corresponding set of four integral equations that apply to static electric fields and steady magnetic fields is

$$\oint_s D.dS = Q = \int_{vol} \rho_v dv \qquad (2.70)$$

$$\oint E.dL = 0 \qquad (2.71)$$

$$\oint H.dL = I = \int_S J.dS \qquad (2.72)$$

$$\oint_s B.dS = 0 \qquad (2.73)$$

Our study of electric and magnetic fields would have been much simpler if we could have begun with either set of equations, (2.66) or (2.71). With a good knowledge of vector analysis, such as we should now have, either set may be readily obtained from the other by applying the divergence theorem or Stokes` theorem. The various experimental laws can be obtained easily from these equations.

As an example of the use of flux and flux density in magnetic fields, let find the flux between the conductors of the coaxial line of fig (2.9a). The magnetic field intensity was found to be

$$H_\emptyset = \frac{I}{2\pi\rho} \ (a < \rho < b) \qquad (2.74)$$

and therefore

The magnetic flux continued between the conductors in a length d is the flux crossing any radial plane extending from $\rho = a$ to $\rho = b$ and from, say, z = 0 to z = d

$$\Phi = \int_s B.dS = \int_s^d \int_a^b \frac{\mu_0 I}{2\pi\rho} \mathrm{a}_\emptyset . d_\rho dz \mathrm{a}_\emptyset \qquad (2.75)$$

$$\Phi = \frac{\mu_0 I}{2\pi} In \frac{b}{a} \qquad (2.76)$$

This expression will be used later to obtain the inductance of the coaxial transmission line.

2.6- FARADY`S LAW:

After Oersted [9]. demonstrated in 1820 that an electric current affected a compass needle, faraday professed his belief that if a current could produce a magnetic field, then a magnetic field should be able to produce a current. The concept of the "field" was not available at that time, and Faraday's goal was to show that a current could be produced by "magnetism".

He worked on this problem intermittently over a period of 10 years, until he was finally successful in 1831[10] He wound two separate on an iron toroid and placed a galvanometer in one circuit and a battery in the other. Upon closing the battery circuit, he noted a momentary deflection of the galvanometer; a similar deflection in the opposite direction occurred when the battery was disconnected. This, of course, was the first experiment he made involving a changing magnetic field, and he followed it with a demonstration that either a moving magnetic field or a moving coil could also produce a galvanometer deflection[10].

In terms of fields, we now say that a time-varying magnetic field produces an electromotive force (emf) which may establish a current in a suitable circuit. An electromotive force is merely a voltage that arises from conductors moving in a magnetic field or from changing magnetic fields, and we shall define it in this section. Faraday`s law is customarily stated as.

$$emf = \frac{d\Phi}{dt}V \qquad (2.77)$$

Equation (2.77) implies a closed path, although not necessarily a closed conducting path; the closed path, for example, might include a capacitor, or it might be a purely imaginary line in space. The magnetic flux is that flux which passes through any and every surface whose perimeter is the closed path, and $d\Phi$ / dt is the time rate of change of this flux.

A nonzero value of $d\Phi$ / dt may result from any of the following situations:

1- A time-changing flux linking a stationary closed path.
2- Relative motion between a steady flux and a closed path.
3- A combination of the two.

The minus sing is an indication that the emf is in such a direction as to produce a current whose flux, if added to the original flux, would reduce the magnitude of the emf. This statement that the induced voltage acts to produce an opposing flux is known as Lenz`s law.[10]

If the closed path is that taken by an N-turn filamentary conductor, it is often sufficiently accurate to consider the turns as coincident and let

$$emf = N\frac{d\Phi}{dt} \qquad (2.78)$$

Where Φ is now interpreted as the flux passing through any one of N coincident paths.

We need to define emf as used in (2.77) or (2.78). The emf is obviously a scalar, and (perhaps not so obviously) a dimensional check shows shows that it is measured in volts. We define the emf as

$$emf = \oint E.d\mathbf{L} \qquad (2.79)$$

and note that it is the voltage about a specific closed path. If any part of the path is changed, generally the emf changes. The departure from static results is clearly shown by (2.79), for an electric field intensity resulting from a static charge distribution must lead to zero positional difference about a closed path. In electrostatics, the line integral leads to a potential difference; with time-varying fields, the result is an emf or a voltage.

Replacing Φ in (2.77) with the surface integral of **B**, we have

$$emf = \oint E.d\mathbf{L} = -\frac{d}{dt}\int_s B.d\mathbf{S} \qquad (2.80)$$

2.7- Maxwell's Equations In Point Form .

already obtained two of Maxwell's equations for time-varying fields,

$$\nabla \times \boldsymbol{E} = \frac{\partial \boldsymbol{B}}{\partial t} \qquad (2.81)$$

and

$$\nabla \times \boldsymbol{H} = \boldsymbol{J} + \frac{\partial \boldsymbol{D}}{\partial t} \qquad (2.82)$$

The remaining two equations are unchanged from their non-time-varying form :

$$\nabla . \boldsymbol{D} = \rho v \qquad (2.83)$$

$$\nabla . \boldsymbol{B} = 0 \qquad (2.84)$$

Equation (2.83) essentially states that charge density is a source (or sink) of electric flux lines. Note that we can no longer say that all electric flux begins and terminates on charge, because the point form of Faraday's law (2.81) shows that **E**, and hence **D**, may have circulation if a changing magnetic field is present. Thus the lines of electric flux may form closed loops. However, the converse is still true, and every coulomb of charge must have one coulomb of electric flux diverging from it.

Equation (2.84) again acknowledges the fact that “magnetic charges," or poles, are not known to exist. Magnetic flux is always found in closed loops and never diverges from a point source.

These four equations form the basis of all electromagnetic theory. They are partial differential equations and relate the electric and magnetic fields to each other and to their sources, charge and current density. The auxiliary equations relating **D** and **E**,

$$\boldsymbol{D} = \epsilon \boldsymbol{E} \qquad (2.85)$$

relating B and H,

$$\boldsymbol{B} = \mu \boldsymbol{H} \qquad (2.86)$$

defining conduction current density,

$$\mathbf{J} = \sigma \boldsymbol{E} \tag{2.87}$$

and defining convection current density in terms of the volume charge density ρv,

$$\mathbf{J} = \rho_v \mathbf{v} \tag{2.88}$$

are also required to define and relate the quantities appearing in Maxwell's equations.

The potentials V and A have not been included because they are not strictly necessary, although they are extremely useful. They will be discussed at the end of this chapter.

If we do not have "nice" materials to work with, then we should replace (2.85) and (2.86) with the relationships involving the polarization and magnetization fields,

$$\boldsymbol{D} = \epsilon 0 \boldsymbol{E} + \boldsymbol{P} \tag{2.89}$$

$$\boldsymbol{B} = \mu 0 (\boldsymbol{H} + \boldsymbol{M}) \tag{2.90}$$

For linear materials we may relate P to E

$$\boldsymbol{P} = X_{e\epsilon 0} \boldsymbol{E} \tag{2.91}$$

and **M** to **H**

$$\boldsymbol{M} = X_m \boldsymbol{H} \tag{2.92}$$

Finally, because of its fundamental importance we should include the Lorentz force equation, written in point form as the force per unit volume,

$$\boldsymbol{F} = \rho v (\boldsymbol{E} + \mathbf{v} \times \boldsymbol{B}) \tag{2.93}$$

2.8- MAXWELL'S EQUATIONS IN INTEGRAL FORM

The integral forms of Maxwell's equations are usually easier to recognize in terms of the experimental laws from which they have been obtained by a generalization process. Experiments must treat physical macroscopic quantities, and their results therefore are expressed in terms

of relationships. A differential equation always represents a theory. Let us now collect the integral forms of Maxwell's equations.

Integrating (2.81) over a surface and applying Stokes' theorem, we obtain Faraday's law,

$$\oint \boldsymbol{E}.d\boldsymbol{L} = -\int_S \frac{\partial \boldsymbol{B}}{\partial t}.d\boldsymbol{S} \qquad (2.94)$$

and the same process applied to (2.82) yields Ampère's circuital law,

$$\oint \boldsymbol{H}.d\boldsymbol{L} = I + \int_S \frac{\partial \boldsymbol{D}}{\partial t}.d\boldsymbol{S} \qquad (2.95)$$

Gauss's laws for the electric and magnetic fields are obtained by integrating (2.83) and (2.84) throughout a volume and using the divergence theorem:

$$\oint_s \boldsymbol{D}.\boldsymbol{dS} = \int_{vol} \rho_v dv \qquad (2.96)$$

$$\oint_s \boldsymbol{B}.d\boldsymbol{S} = 0 \qquad (2.97)$$

These four integral equations enable us to find the boundary conditions on **B**, **D**, **H**, and **E** which are necessary to evaluate the constants obtained in solving Maxwell's equations in partial differential form. These boundary conditions are in general unchanged from their forms for static or steady fields, and the same methods may be used to obtain them. Between any two real physical media (where K must be zero on the boundary surface), (2.94) enables us to relate the tangential E-field components,

$$E_{t1} = E_{t2} \qquad (2.98)$$

and from (2.45),

$$H_{t1} = H_{t2} \qquad (2.99)$$

The surface integrals produce the boundary conditions on the normal components,

$$D_{N1} - D_{N2} = PS \qquad (2.100)$$

and

$$B_{N1} = B_{N2} \qquad (2.101)$$

It is often desirable to idealize a physical problem by assuming a perfect conductor for which o is infinite but J is finite. From Ohm's law, then, in a perfect conductor,

$$\mathbf{E}=0$$

and it follows from the point form of Faraday's law that

$$\mathbf{H} = 0$$

for time-varying fields. The point form of Ampère's circuital law then shows that the finite value of J is

$$\mathbf{J} = 0$$

and current must be carried on the conductor surface as a surface current K. Thus, if region 2 is a perfect conductor, (2.98) to (2.101) become, respectively,

$$E_{t1} = 0 \qquad (2.102)$$

$$H_{t1} = K \qquad (\boldsymbol{H}_{t1} = \boldsymbol{K} \times \mathbf{a}_N) \qquad (2.103)$$

$$D_{N1} = \rho_s \qquad (2.104)$$

$$B_{N1} = 0 \qquad (2.105)$$

where an is an outward normal at the conductor surface.

Note that surface charge density is considered a physical possibility for either dielectrics, perfect conductors, or imperfect conductors, but that surface current density is assumed only in conjunction with perfect conductors.

The preceding boundary conditions are a very necessary part of Maxwell's equations. All real physical problems have boundaries and require the solution of Maxwell's equations in two or more regions and the matching of these solutions at the boundaries. In the case of perfect conductors, the solution of the equations within the conductor is trivial (all time-varying fields are zero), but the application of the boundary conditions (2.102) to (2.105) may be very difficult[10].

Chapter 3

Performance Of High-voltage power Transmission lines

3- The Libyan Electricity Network:

General Electric Company Of Libya (GECOL) is a state-owned power utility responsible for generation, transmission and distribution of electric power throughout Libya and it is the only supplier of electricity in the country.

The data related to the peak generation and distribution circuits lengths as listed in GECOL Site. The 400KV power lines, network extended through Libyan land for more than 2,823km .The next map Fig(3. 1) shows the 400KV lines which are in operation (red color) and which under Construction (blue color).

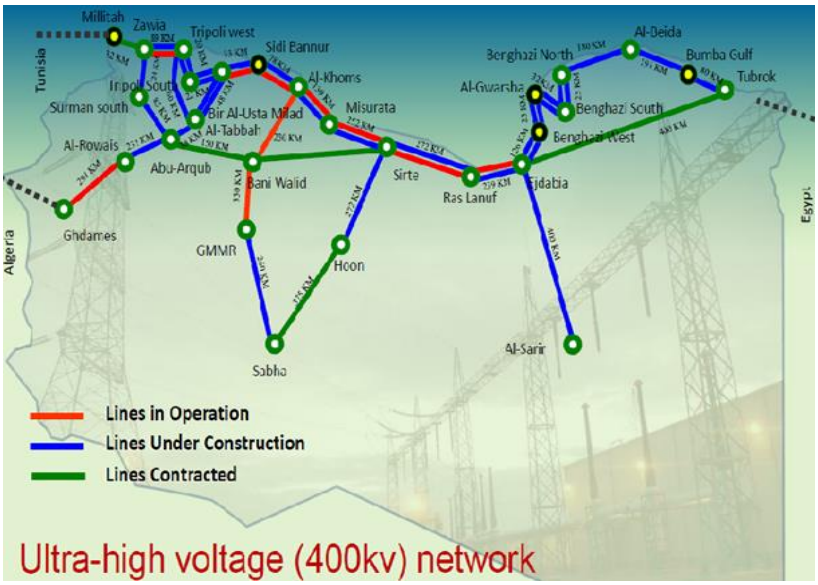

Fig (3.1) Libyan high voltage coverage[GECOL]

3.1 Electric field of the High voltage Transmission line.

The electric field created by a high-voltage transmission line, extends from the energized conductors to other conducting objects such as the ground, towers, vegetation, buildings, vehicles, and people. The calculated strength of the electric field at a height of 3.28 ft. (1 m) above an vegetated, flat earth is frequently used to describe the electric field under straight, parallel transmission lines. The most important

transmission-line parameters that determine the electric field at a l-m height are conductor height above ground and line voltage.

Calculations of electric fields from transmission lines are performed with computer programs based on well-known physical principles[11]. The calculated values under these conditions represent an ideal situation. When practical conditions approach this ideal model measurements and calculations agree. Often, however, conditions are far from ideal because of variable terrain and vegetation. In these cases, fields are calculated for ideal conditions, with the lowest conductor clearances to provide upper bombs on the electric field under the transmission lines. With the use of more complex models or empirical results, it is also possible to account accurately for variations in conductor height, topography, and changes in line direction. Because the fields from different sources add vector ally, it is possible to compute the fields from several different lines if the electrical and geometrical properties of the lines are known. However, in general, electric fields near transmission lines with vegetation below are highly complex and carrot be calculated. Measured fields in such situations are highly variable.

For evaluation of EMF from transmission lines, the fields must be calculated for a specific line condition. The NESC states the condition for evaluating electric-field-induced short-circuit current for lines with voltage above 98 kV, line-to-ground, as follows: conductors are at a minimum clearance from grated corresponding to a conductor temperature of l22°F (50°C), and at a maximum voltage[12]. Echini's has supplied the information for calculating electric and magnetic fields from the proposed transmission line: the maximum operating voltage, the estimated peak currents, and the minimum conductor clearances.

There are standard techniques for measuring transmission-line electric fields[43]. Provided that the conditions at a measurement site

closely approximate those of the ideal side for calculations, measurements of electric fields agree well with the calculated values. If the ideal conditions are not approximated, the measured field can diver substantially from calculated values. Usually, the actual electric field at ground level is reduced from the calculated values by various common objects that act as shields.

Maximum or peak field values occur over a small area at midspan, where conductors are closest to the ground. As the location of an electric-field profile approaches a tower, the conductor clearance increases, and the peak field decreases. A grounded tower will reduce the electric field considerably, by shielding.

For traditional transmission lines, such as the proposed line, where the right-of-way extends laterally well beyond the conductors, electric fields at the edge of the right-of-way are not as sensitive as the peak field to conductor height. Computed values at the edge of the right-of-way for any line height are fairly representative of what can be expected all along the transmission-line corridor. However, the presence of vegetation on and at the edge of the right-of-way will reduce actual electric-field levels below calculated values.

The ma etic field generated by currents on transmission-line conductors extends from the conductors through the air and into the ground. The magnitude of the field at a height of 3.28 ft. (l m) is frequently used to describe the magnetic field under transmission lines. Because the magnetic field is not affected by non-ferrous materials, the field is not influenced by normal objects on the ground under the line. The direction of the maximum field varies with location. (The electric field, by contrast, is essentially vertical near the ground.) The most important transmission-line parameters that determine the magnetic field at 3.28 ft. (1 m) height are conductor height above ground and magnitude of the

currents flowing in the conductors. As distance from the transmission-line conductors increases, the magnetic field decreases.

Calculations of magnetic fields from transmission lines are performed using well-known physical principles[11]. The calculated values usually represent the ideal straight parallel-conductor configuration. For simplicity, a flat earth is usually assumed. Balanced currents) currents of the same magnitude for each phase) are also assumed. This is usually valid for transmission lines, where loads on all three phases are maintained in balance during operation. Induced image currents in the earth are usually ignored for calculations of magnetic field under or near the right-of-way. The resulting error is negligible. Only at distances greater than 300 ft. (91 m) from a line do such contributions become significant[11]. The clearance for magnetic-field calculations for the proposed line was the same as that used for electric-field evaluations.

Standard techniques for measuring magnetic fields near transmission lines are described in ANSI IEEE Standard No. 644-1994[13]. Measured magnetic fields agree well with calculated values, provided the currents and line heights that go into the calculation correspond to the actual values for the line. To realize such agreement, it is necessary to get accurate current readings during field measurements (because currents on transmission lines can vary considerably over short periods of time) and also to account for all field sources in the vicinity of the measurements.

As with electric fields, the maximum or peak magnetic fields occur in areas near the centerline and at misspent where the conductors are the lowest. The magnetic field at the edge of the right-of-way is not very dependent on line height. For a double-circuit line or if more than one line is present, the peak field will depend on the relative electrical phasing of the conductors and the direction of power flow.

3.2 Types of Overhead transmission line conductor:

In early days copper Cu conductors was used for transmitting energy in stranded hard drawn form to increase tensile strength. But now it has been replaced by aluminum 'Al' due to following reasons:

1. It has lesser cost than copper.
2. It offers larger diameter for same amount of current which reduces corona.

Corona is ionization of air due to higher voltage (usually voltage above critical voltage which causes violet light around the conductor and hissing sound. It also produces ozone gas therefore it is undesirable condition).

Aluminum also has some disadvantages over copper i.e.

1. It has lesser conductivity.
2. It has larger diameter which increase surface area to air pressure thus it swings more in air than copper so larger cross arms required which increases the cost.
3. It has lesser tensile strength ultimately larger sag.
4. It has lesser specific gravity (2.71gm/cc) than copper (8.9gm/cc).

Due to lower tensile strength aluminum is used with some other materials or its alloys[14].

TAB.3.1 Resistivity and Temperature Coefficient of Some Conductors [14]

Material	Resistivity at 20°C (Ω-m)	Temperature Coefficient (°C)
Silver	1.59×10^{-8}	243.0
Annealed copper	1.72×10^{-8}	234.5
Hard-drawn copper	1.77×10^{-8}	241.5
Aluminum	2.83×10^{-8}	228.1

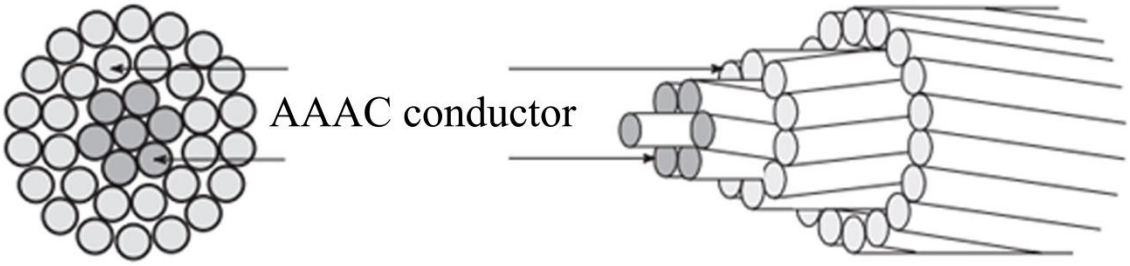

Fig (3.2) AAAC (All Aluminum Alloy Conductor)[14]

I - It has same construction as AAC except the alloy.

II -Its strength is equal to ACSR but due to absence of steel is light in weight.

III - The presence of formation of alloy makes it expensive.

IV - Due to stronger tensile strength than AAC, it is used for longer spans.

V -It can be used in distribution level, i.e. river crossing.

VI - It has lesser sag than AAC.

VII - The difference between ACSR and AAAC is the weight. Being lighter in weight, it is used in transmission and sub-transmission where lighter support structure is required such as mountains, swamps etc .[15] Fig (3.2).

3.3 Types of transmission lines:

Based on number of phases (R.Y.B) used:

1. Sigel circuit transmission lines.
2. Double circuit transmission lines.
3. Multi circuit.

3.3.1 Single Circuit Transmission Lines

These type of Transmission lines have only one set of RYB. These are used shorter distance Transmission because of the following reasons:

1. These transmit less power when compared to other types of transmission lines.

2. This type is not suitable for long distance transmission because if the load increases then a transmission line parallel to this has to be constructed which increases the cost of construction.

In single circuit transmission line system, electrical power is transmitted over a group of conductors constituting the 3-phase sequence of the total or part of the power generated. Each group of conductors may be made up of a single conductor or more bundled conductors arranged in a technical way. Two, three, and four bundled conductor per phase are widely used in one way or another as shown in fig (3.3). In the case of single circuit transmission line systems, the phases are usually configured horizontally or in a triangular configuration. The supporting tower is usually designed with a configuration convenient to support the conductors. More flexibility and space are available on the tower in the case of single circuit to construct the best configuration. Anther wire, sometimes two, is used for earthling with the single circuit transmission system. A single circuit transmission line system is usually used in case of extra high voltages where large insulation spacing between phases is required as well between conductors and the support structures.

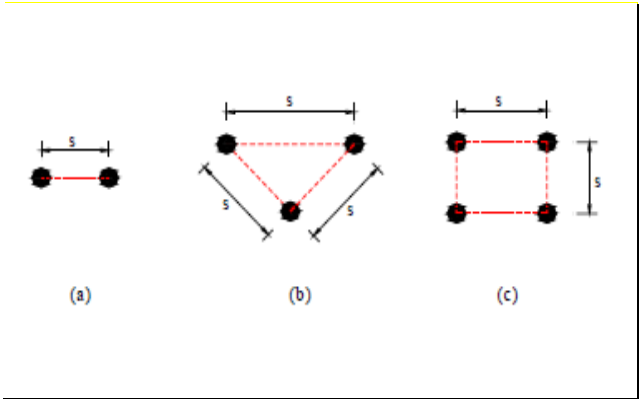

Fig (3.3): Bundled conductors, (a) two bundled conductors, (b) three bundled conductors, (c) Four bundled conductors. [16]

A 400kV single circuit 3-phase typical line configuration constructed in Libya is shown in Fig (3-4), with the phasing arrangement confirmed from the substation side.[16]

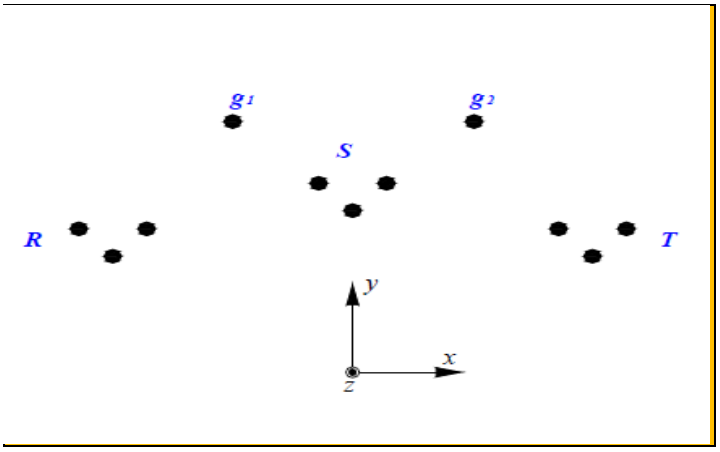

Fig (3.4): Typical 400kv single circuit line configuration using bundled conductors and two earth wires (cross-sectional view).[16]

3.3.2 Double Circuit 3-Phase Transmission Lines

These types of transmission lines have two sets of RST for more power transmission, The following are the advantages of double circuit transmission lines,

1. These carry twice the amount of power than the single circuit transmission lines.
2. The constriction cost is reduced when compared to the single circuit transmission lines.
3. The right of way is reduced when compared to the single circuit transmission.

For larger amounts of power or in case of a part load centers, double circuits can be used to transmit power instead of single circuit system. Two single circuits on each side of a transmission tower can be supported with enough spacing between them. A common ear thing wire can be used for protection. The two single circuits supported by the single tower are called double circuits. The two circuits may supply the same load center or at some point they may separate to supply different load

center. The line configuration of the two circuits is usually vertical on either tower sides.

A 400kV typical line configuration for double circuit system is shown in Fig (3.5) [16].

The magnetic field analysis will be discussed later for the single and double circuits described above.

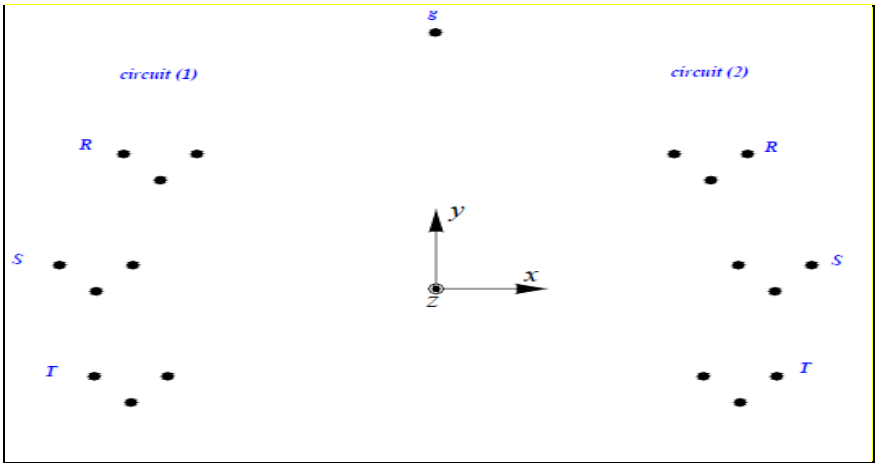

Fig (3.5): Typical 400kv double circuit line configuration using triangular bundled conductors and single earth wire (cross-sectional).[16]

3.3.3 Multi-Circuits 3-Phase Transmission Lines:

These type transmission lines have more than 2sets of RST. These are helpful at the generation and where large amounts of power has to distributed between substations for the power distribution to the end consumer.

When compared to other types of transmission lines the following are a drainages of the lines:

1. The construction cost is greatly reduced.
2. The power transmitted is more also reliable.
3. Row decreases.

In multi-circuit systems, the span is constituted from more than two circuits that may be charged with the same voltage or may have different voltages. The line configuration of these circuits and the spacing between them is a design issue that has to take into consideration the line voltages

and the maximum load for each circuit. No such system exists in Libya.[16]

3.4 Transmission line Models:

3.4.1 The Short Transmission Line:

The equivalent circuit of a short transmission line is shown in Fig.(3.6), w here Is and I_R are the sending- and receiving-end currents, respectively, and V_S and V_R are the sending- and receiving-end line-to-neutral voltages. The circuit is solved as a simple series ac circuit. So,

$$I_S=I_R \tag{3.1}$$

$$V_S=V_R+I_RZ \tag{3.2}$$

where Z is zl, the total series impedance of the line .The effect of the variation of t h e power factor of t h e load on t h e voltage regulation of a line is most easily understood for the short line and therefore will be considered at this time. Voltage regulation of a transmission line is the rise in voltage at the receiving end, expressed in percent of full-load voltage, when full load at a specified power factor is removed while the sending-end

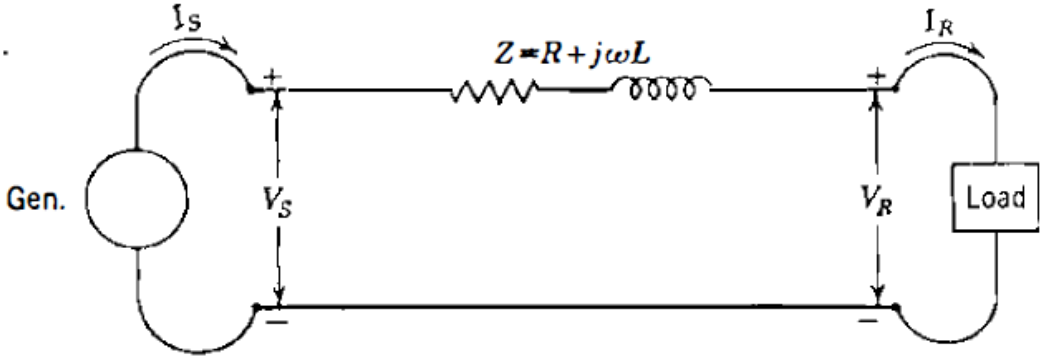

Fig (3.6) Equivalent circuit of a short transmission line where the resistance R and inductance L are values for the entire length of the line [16]

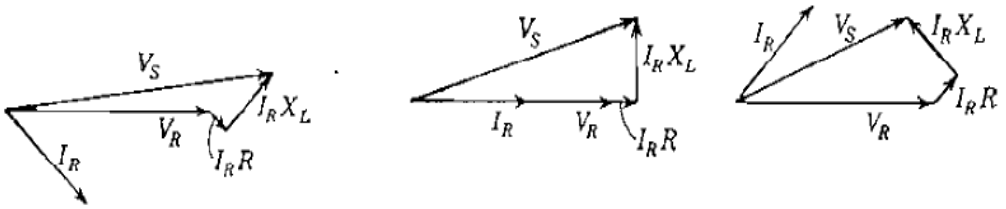

(a) Load p. f. = 70 % lag **(b) Load p. f. = 100 %** **(c) Load p. f. =70 %lead**

Fig (3.7) Phasor diagrams of a short transmission line . All diagrams are drawn for the same magnitudes of I_R and V_R ' [16]

$$\text{Percent regulation} = \frac{(|V_{R.NL}| - |V_{R.FL}|)}{|V_{R.FL}|} \times 100 \qquad (3.3)$$

where $|V_{R.NL}|$ is the magnitude of receiving-end voltage at no load and $|V_{R.FL}|$ is the magnitude of receiving-end voltage at full load with $|V_S|$ constant . After the load on a short transmission line , represented by the circuit of Fig.(3.6), is removed, the voltage a t the receiving end is equal to the voltage at the sending end . In Fig.(3.6), with the load connected , the receiving-end voltage is designated by VR , and $|VR| = |VR_{FL}|$. The sending-end voltage is Vs ; and $|Vs| = |VR._{NL}|$. The phasor diagrams of Fig. (3.7) are drawn for the same magnitudes of the receiving end voltage and current and s how that a larger value of the sending-end voltage is required to maintain a given receiving-end voltage when the receiving-end current is lagging the voltage than when the same current and voltage are in phase. A still smaller sending-end voltage is required to maintain the given receiving-end voltage when the receiving-end current leads the voltage. The voltage drop is the same in the series impedance of the line in all cases; because of the different power factors, however, the voltage drop is added to the receiving - end volt ilgeilt different angle in each case . The regulation is greatest for R lagging power factors a n d least, or even negative, R or leading power factors .The inductive reactance of transmission line is larger than the resistance, and the principle of

regulation illustrated in Fig (3.7) is true for any load supplied by a predominantly inductive circuit . The magnitudes of the voltage drops I_R R and I_R X_L for a short line have been exaggerated with respect to V_R in drawing the phasor diagrams in order to illustrate the point more clearly. The relation between power factor and regulation for longer lines is similar to that for short lines but is not visualized so easily[16].

3.4.2 The Medium Transmission line:

The shunt admittance, usually pure capacitance, is included in the calculations for a line of medium length. If the total shunt admittance of the line is divided into two equal parts placed at the sending and receiving ends of the line, the circuit is called a nominal . it refers to Fig(3.8) to derive equations. To Obtain an ' expression for Vs we note that the current in the capacitance at the.

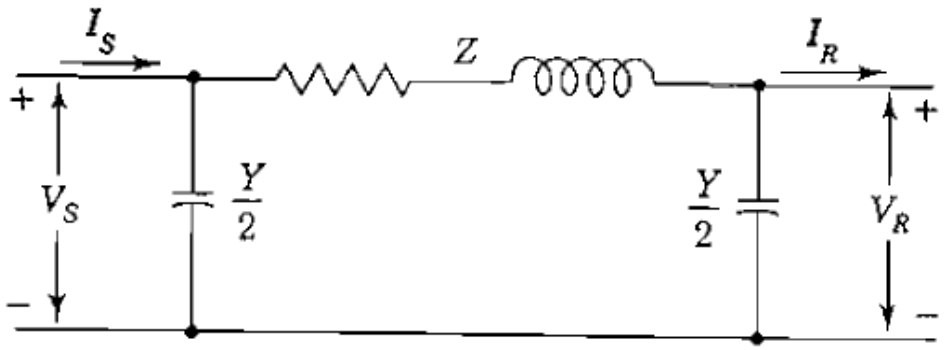

Fig (3.8) Nominal π circuit of a medium-length transmission line.[16]

receiving end is V_R Y/2 and the current in the series arm is I_R + V_RY/2. Then.

$$V_S=(V_R \frac{Y}{2}+I_R)Z+V_R \quad (3.4)$$

$$V_S=(\frac{ZY}{2}+1)V_R+ ZI_R \quad (3.5)$$

To derive Is , we note that the current in the shunt capacitance a t the

sending end is Vs Y / 2 , which added to the current in the series arm gives.

$$I_S=V_S\frac{Y}{2}+V_R\frac{Y}{2}+I_R \tag{3.6}$$

Substituting Vs , as given by Eq. (3.5), in Eq . (3.6) yields

$$I_s = V_R Y\left(1+\frac{ZY}{4}\right)+\left(\frac{ZY}{2}+1\right)I_R \tag{3.7}$$

Equations (3.5) and (3.7) may be expressed in the general form

$$V_S=AV_R+BI_R \tag{3.8}$$

$$I_S=CV_R+DI_R \tag{3.9}$$

Where

$$A=D=\frac{ZY}{2}+1$$

$$B=Z \qquad C=Y\left(1+\frac{ZY}{4}\right) \tag{3.10}$$

These ABCD constants are sometimes called the generalized circuit constants of the transmission line . In general, they are complex numbers. A and D are dimensionless and equal each other if the line is the same when viewed from either end. The dimensions of B and C are ohms and mhos or Siemens, respectively. The constants apply to any linear, passive, and bilateral four- terminal network having two pairs of terminals. Such a network is called a two-port network .A physical meaning is easily assigned to the constants. By letting $I_R<$ be zero in Eq. (3.8), we see that A is the ratio V_S/ V_R at no load . Similarly, B is the ratio Vs $/I_R$ when the receiving end is short-circuited. The constant A is useful in computing regulation. If $V_{R,FL}$ is the receiving-end voltage at full load for a sending-end voltage of V_S., Eq. (3.3) becomes[16].

$$\text{Percent regulation}=\frac{|V_S|/|A|-|V_{R,FL}|}{|V_{R,FL}|}\times 100 \tag{3.11}$$

3.4.3 The Long Transmission Line:

The exact solution of any transmission line and the one required for a high degree of accuracy in calculating 60-H z lines more than approximately (150 mi) long must consider the fact that the parameters of the lines are not lumped but, rather, are distributed uniformly throughout the length of the line. Lumped parameters are not shown because we are ready to consider the solution of the line with the impedance and admittance uniformly distributed .In Fig(3.9) we consider a differential element of length dx in the line at a distance x from the receiving end of the line. Then $z\,dx$ and ydx are, respectively, the series impedance and shunt admittance of the elemental section . V and I are phases which vary with x .Fig(3.8) show the Schematic diagram of a transmission line[16].

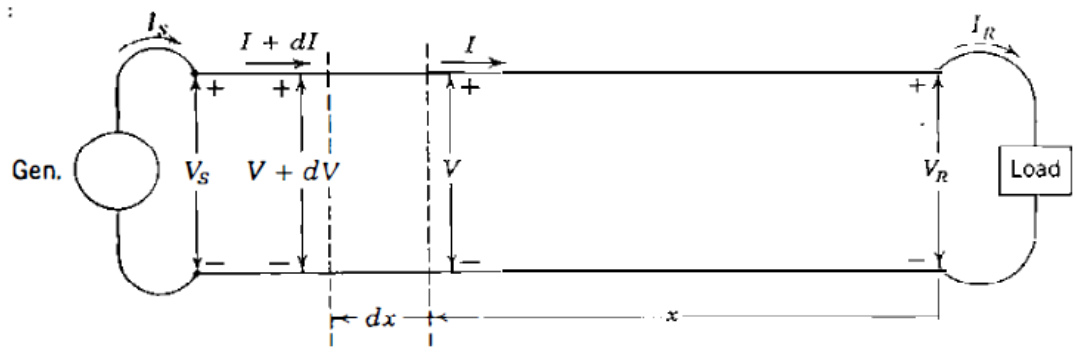

Fig (3.9) Schematic diagram of a transmission line showing one phase and the neutral return. Nomenclature for the line and the elemental length are indicated[16]

Average line current in the element is (I + I + dI) /2, and the increase of V in the distance dx is quite accurately expressed as

$$dV = \frac{I+I+dI}{2} + zdx = Iz\,dx \qquad (3.12)$$

when products of the differential quantities are neglected. Similarly,

$$dI = \frac{V+V+dV}{2} ydx = Vdx \tag{3.13}$$

Then , from Eqs . (3.12) and (3.13) we have

$$\frac{dv}{dx} = Iz \tag{3.14}$$

and

$$\frac{dI}{dx} = Vy \tag{3.15}$$

Let us differentiate Eqs. (3.14) and (3.15) with respect to x , and we obtain

$$\frac{d^2V}{dx^2} = z\frac{dI}{dx} \tag{3.16}$$

and

$$\frac{d^2I}{dx^2} = y\frac{dV}{dx} \tag{3.17}$$

If we substitute the values of $^{dy}/_{dx}$ and d $^{V}/_{dx}$ from Eqs. (3.15) and (3.14) in Eqs . (3.16) and (3.17), respectively, we obtain

$$\frac{d^2V}{dx^2} = yzV \tag{3.18}$$

And

$$\frac{d^2I}{dx^2} = yzI \tag{3.19}$$

Now we have Eq . (3.18) in which the only variables are V and x and Eq. (3.19) in which the only variables are I and x . The solutions of those equations for V and I, respectively, must be expressions which when differentiated twice with respect to x yield the original expression times the constant y z . For instance ,the solution for V when differentiated twice with respect to x must yield yzV This suggests an exponential form of solution . Assume t hat the solution of Eq.(3.18) is

$$V = A_1 \in^{\sqrt{yzx}} + A_2 \in^{-\sqrt{yzx}} \tag{3.20}$$

$$\frac{d^2V}{dx^2} = yz\left[A_1 \in^{\sqrt{yzx}} + A_2 \in^{-\sqrt{YZX}}\right] \tag{3.21}$$

which is yz times the assumed solution for V. Therefore, Eq. (3.20) is the solution of Eq. (3.18) .when we substitute the value given by Eq. (3.20) for V in Eq. (3.14), we obtain

$$I = \frac{1}{\sqrt{z/y}} A_1 \in^{\sqrt{yzx}} - \frac{1}{\sqrt{z/y}} A_2 \in^{-\sqrt{YZX}} \tag{3.22}$$

The constants A_1 and A_2 can be evaluated by using the conditions at the receiving end of the line; namely, when x = 0 , V = V_R and I = I_R' Substitution of these values in Eqs. (3.20) and (3.22) yields

$$V_R = A_1 + A_2 \quad \text{and} \quad I_R = \frac{1}{\sqrt{z/y}}(A_1 - A_2)$$

Substituting $Z_C = \sqrt{z/y}$ and solving for A_1give

$$V = \frac{V_R + I_R Z_C}{2} \in^{yx} + \frac{V_R - I_R Z_C}{2} \in^{-yx} \tag{3.23}$$

$$I = \frac{V_R/Z_C + I_R}{2} \in^{yx} - \frac{V_R/Z_C - I_R}{2} \in^{-yx} \tag{3.24}$$

where $Z_C = \sqrt{z/y}$ and is called the characteristic impedance of the line, and $y = \sqrt{z/y}$ and is called the propagation constant Equations (3.23)

and (3.24) give the rms values of V and I and their Phase angles at any specified point along the line in terms of the distance x from the receiving end to the specified point , provided V_R,I_R and the parameters of the line are known[16].

3.4.4 Hyperbolic Form Of The Equation:

The incident and reflected waves of voltage are seldom found when calculating the voltage of a power line. The reason for discussing the voltage and the current of a line in terms of the incident and reflected components is that such an analysis is helpful in obtaining a better understanding of some of the phenomena of transmission lines . A more convenient form of the equations for computing current and voltage of, power line is found by in traducing hyperbolic functions. Hyperbolic functions are defined in exponential form[16]:

$$\sinh\theta = \frac{\varepsilon^{\theta} - \varepsilon^{-\theta}}{2} \tag{3.31}$$

$$\cosh\theta = \frac{\varepsilon^{\theta} - \varepsilon^{-\theta}}{2} \tag{3.32}$$

By rearranging Eqs. (3.23) and (3.24) and substituting hyperbolic functions for the exponential terms, we find a new set of equations. The new equations, giving voltage and current anywhere along the line, are

$$V = \mathrm{V_R}\cosh yx + I_R Z_C \sinh yx \tag{3.33}$$

$$I = \mathrm{I_R}\cosh yx + \frac{V_R}{Z_C}\sinh yx \tag{3.34}$$

Letting x = / to obtain the voltage and the current It the sending end , we have

$$V_S = \mathrm{V_R}\cosh yl + I_R Z_C \sinh yl \tag{3.35}$$

$$I_S = \mathrm{I_R}\cosh yl + \frac{V_R}{Z_C}\sinh yl \tag{3.36}$$

From examination of these equations we see that the generalized circuit constants for a long line are

$$A = \cosh yl \qquad c = \frac{\sinh yl}{Z_C} \tag{3.37}$$

$$B = Z_C \sinh yl \qquad D = \cosh yl$$

Solving Eqs. (3.35) and (3.36) for V_R and I_R in terms of V_S and I_S, we obtain

$$V_R = V_S \cosh yl + I_S Z_C \sinh yl \tag{3.38}$$

$$I_R = I_S \cosh yl + \frac{V_S}{Z_C} \sinh yl \tag{3.39}$$

For balanced three-phase lines the currents in the above equations are line currents and the voltages are line-to- neutral voltages, that is, line voltages divided by 13 . In order to solve the equations, the hyperbolic functions must be evaluated. Since "II is usually complex , the hyperbolic functions are also complex and can be evaluated with the assistance of a calculator or computer. For solving an occasional problem without resorting to a computer there are several choices. The following equations give the expansions of hyperbolic sins and cosines of complex arguments in terms of circular and hyperbolic functions of real arguments[16]:

$$\cosh(\alpha l + j\beta l) = \cosh \alpha l \cos \beta l + j \sinh \alpha l \sin \beta l \tag{3.40}$$

$$\sinh(\alpha l + j\beta l) = \sinh \alpha l \cos \beta l + j \cosh \alpha l \sin \beta l \tag{3.41}$$

Equations (3.40) and (3.41) make possible the computation of hyperbolic functions of complex arguments. The correct mathematical unit for βl is the radian, and the radian is the unit found for βl by computing the quad rapture component of "yl. Equations (3.40) and (3.41) can be verified by substituting in t hem the exponential forms o f t

h e hyperbolic functions and the similar exponential forms of the circular functions. Another method of evaluating complex hyperbolic functions is suggested by Eqs . (3.31) and (3.32). Substituting a + j{3 for $\alpha + j\beta$ forθ, we obtain :

$$\cosh(\alpha + j\beta) = \frac{\varepsilon^{\alpha}\varepsilon^{j\beta} + \varepsilon^{-\alpha}\varepsilon^{-j\beta}}{2} = \frac{1}{2}\left(\varepsilon^{\alpha}\angle\beta + \varepsilon^{-\alpha}\angle -\beta\right) \quad (3.42)$$

$$\text{sinsh}(\alpha + \text{j}\beta) = \frac{\varepsilon^{\alpha}\varepsilon^{\text{j}\beta} - \varepsilon^{-\alpha}\varepsilon^{-\text{j}\beta}}{2} = \frac{1}{2}(\varepsilon^{\alpha}\angle\beta - \varepsilon^{-\alpha}\angle -\beta) \quad (3.43)$$

3.4.5 The Equivalent Circuit Of a Long Line:

The nominal-π circuit does not represent a transmission line exactly because it does not account for the parameters of the line being uniformly distributed. The discrepancy between the nominal π and the actual line becomes larger as the length of line increases. It is possible, however, to find the equivalent circuit of along transmission line and to represent the line accurately, in so far as measurements at the ends of the line are concerned, by a network of lumped parameters .Let us assume that a π circuit similar to that of Fig (3.9) is the equivalent circuit of a long line, but let us call the series arm of our equivalent-π circuit z'and the shunt arms $Y/2$ to distinguish them from the arms of the nominal-πcircuit. Equation (3.5) gives the sending-end voltage of a symmetrical -π circuit in terms of its series and shunt arms and the voltage and current at the receiving end . By substituting Z' and $Y/2$ for Z and $Y/2$ in Eq. (3.5), we obtain the sending-end voltage of our equivalent circuit in terms of its series and shunt.

arms and the voltage and current at t h e receiving end:

$$\text{V}_\text{S} = \left(\frac{\text{Z}'\text{Y}'}{2} + 1\right)\text{V}_\text{R} + \text{Z}'\text{I}_\text{R} \quad (3.44)$$

For our circuit to be equivalent to the long transmission line the coefficients of V_R and I_R in Eq . (3.44) must be identical, respectively, to

the coefficients of V_R and I_R in Eq. (3.35). Equating the coefficients of I_R in the two equations yields

$$Z' = Z_C \sinh yl \tag{3.45}$$

$$Z' = \sqrt{\frac{Z}{Y}} \sinh yl = zl \frac{\sinh yl}{\sqrt{zy}\, l}$$

$$Z' = Z \frac{\sinh yl}{yl} \tag{3.46}$$

where Z is equal to zl, the total series impedance of the line. The term$(\sinh yl)/yl$ is t he factor by which the series impedance of the nominal π must be multiplied to convert the nominal π to the equivalent π . For small values of yl, both $\sinh yl$ and yl are almost identical, and this fact shows that the nominal π represents the medium-length transmission line quite accurately ,insofar as the series arm is concerned .To investigate the shunt arms of the equivalent-π" circuit, we equate the coefficients of V_R in Eqs. (3.35) and (3.44) and obtain

$$\frac{Z'Y'}{2} + 1 = \cosh yl \tag{3.47}$$

Substituting $Z_C \sinh yl$ for Z' gives

$$\frac{Y' Z_C \sinh yl}{2} + 1 = \cosh yl \tag{3.48}$$

$$\frac{Y'}{2} = \frac{1}{Z_C} \frac{\cosh yl - 1}{\sinh yl} \tag{3.49}$$

Another form of the expression for the shunt admittance of the Equivalent circuit can be found by substituting in Eq. (3.49) the identity

$$\tanh \frac{yl}{2} = \frac{\cosh yl - 1}{\sinh yl} \tag{3.50}$$

The identity can be verified by substituting the exponential forms of, Eqs. (3.31)

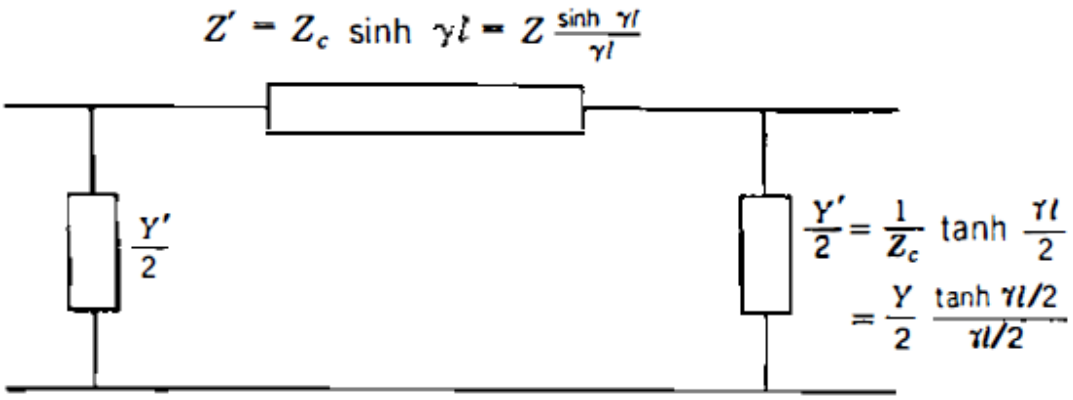

Fig (3.10) Equivalent -π circuit of a transmission line.[16]

and (3.32) for the hyperbolic functions and by recalling that $\tanh\theta = \sinh\theta / \cosh\theta$. Now

$$\frac{Y'}{2} = \frac{1}{Z_C} \tanh \frac{y}{l} \tag{3.51}$$

$$\frac{Y'}{2} = \frac{Y}{2} \frac{\tanh(yl/2)}{yl/2} \tag{3.52}$$

where Y is equal to yl, the total shunt admittance of the line. Equation (3.52) shows the correction factor used to convert the admittance of the shunt arms of the nominal $\pi$to that of the equivalent π Since $\tanh(yl/2)$ and $yl/2$ are very nearly equal for small values of yl, the nominal π represents the medium-length transmission line quite accurately, for we have seen previously that the correction factor for the series arm is negligible for medium-length lines. The equivalent -π circuit is shown in Fig (3. 10). An equivalent-T circuit can also be found for a transmission line[16].

Chapter Four

Experiment with the use of nuclear impact detectors (CR-39) in radiometric measurements and Experiment of Electromagnetic Field

4.1- Introduction

God almighty created the universe of which we live, from materials such as water, air, sand, iron and wood. The material in this universe is in the form of separate elements or compounds of these elements or in the form of mixtures of several materials. The element is the primary image and cannot be transformed into a simpler one by chemical methods. All the materials in this universe are composed of ninety-two natural elements such as hydrogen, oxygen, iron, gold and others. Several dozen other elements can also be produced by industrial methods, such as plutonium, which is critical in 4185 nuclear weapons and some reactors[17]. The purpose of this preliminary study is to measure the concentration of radioactive radon in the soil surrounding high-voltage trans mission lines wires and faraway of high-voltage and to draw a preliminary the distribution of radon concentration.

4.2 Radon sources:

The main sources of radon are soil, rock, water, and building materials. Radon is emitted from these sources to the surrounding environment and mixed with atmospheric air.[18]

4.2.1- Soils and rocks:

The proportion of radon emitted from the top layer of the earth's crust is about 80% of the total radon emitted to the outer medium, so the soil is the main source of radon in the environment. Usually the amount of uranium present somewhere in a millionth of a pound of weight or the specific radioactivity (Specific activity) expressed in pico-curie in one gram of material[19-20].

The relationship between these two formats is (1pCi / g = 1ppm). In general, the rocks in the Earth's crust contain about 1pCi / g, and the

soil is about 0.7pci / g [21]. The presence of uranium-238 and thus radium-226 is the cause of radon emission from soil and rocks. The amount of radium and uranium varies from one place to another according to the geological nature of the place, that is, every dissociation of a radium atom present in the grains of soil or rocks will give an atom of radon, and it is believed that the departure of radon from the soil granule is the result of the reflux that occurs when the radium atom dissolves a massive alpha particle [22]. The amount of radon emitted from the soil depends on the porosity and moisture of the soil. Frequently the place of production of this atom is close to the surface of the soil, the greater the probability of its leakage to the outer medium. Several studies on the effect of humidity on the radon emission rate from the soil showed that the emission rate increases with the increase in humidity up to 18% and then decreases as the humidity increases above this level [23]. Radon enters between the grains of the soil as a result of the reflux of the radon atom resulting from the dissociation of radium. If the medium is dry, then the radon atoms that are rebound may be embedded in the neighboring grains[24].

4.3- Health risks of radon gas:

Exposure to atomic radiation of various levels is undesirable, and the biological effects of radiation when exposed to high doses are well known. The assessment of the health risk posed by exposure to low doses of atomic radiation from radioactive natural isotopes, especially uranium (238U) and thorium (232Th) has become of interest due to the discovery of radon as a possible source of high incidence of lung cancer among miners[25]. The researchers and organizations concerned with health and environmental radiological protection during the last half of the

nineteenth century were interested in studying the concentration of radon in populated places such as homes to know levels of exposure to homes and take preventive measures for general protection[26]. Estimation of the risk of lung cancer due to inhalation of radon and its births is based on a study of the emergence of cancer among uranium miners in Canada and the USA, iron miners in Sweden and uranium miners in Czechoslovakia. Radon was not previously thought to be a health hazard in other places far from mines because of its low concentration, but it was discovered that radon concentrations in some homes vary by at least 100 times depending on their composition and location. That means the possibility of up High concentrations in some dwellings to levels comparable to its concentration in mines have been shown to cause lung cancer [27]. The UK Radiological Protection Agency has estimated that radon causes about 5% -6% of lung cancer deaths in the UK, which is equivalent to about 2,000 deaths a year out of a total of 40,000 cases. In Sweden, which suffers from the problem of high concentrations of radon in its dwellings, 30% of the total annual cancer incidence of 3,000 cases is attributable to exposure to radon, while Sweden's population is only 8.4 million. According to a report by the US Environmental Protection Agency (EPA), about 13,000 to 15,000 deaths a year from lung cancer can be attributed to radon [27], and the agency's own statistics indicate that radon is second only to smoking in the states. At the same time, it is the leading cause of lung cancer for non-smokers. The risk of lung cancer increases for smokers. In several reports published by the National Academy of Sciences of the United States in 1999, research results show that 15,000 to 22,000 people die annually from lung cancer caused by exposure to radon. The report issued by the same authority on assessing radon risk also states that 21,100 people died out of a total of 146,600 cases of lung cancer deaths during 1995, or 14.4% attributable to

exposure to radon at homes See Fig (4.1). These results were based on a radon risk assessment from data obtained from the exposure of miners to radon during their working periods[27].

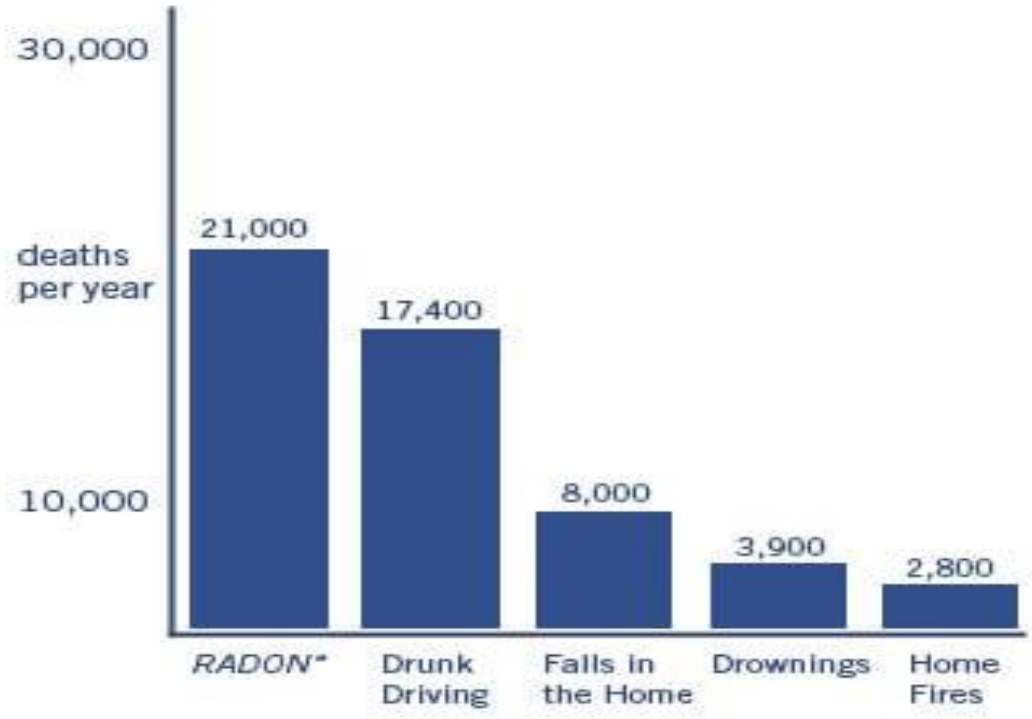

Fig (4.1) Percentage of causes of death in the United States[27]

4.4- Electromagnetic waves and their impact on human and environment:

Aerobic electricity poles pose a threat to people's lives because they carry electromagnetic radiation, cancer, childhood immunity, and environmental pollution. Global and health studies by the British Cancer Research Institute, the American National Cancer Institute and the Karolinsky Institute Al Suwaidi several years ago about the danger of exposure or housing near power lines or power transformers, and studies conducted on this matter that there is a relationship between electromagnetic pollution and the incidence of many children with leukemia and acne of dangerous diseases[28].

The electrical system in any country is a symbol of civilization and a criterion of progress and development in this country, the electrical system is developing and increasing steadily with the increase of population and urban and industrial buildings, and technological development in the world and the spread of various industries and increase population and high standard of living imposed a continuous increase in energy consumption of all Types. It is known that electrical energy is one of the most common and widely used types of energies because of its many advantages such as:

1. Easy to generate and transport in large quantities over long distances with high efficiency and easy distribution.
2. Can be converted into different images of energy in simple and easy ways.
3. High economic feasibility.

The proliferation of generating stations, switching stations and power transmission lines everywhere has led to a large number of studies and research into the potential health damage caused by the electrical system, and the recent advantage of electric power has recently become the subject of considerable controversy after conducting these studies and research that has raised global concern As the electricians responsible for generating, distributing and distributing electrical energy to consumers, researchers should study the harmful effects of using this energy in cooperation with specialists. The other sciences such as medicine, biochemistry and statistics. Electromagnetic energy is produced from natural sources and from many artificial sources in the form of electromagnetic waves. These waves consist of oscillating electrical and magnetic fields, and interact directly with biological systems such as human cells, animals and plants. Therefore, in this work the possible negative effects of using high and high voltage transmission in particular and electric power in general is studied[28].

4.5 Safety and Methods of Dealing with Electromagnetic Radiation

Energy and matter are two different forms of one thing. Material can be converted into energy and energy into matter. Even to a lesser extent than the conversion of energy into matter in the accelerators, although this still exists at the particle level. The transformation of matter into energy and energy into matter is scientifically and practically possible. The matter and energy are coupled, and the occurrence of this shift on a large scale only hinders the difficulty of its occurrence and control under the current scientific and practical conditions and possibilities. Energy at ease calls for tremendous scientific and technical progress.

The science of magnetism arose from the observation that some stones are called Magnetite (Fe3O4) attract iron particles. The word magnetism is derived from the region of Magnesia in Asia Minor where these stones are found. The globe itself is also known as a permanent magnet. In 1820, the scientist Orested noted that if a current passed through a wire, a magnetic effect was created, namely the deviation of a magnetic needle placed next to the wire, that the magnetic field arises from charges in the state of motion (electric current).

The area around a permanent magnet or conductor through which a current passes is known as a magnetic field. A field is a physical effect that takes different values in a vacuum. The basic vector in magnetic effects is called a magnetic induction vector. The magnetic field can be represented by magnetic force lines so that the density of lines per unit area of a space element perpendicular to the direction of the power lines is the magnitude of the magnetic field. The tangent direction of the power line at any point on it is given the direction of the magnetic field at that point[28].

4.6- Electromagnetic radiation:

The reason for the formation of electromagnetic radiation, the fluctuation of the constituent charges of the atom leads to the emission of the electromagnetic spectrum that acts as a spring is the temperature that supplies the charges with energy or any type of excitation such as collisions and others. The wavelength of the electromagnetic radiation depends on the degree of excitation of the charge, and from here we find that the electromagnetic spectrum has a wide range.

Electromagnetic radiation propagates in a vacuum at a constant speed, the speed of light and its value is 3 X 10^8 m / s. These rays travel in a vacuum and transfer energy from the source to the receiver. These rays were discovered in stages where the scientist Hertz (1887 AD) was the first to work in this field and only at that time were radio and visible rays, and then the rest of the electromagnetic spectrum was discovered through physical observations and phenomena. Electromagnetic radiation has a wavelength and frequency that determines its properties. The speed of the electromagnetic radiation is related to the frequency and wavelength by the formula:

$$c = \lambda \times f \ldots\ldots\ldots\ldots\ldots\ldots\ldots\ldots\ldots (4.1)$$

Where:

c-speed electromagnetic radiation (m / s), λ-wavelength (m), f-frequency (Hz).

As shown in Fig (4.2), a blueprint for the entire electromagnetic spectrum is started, starting from radio waves of long wavelength and low frequency, then the microwave ray region, the infrared region, then the visible ray area, then the ultraviolet area, then the X-ray region, then the gamma-ray region. this sequence is depending on the increased frequency of these waves. Each region of the electromagnetic spectrum has

characteristics that distinguish it from each other, and accordingly different applications of these rays have been produced, and for science it is the area of the visible spectrum that God Almighty has given us the ability to see and it is the region to which the retina responds to be able to see the things that have been transformed. It should be noted that electromagnetic radiation has an energy given by equation (4.1). It follows from this that the greater the frequency, the greater the energy[28].

4.6.1- Electromagnetic waves:

Image of energy disturbance in the vacuum in the form of two hesitating fields, one electric field (E) and the other magnetic field (B) in two levels perpendicular to each other as they perpendicular to the direction of wave propagation as shown in Fig (4.2).

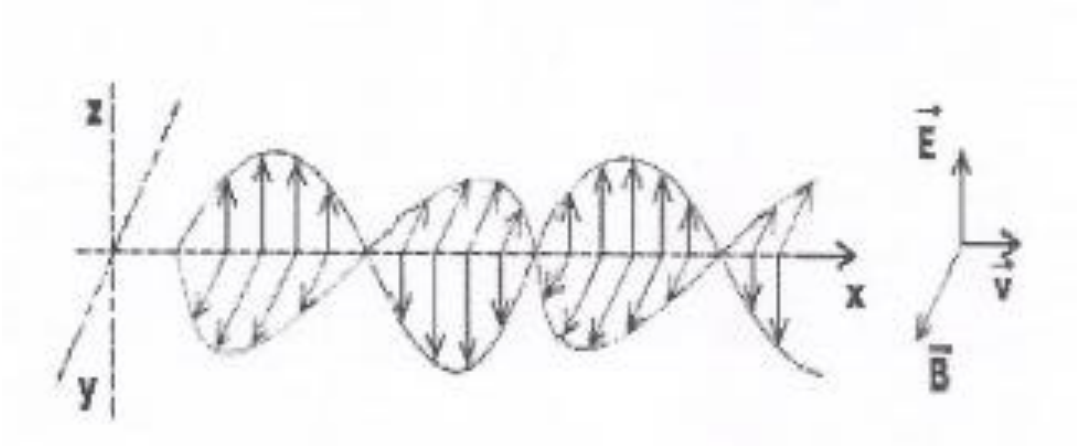

Fig (4.2) The direction of the electric and magnetic field[28].

4.6.2 Electromagnetic wave characteristics

The main characteristics of Electromagnetic waves are:-

1. Spread out in a vacuum at a constant speed equal to $3X10^8$ m / s.
2. Not affected by electric or magnetic fields.
3. It is spread in straight lines and is subject to suggestive properties of diffraction and interference.
4. Polarized cross waves.

4.6.3 Spectrum of electromagnetic waves:

Electromagnetic waves occupy a large area of frequencies and vary and differ from each other in the nature of their source and the method of their discovery and penetration of different media, but they are in agreement with the general characteristics. The spectrum of electromagnetic waves is divided into radio waves, infrared radiation, visible light, ultraviolet rays, X-rays and gamma rays.

4.7- Absorbing electromagnetic radiation in the body:

Studies have shown that the rate of the body's absorption of electromagnetic energy depends to a large extent on the orientation of the largest axis of the human body in relation to the electric field and the rate of absorption reaches its peak when the length of the body is equal to approximately 0.4 of the wavelength and at vibrations of a value ranging from 70-80 MHz when the person is isolated From the ground contact. It has been observed that human contact with the earth under these conditions reduces oscillations to nearly half (35-40 MHz), and this explains the importance of caring for establishing ground connection systems in electrical networks in schools, homes and various work facilities[28].

4.7.1 Health Effects of Electromagnetic Radiation:

• The complaints of exposure to electromagnetic radiation are concentrated in chronic headaches, tension, horror, abnormal agitation, frustration, increased sensitivity to the skin, chest, eye, arthritis, osteoporosis, sexual dysfunction, heart disorders and early aging symptoms.

• Many clinical scientific researchers agree that no confirmed health damage was demonstrated as a result of exposure to electromagnetic radiation at levels less than 0.5 mW / cm^2, but exposure to higher levels

of these radiation and cumulative doses may cause the appearance of many pathological symptoms, including general symptoms and include feelings Fatigue, headache and tension. Organic symptoms appear in the cerebral nervous system and cause lower rates of mental focus, behavioral changes, frustration and a desire to commit suicide, and organic symptoms appear in the visual system, cardiovascular system and immune system.

• Feeling of temporary effects including forgetfulness, inability to concentrate and increase nervous pressure after exposure to electromagnetic radiation levels from 0.01 mW / cm^2 to 10 mW / cm2, and these symptoms are called psychological changes.

• Exposure to electromagnetic radiation at levels starting from 120 mW / cm^2 affects the function of hormonal secretion from the pituitary gland, which may affect the level of sexual fertility. Also exposed to electromagnetic radiation at levels starting at 700 mW / cm^2, sounds can be heard as if they were coming from or near the head.

• Exposure to electromagnetic radiation damages the retina and crystalline lens, and that the high temperature of the lens of the lens to about 41 degrees Celsius, can lead to the emergence of opacities in the lens of the eye (Cataract).

• Although there are insufficient studies on the effect of electromagnetic radiation in metals, it is advised not to be exposed to the levels of impact of these radiation, for patients with bone fractures with slices or nails used in fixing fractures.

• There is increasing concern about the effect of exposure to electromagnetic radiation on the mechanism of nervous stimulation with vivo systems if taking into account the results of scientific research about the effect of radiation emitted by the mobile on the electronic chips that regulate the work of gasoline pump stations counters and the interference it causes in electronic control of the takeoff and landing of aircraft[58].

4.8 Experiment with the use of nuclear impact detectors (CR-39) in radiometric measurements

Plastic reagents played an important role in detecting and measuring ionizing particles for their simplicity, light weight, small size and ease of handling. These reagents have become an excellent means in many scientific fields such as physics, chemistry, biology, space science, medicine, geology and radiation dosimeter. Nuclear impact reagents are insulating materials such as crystal, glass, plastic, etc.

The principle of action of these reagents depends on the fact that when a charged particle passes through the reagent (which is an insulating material such as glass or plastic), there is vandalism along its path. This sabotage is caused by the attenuation of the ionized particle falling by the reagent atoms by giving them their energy. This results in a breakdown of the chemical bonds formed by the reagent's body and its free radicals. The energy threshold required to produce such effects varies from several electron volts to several million electron volts, depending on the type of detector. These effects are very small and can only be seen with an electron microscope. In order to show these effects to be visible to the normal microscope, the reagent must be chemically treated.

4.8.1 Objective of the experiment:

1. Identify plastic reagents in general and CR-39.
2. Learn how to prepare the antimatter and how to show the effects by chemical induction.
3. Identify how to count the effects with a microscope and calculate the intensity of the effects on the detector.
4. Learn how to calculate the yield of these reagents in recording the falling particles perpendicular to the detector.
5. Learn how to measure the range of alpha particles in the air.

4.8.2 Devices used:

1. CR-39 detectors with 1mm thickness.
2. Sources of Americum-241 (Am-241) source of particles with low activity.
3. Package selectors.
4. Sodium hydrate and distilled water.
5. Suitable water and bath.
6. Suspension springs for reagents.
7. Micrometer slide included.
8. Optical microscope.
9. Manual digital counters and timer.

4.9 Chemical Abrasion

The magnification of the effects to be visible under a light microscope depends on the concentration of the solution used to scratch the reagents, temperature and rubbing time. To determine the best time to scratch the plastic reagents (CR-39), the following experiment was conducted:

Cut a slice of CR-39 with a thickness (1mm) into small pieces of equal dimensions about (1.5cm × 1.5cm). The reagents are numbered and washed with distilled water in the ultrasonic bath to be cleaned from the chopping residue and then dried with a soft paper. Display each detector separately for the standard alpha source (Am-241) for one hour. After exposure, the reagents are placed with a chemical abrasion solution and are loaded onto a spiral wire to prevent adhesion to each other when placed inside the solution. A chemical solution of NaOH is used for itching. The solution is placed in a beaker and the beaker is placed in a water bath about a degree (70^{o}C) For a sufficient period of time to make the chemical solution in the flask and the water bath in equilibrium before placing the reagents in the solution. The reagents are placed in the

solution in one vessel. After the first hour of scratching, the first reagent is withdrawn and then after two hours of scratching, the second reagent is withdrawn and thus the reagent is withdrawn whenever an hour has elapsed until five hours. When withdrawing any reagent placed directly in a beaker with water and placed under tap water for an hour until the caustic soda solution is neutralized, the reagents are transferred to a beaker with distilled water and washed using an ultrasonic bath to clean the reagents from any trace of the caustic soda solution, It is then pulled and dried with fine paper and the reagents are ready to count using a 500X magnification light microscope. The numerical density of nuclear effects (density) (Track density) on each detector is counted and plotted as a function of time as shown in Fig (4.3). From the curve we notice that the numerical density increases with increasing abrasion time and then the value of numerical density is confirmed with increasing abrasion time. Usually the time corresponding to the beginning of the numerical density is proven to be the best scratching time, from the figure we note that the best time to show the effect is 3.5 hours.

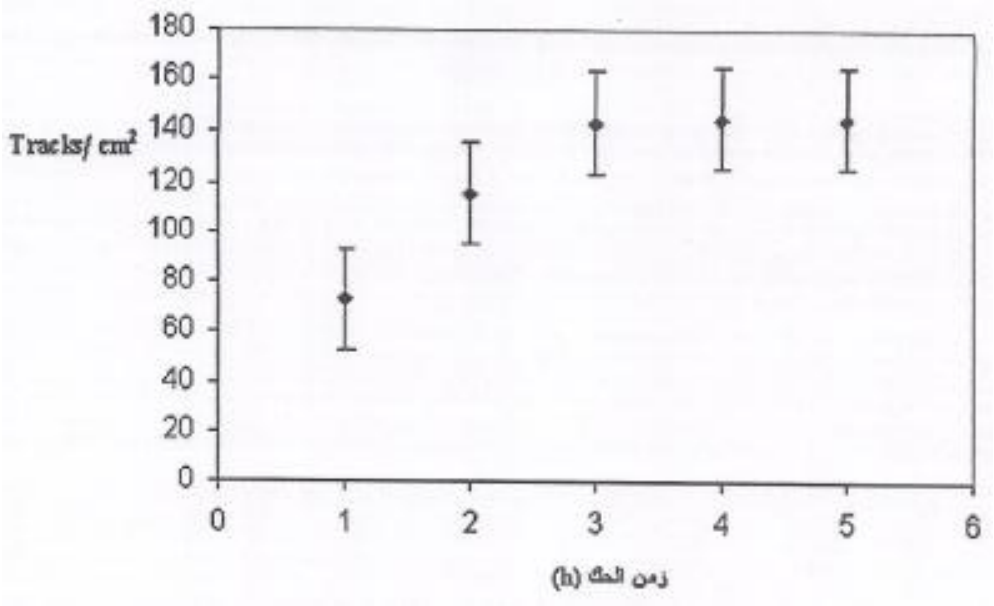

Fig (4.3) The numerical density of alpha particles as a function of chemical abrasion time[28]

4.10 Calculation of the numerical density of the effects of alpha particles:

Griffin optical microscope was used to measure the numerical density of the reagents, and a 10 mm graduated ruler divided into 100 scales, each calibrator (0.1mm), was used to calibrate the field of view and found that the field area using a 40X magnification lens and a 12.5 magnification eye lens X is equal to 0.000625cm2. If we denote the number of alpha traces in the field of vision with the symbol (N) and the number of fields (n) and the area of the field of view (A), the numerical density (ρ) of the alpha effects is calculated from the following relationship:

$$\rho = \frac{\sum_{i=1}^{n} N_i}{nA} \qquad \text{Tracks/cm}^2 \ldots . (4.2)$$

It is usually assumed that the number of effects is subject to the Poisson statistical distribution [29-30] and therefore the standard deviation in numerical density (σ) is calculated from the following relationship[28]:

$$\sigma(\rho) = \frac{\sqrt{\sum_{i=1}^{n} N_i}}{nA} \qquad \text{Tracks/cm}^2 \ldots . (4.3)$$

4.11- Conversion of alpha particle density to radioactivity:

To convert the numerical density (Tracks / cm^2) of alpha particles to radioactivity (Bq/cm^3) requires calibration of doses using a calibration chamber of about $1m^3$ size containing a standard source of radon (226Ra). The doses used in this project have been calibrated by the Libya Atomic Energy Agency's coefficient Fig (4.4).

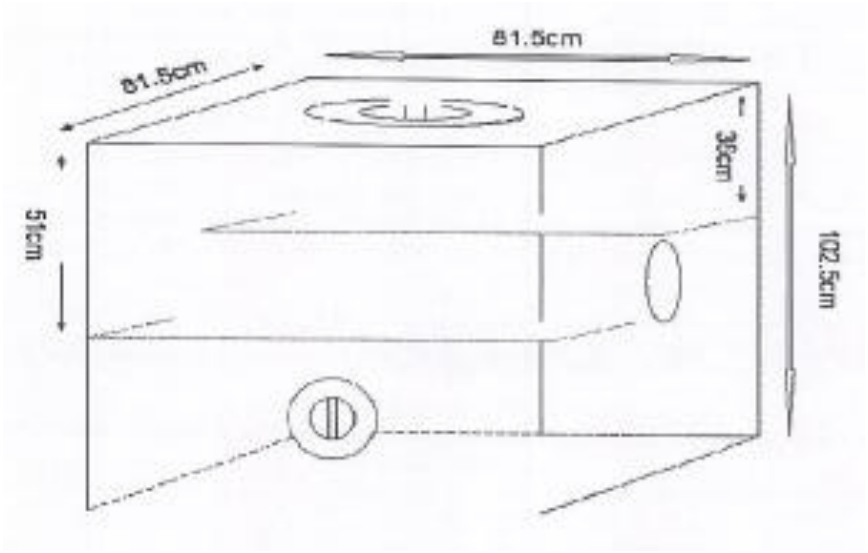

Fig (4.4) Calibration chamber of radon measurements in the study area

Fig (4.5) shows the radon exposure curve of the numerical density of the standard source (ρs) as a function of radon (Es) exposure in Bq / m3, which gives a linear relationship, the slope of the best line passing through the measurement points (k = 0.0024).

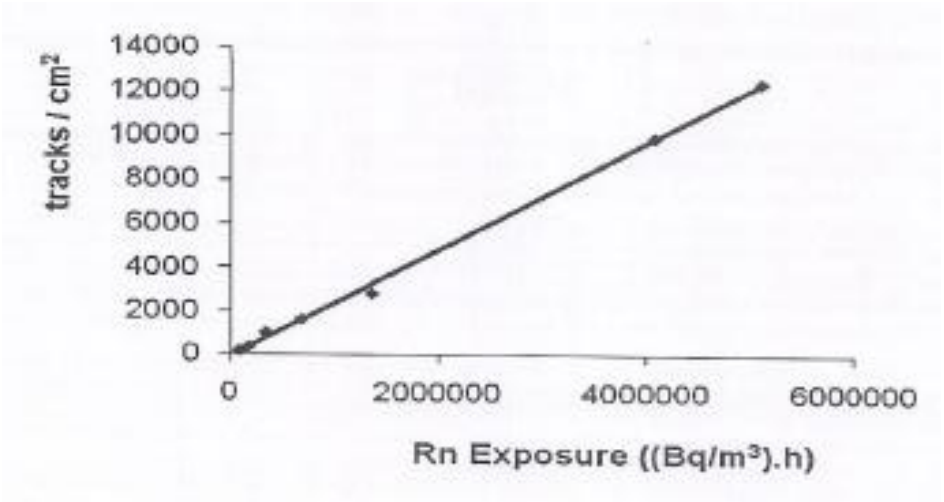

Fig (4.5) Exposure curve for radon

The numerical density of the measurement site can be converted to the equivalent concentration of radon (C) according to the following:

$$k(\text{slope}) = \frac{\Delta\rho_s}{\Delta E_s} \dots\dots\dots\dots\dots\dots\dots\dots\dots (4.4)$$

Thus, the concentration of radon can be calculated from the following relationship:

$$c = \frac{E_s}{t} = \frac{\rho_s}{kt} \quad Bq/m^3 \dots\dots\dots\dots\dots\dots\dots\dots\dots (4.5)$$

Where:

c: concentration of radon in measurement places (Bq/m^3).

t: exposure time of reagents at home (h).

Es: exposure to radon with a calibration curve corresponding to the numerical density value ($Bq/m^3.h$).

4.12 Calculation of the Radiation Background with Reagents Used (CR-39):

The CR-39 strips are kept cooled to 0°C in order to minimize exposure to radon during storage. Perform the required measurements 8 pieces are numbered to calculate the numerical density of the background (4 pieces in each region).

4.13 Radon measurement with high-pressure soil lines (wires):

Radon measurement inside the homes is generally important as a database on the concentration of the largest source that contributes to the natural radiological background to which human and organism are permanently exposed; Oil industries are given special importance in measurements because the phosphate residues are rich in uranium, and the oil extracted from the ground passes through rock layers that may be rich in uranium and therefore rich in radium in addition to the refining processes accompanied by gases It is in the air that may be accompanied by radon resulting from radioactive decay of radium Therefore, the measurements targeted radon gas concentration in two areas: the first area near the high-pressure lines, and the second area far or free of high-pressure lines, where the reagents were distributed to eight sites of the free zone, and four to the area exposed to the lines, after being placed in compartments (doses), The compartment, as shown in Fig (4.6), consists

of a cylindrical plastic tube on one end with a lid. The detector is attached to the inside of the lid of the tube using adhesive tape on both sides. The lower end of the tube has a clogged opening from the inside with a 0.8μm porous paper filter that allows only radon to enter and does not allow radon births suspended by air or soil. The filter is fixed to the opening of the compartment with a piece of synthetic sponge.

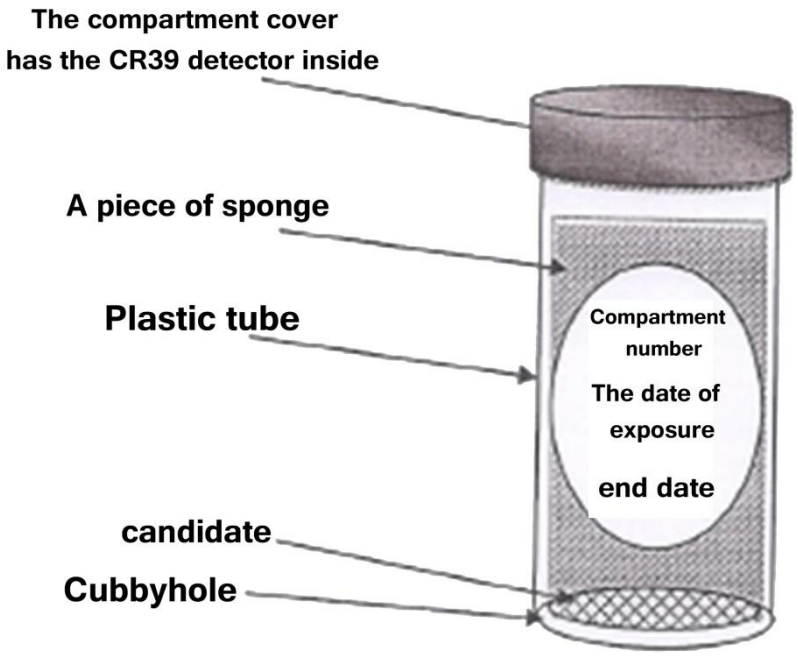

Fig (4.6) Installation of a radon measurement compartment

4.14- Distribution and Collection of Compartments:

The plastic detector (CR-39 type) with a thickness of (1mm) was cut into small pieces each piece with dimensions of about (1.5cm × 1.5cm). Each piece is labeled with a number or mark at the bottom right corner of each detector using a pointed metal tool. Then, the reagents are washed in a water bath (distilled water) using an ultrasonic bath to remove the cutting products from the surface of the reagents and dry with a soft paper. Fix one detector inside the lid of each compartment with adhesive tape on both sides so that the numbered side is exposed. Number the compartment from the outside with a number identical to the detector number. Measurements included the preparation of (16) compartments

and their distribution so that eight doses are placed in both locations. Due to the measurements required by the direct dealings with the population in the region and what may see some interference in their privacy, which requires the preparation of a program to educate and educate the landowners in the study area in order to accept the status of dangers in their land for three months from 22/9/2018 to 7/1/2019. Fig (4.7) shows how to place doses at a depth of one meter below the soil.

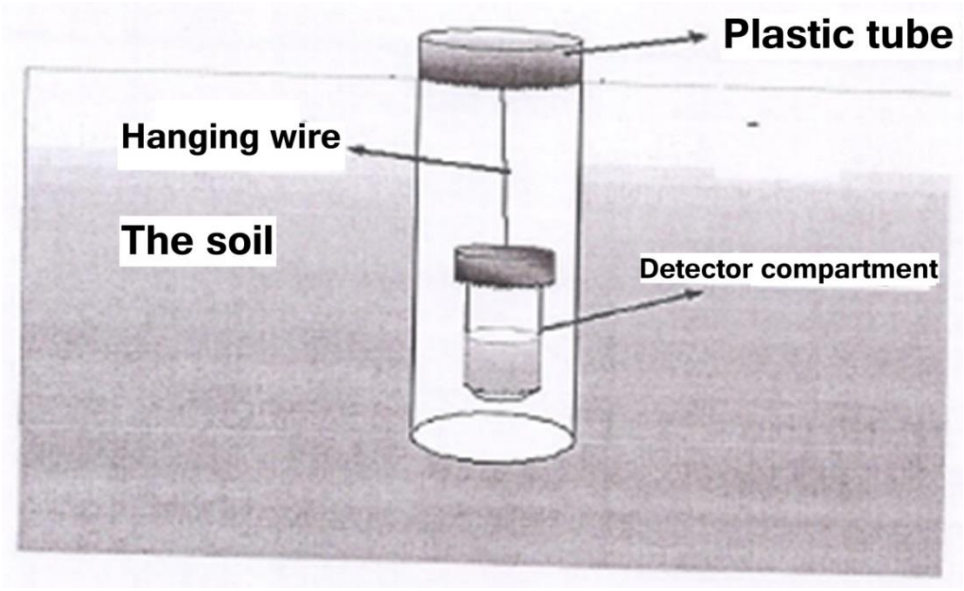

Fig (4.7) Laying the compartment under the soil

After the expiration of the exposure period the compartments were collected and the total compartments retrieved were complete. The reagents collected after exposure are carried on spiral wires and placed with NaOH solution at a concentration of (6N) and at a temperature of (70 C) for three and a half hours to chemically rub the reagents and show the effects of alpha particles resulting from the dissolution of radon and its births inside the doses. After the rubbing period, the reagents are placed in a beaker with water and left under tap water for about 1 hour to ensure that the caustic soda solution is tied. Ready to count and calculate the numerical density of the effects of alpha particles (ρ) using a light microscope at a magnification of 500x.

Table 4.1 Density ρ $(Tracks/cm^2)$ And the concentration of radon $C(Bq/m^3)$ In the soil of high-voltage wires in the study area

σci	Dci	pBg	Σpf	the focus (c)	the college (pf)	σpi	Each detector (σ)	Radiation background (pBg)	Number of relics (t)	Number of fields (n)	Detector number
168.2816886	0.035027154	587.92	1017.74507	4804.320885	29056.5327	830.7557415	30194.29	1137.753	1321	70	13
153.2885382	0.029930964	587.92	927.0609076	5121.403274	30974.247	716.7928571	32112	1137.753	2007	100	31
135.1844187	0.054498194	587.92	817.5878708	2480.530258	15002.247	568.1549085	16140	1137.753	807	80	4
117.3664751	0.081121418	587.92	709.8295052	1446.800099	8750.247	397.7536926	9888	1137.753	618	100	25
				13853.05452	Total						
				3463.263629	Average arithmetic						

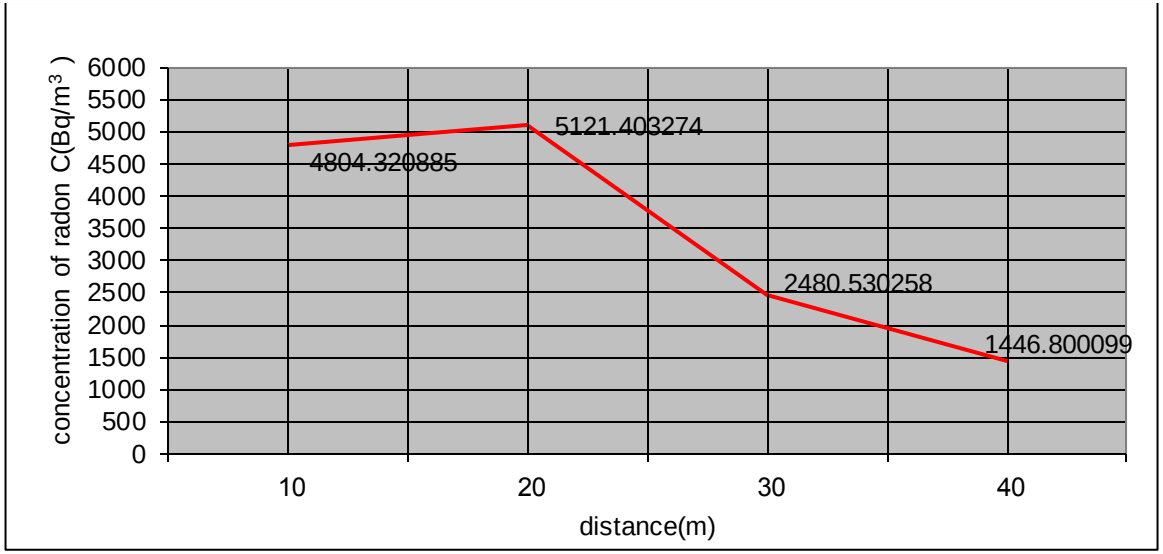

Fig (4.8) Radon concentration and distance in high voltage soil in the study area

Table 4.2 Density ρ ($Tracks/cm^2$) and the concentration of radon C(Bq/m^3) In free soil in the study area

σci	Dci	pBg	σpf	the focus (c)	the college (pf)	σpi	Each detector (σ)	Radiation background (pBg)	Number of relics (t)	Number of fields (n)	Detector number
131.7252049	0.047067376	587.92	796.6642495	2798.651951	16926.247	537.6095237	18064	1137.753	1129	100	21
134.590039	0.04359881	587.92	813.9888982	3087.011739	18670.247	562.9635867	19808	1137.753	1238	100	35
130.658144	0.048520721	587.92	790.2113176	2692.831845	16286.247	528	17424	1137.753	1089	100	7
149.9513427	0.03994784	587.92	906.8902505	3753.678406	22702.247	690.5070601	23840	1137.753	1192	80	47
				12332.17394	Total						
				3083.043485	Average arithmetic						

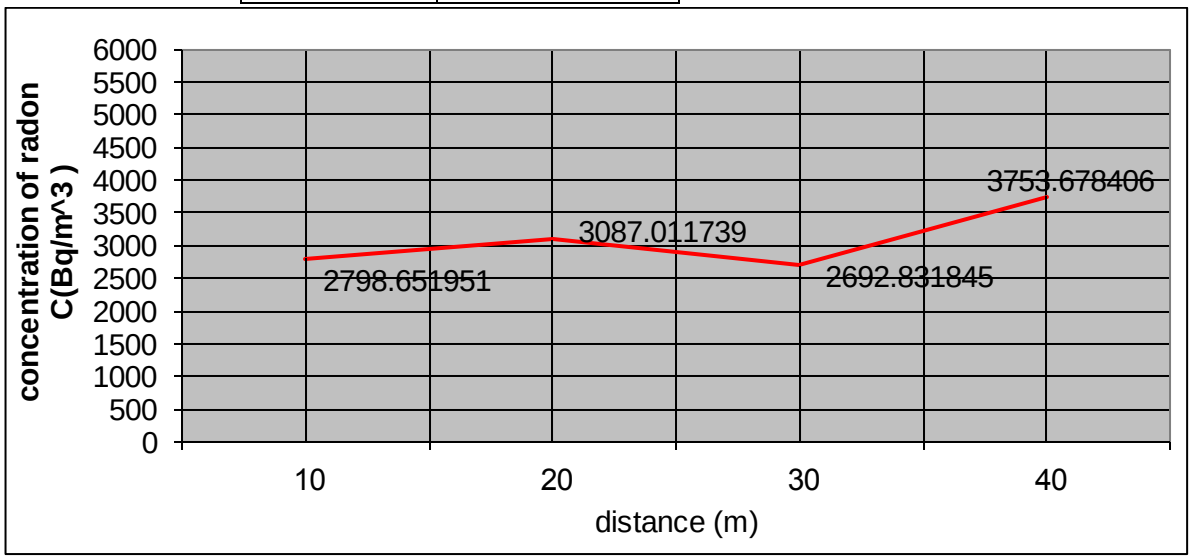

Fig (4.9) Radon concentration and distance in free soil in the study area

Table (4.3) Number of rooms in which measurements were made in the study area and average radon concentration.

Site	Exposure time (month)	Number of compartments	Arithmetic mean of radon concentration (Bq/m3)
1. High voltage lines area.	3.5	4	3463.26
2. Free zone of high voltage lines.	3.5	4	3083.04

Summary the eight reagents were divided into two groups for comparative purposes, and four were used as a radiological background to estimate the statistical confidence level in the data obtained. The CR39 nuclear impact detectors were used in this study and are the first time these detectors have been used in conducting such studies. After etching the reagents using sodium hydroxide solution and reading and recording the results found that the concentration of radon gas is high and poses a risk to public health compared to the results of studies conducted in many countries of the world.

From table it can be seen that the concentration of radon in the first region is approximately (3463.26 Bq/m^3) In the second area about (3083.04 Bq/m^3) The data showed that the radon level in the first region compared to the second zone. As a result, the level of radon concentration and respiration rate in the soil of high-pressure wires is relatively high than the empty soil because of the presence of high-pressure wires and their electromagnetic radiation.

The level of radon concentration and its rate of respiration in field sites (soil free) is low compared to the site (high pressure wires), which indicates a low radon . The concentration of radon gas and its rate of respiration in the soil of high pressure wires is relatively high than the empty soil because of the presence of high pressure wires.

Radon concentration was generally found to be high in both locations.

Human health is very important especially with the development of these days, so there are many studies have been concerned with the negative effects of electric and magnetic fields on humans and animals surrounding the power lines. Many of these studies were computational using programming and few in the field. In these studies there has been considerable debate about the impact of these fields on human health.

The computational study does not simulate the real conditions surrounding the transmission lines of electricity, so a comprehensive field study was required under the high voltage lines to determine the percentage of air pollution by the electric and magnetic fields with their conformity with the World Health Organization.

In this theses presented the possible negative effects of the electrical and magnetic fields under 400 kV transmission line in city of Sabratha were conducted experimentally and compared with computer simulation using Appendix.

4.15- Effect of electromagnetic field on human:

Humans are constantly exposed to many different sources of radiation and the effects that chase him everywhere in the workplace, the street and at home. The most important of these radiations resulting from the lines of the conductor of the electric current, and noted electromagnetic for example during the passage of electricity in a wire, it consists of a magnetic field associated with the electric field consisting of the passage of electrical current in the wires.

Diseases caused by electromagnetic pollution such as brain function disorder, lack of concentration, destruction of the chemical structure of the cells of the body and fetal deformity .

4.16- Standard Guidelines Limits:

There are European Union and International Commission no Non-Ionizing Protection (ICNIRP), standards. In these criteria, the frequencies of different Electromagnetic field have a "reference value". In 1999, the World Health Organization (WHO) set the limit values of electric and magnetic fields for public and occupation area as shown in the Table(4.4).

Table (4.4): Recommendation limits the strength of electric and magnetic fields.

Organization	Public Area		Occupational Area	
	E (kv/m)	$B(\mu T)$	E (kv/m)	$B(\mu T)$
ICNIRP	5	100	10	500
European	5	100	10	500

Note: All values are rms values

Occupational limits of exposure apply to employees and contractors of the business who, by their training or experience, would be aware of possible risks associated with EMF from various sources.

General public limits of exposure apply to all others, such as employees of the business, visitors, etc. who from their backgrounds would be unaware of possible risks associated with EMF from various sources.

The test field was carefully selected so that the ground was flat, as well as weather conditions were taken into account The current passing through the transmission line sat the time of the experiments was recorded by the power plant was 200A, and it will be used for calculation and programming using Appendix.

The electric and magnetic field was measured in several directions at the side and under the 400 kV transmission line in the city of Sabratha. In this study, a type Survey Meter model Model HI-3604 device was used as shown in Fig (4.10). The electrical specifications of device are indicated in Table (4.5). All measurements were done in flat area and at a

height of approximately one meter from the ground. The electric and magnetic field was measured every 10 meters in several directions starting from the center of the tower base.

Direct digital readout of field strength is provided by the instrument with the ability to read the meter remotely via a fiber optic remote control (Model HI-3616) which is available as an option. The HI-3604 finds applications in research and environmental field studies where knowledge of the strength of power frequency fields is required. It is designed to provide engineers, industrial hygienists and health and safety personnel with a sophisticated tool for the accurate investigation of power frequency electrical environments.

Fig (4.10) Electromagnetic meter survey

Table (4.5) Electrical specifications of meter survey[28]

Frequency range(nominal)	30-2000Hz	
Frequency response (typical)	Magnetic Field	Electrical Field
	+0.5,-2.0 dB(30-1000Hz) -2, -6 dB(1000-2000Hz)	+0.5, -2.5 dB(30-2000Hz)
Dynamic range	Electric	Magnetic
	1 V/m -200kV/m	0.2mG-20G
Response	True RMS	
Logging	On-Board, 112 Readings (max)	
Sensitivity	Electric	Magnetic
	1 V/m-199 kV/m	0.1 mG-20 G

4.16.1- Power Frequency Fields:

The HI-3604 finds application in numerous circumstances involving 60-Hz fields. A prime example of the HI-3604's utility is evaluation of electric the high-voltage transmission line (400kv). In this case, the electromagnetic field environment surrounding a typical power transmission line can be visualized through Fig (4.11). This fig illustrates a single-circuit, three phase power line consisting of three separate electrical conductors, each having an impressed voltage which is 120 degrees out of phase with its neighboring conductors. A shield wire may be present above the three phases of the line; this wire, which is grounded, acts as a preferred point for lightning strikes which could, if unprotected, strike the current carrying conductors, potentially damaging and removing the line from service for repairs. A double circuit line would consist of two sets of the three phase conductors[31].

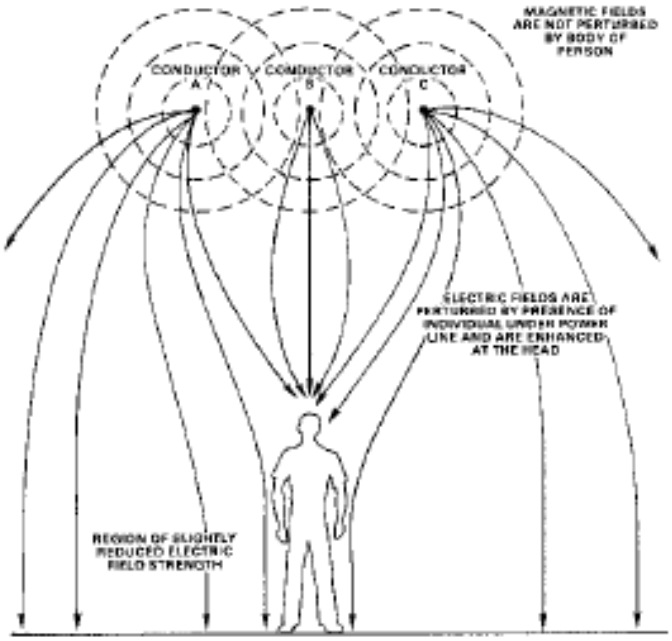

Fig 4.11: Single-circuit, three phase power line consisting of three separate electrical conductors

Fig 4.12 indicates that the maximum electric field strength beneath the 345 kV line is expected to be about 3.4 kV/m. The maximum

magnetic field strength will be dependent on the magnitude of current flowing in the line; Fig 4.12 represents the magnetic fields if the line was carrying a current of 1000 A and indicates a maximum value of 175 mG (equivalent to 14 A/m).

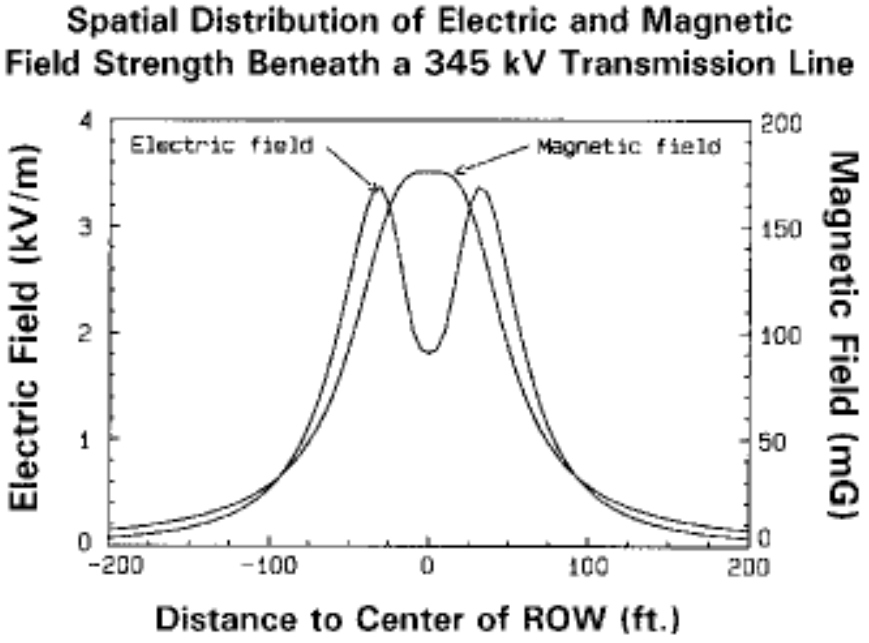

Fig 4.12: Spatial Distribution of Field Strength

4.16.2- Using the HI-3604

4.16.2.1- DIGITAL DISPLAY

The HI-3604 uses a custom LCD to provide information on instrument settings as well as the variables being measured Fig (4.13).

When the meter is turned on, a self-test procedure is automatically performed. As part of this procedure, all segments of the display are lit for about two seconds.

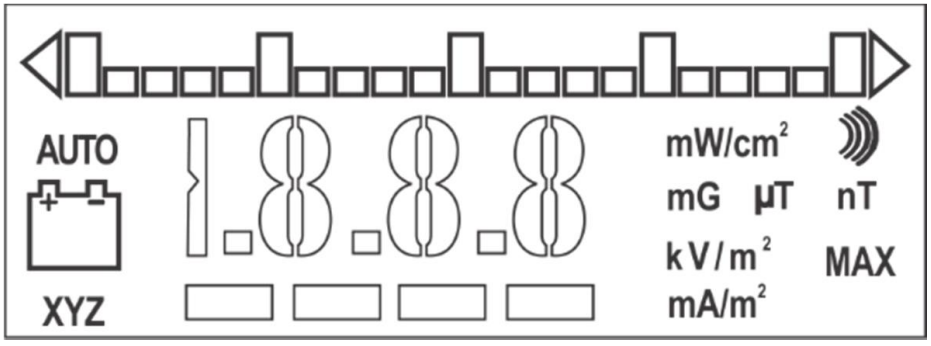

Fig(4.13) HI-3604 Custom LCD.

4.16.2.2- Electric Field/Magnetic Field Mode Selection

The HI-3604 measures both electric (E) and magnetic (H) fields. The unit is switched between the E and H field modes using the membrane switch panel keypads. The units being measured are shown on the LCD display.

Chapter Five

results and discussion

5.1- Results and Simulation:

As mentioned above, the electric and magnetic fields were measured around the tower base of 400 KV in several directions every 10 meters starting from the center of the tower, and the measurements were repeated more than once to take into account any error that may occur during the measurement. The Fig (5.1-5.2) shows the relationship between the magnetic field and the distance from the base of the tower in direction of southeast to northwest of the tower base .it is clearly that the electric field is concentrated around the point of origin (center of the tower base) and decreases gradually as we move away from the tower base. However, the electric field is almost non-existent around the point of origin and gradually increases as we move away from the center of the tower could be attributed to parasitic capacitances, as shown in Fig 5.1-5.2 **(a,b)**.

Table (5.1) Electromagnetic field measured from the center of tower base measured in South East (SE) and North West (NW) (a)

μT	SE
0.89	0
0.578	10
0.376	20
0.175	30
0.15	40
0.082	50
μT	**NW**
0.89	0
0.502	10–
0.364	20–
0.263	30–
0.138	40–
0.125	50–

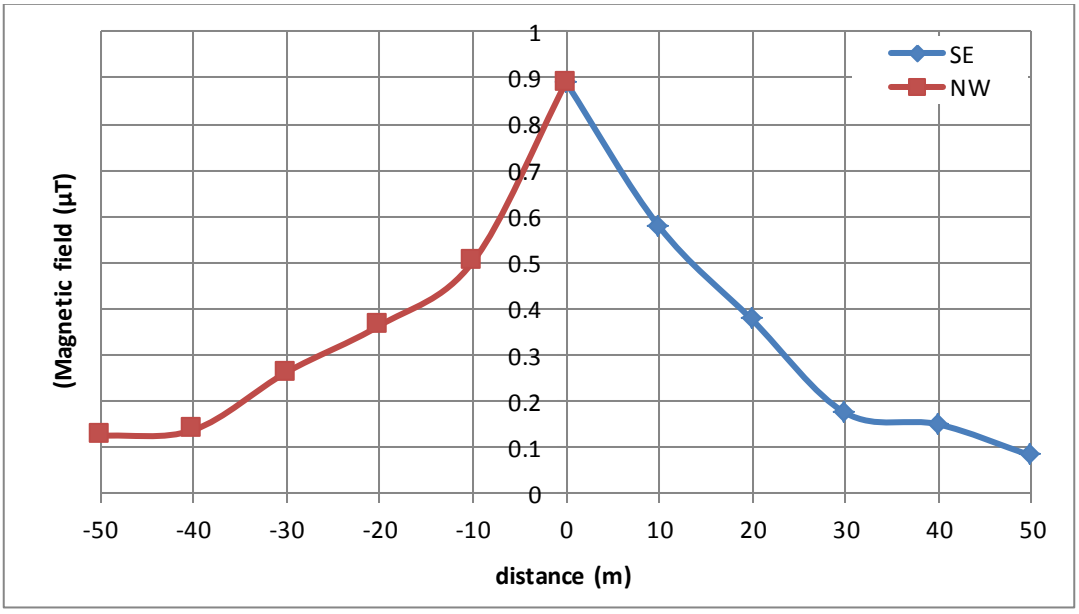

Fig 5.1. Electromagnetic field measured from the center of tower base measured in South East (SE) and North West (NW) (a)

Table (5.2) Electromagnetic field measured from the center of tower base measured in South East (SE) and North West (NW) (b)

KV/m	SE
0.022	0
1.07	10
0.73	20
0.49	30
0.26	40
0.25	50
KV/m	**NW**
0.022	0
0.68	10–
0.66	20–
0.48	30–
0.3	40–
0.12	50–

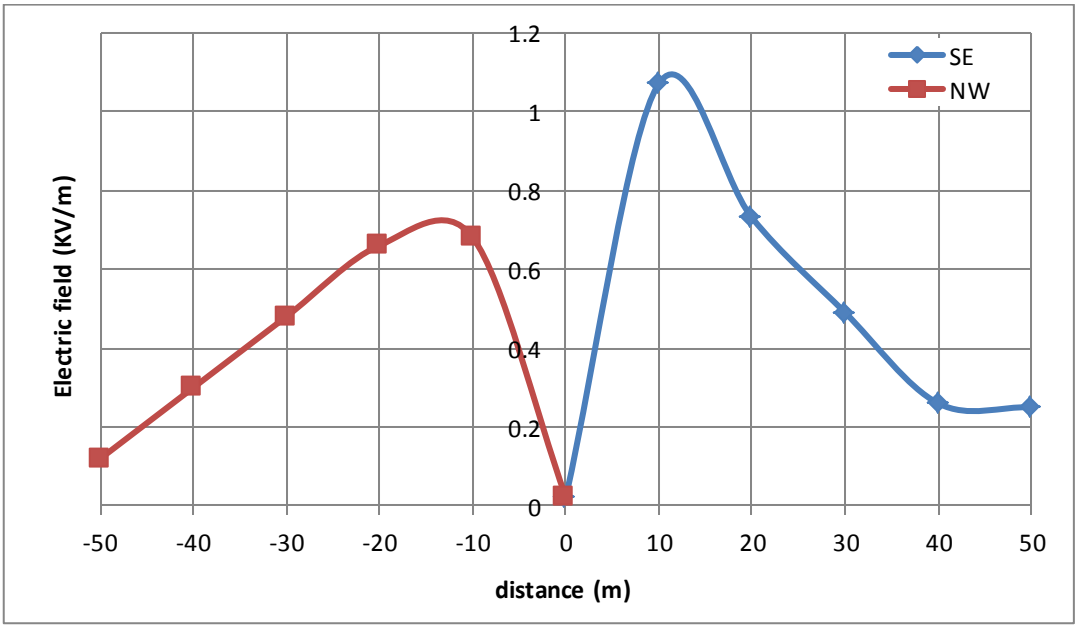

Fig 5.2. Electromagnetic field measured from the center of tower base measured in South East (SE) and North West (NW) (b)

Table (5.3) Electromagnetic field measured from the center of tower base measured in South West(SW)and North East (NE) (a)

μT	SW
0.89	0
0.49	10
0.515	20
0.238	30
0.15	40
0.389	50
μT	NE
0.89	0
0.52	10–
0.389	20–
0.289	30–
0.105	40–
0.201	50–

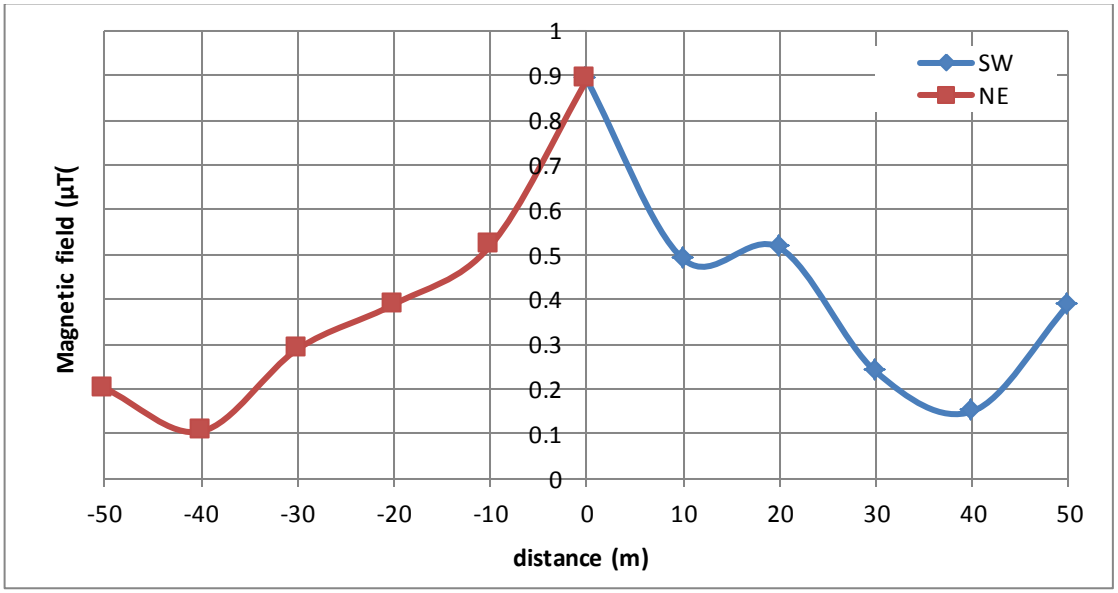

Fig 5.3 Electromagnetic field measured from the center of tower base measured in South West(SW)and North East (NE) (a)

Table (5.4) Electromagnetic field measured from the center of tower base measured in South West (SW) and North East (NE) (b)

KV/m	SW
0.022	0
0.6	10
0.51	20
0.48	30
0.25	40
0.15	50
KV/m	**NE**
0.022	0
1.19	10-
0.8	20-
0.62	30-
0.36	40-
0.24	50-

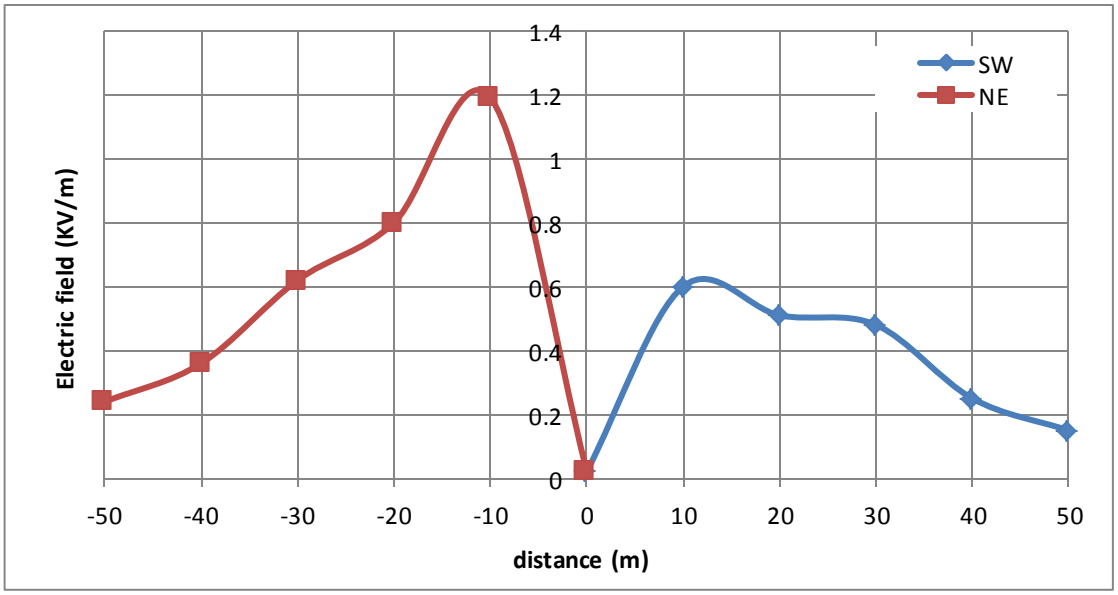

Fig 5.4 Electromagnetic field measured from the center of tower base measured in South West(SW)and North East (NE) (b)

The electromagnetic field under the 400 kV transmission line also was tested at both sides of the tower base as shown in Fig (5.5a-5.6b) and b. Each distance of profile is 90m for each direction (from North to South). As can be seen from figures that there are some oscillations were achieved, and might be due to the soil resistivity at horizontal line is non-uniform.

Table (5.5) Electromagnetic field measured in North-South direction (a)

µT	**South**
0.89	0
0.96	10
0.093	20
52	30
0.804	40
34.8	50
8.29	60
5.6	70
93.1	80
12.4	90
µT	**North**
0.89	0
2.7	10-
6.3	20-
53.1	30-
16.9	40-
19.2	50-
0.039	60-
0.133	70-
18	80-
23.1	90-

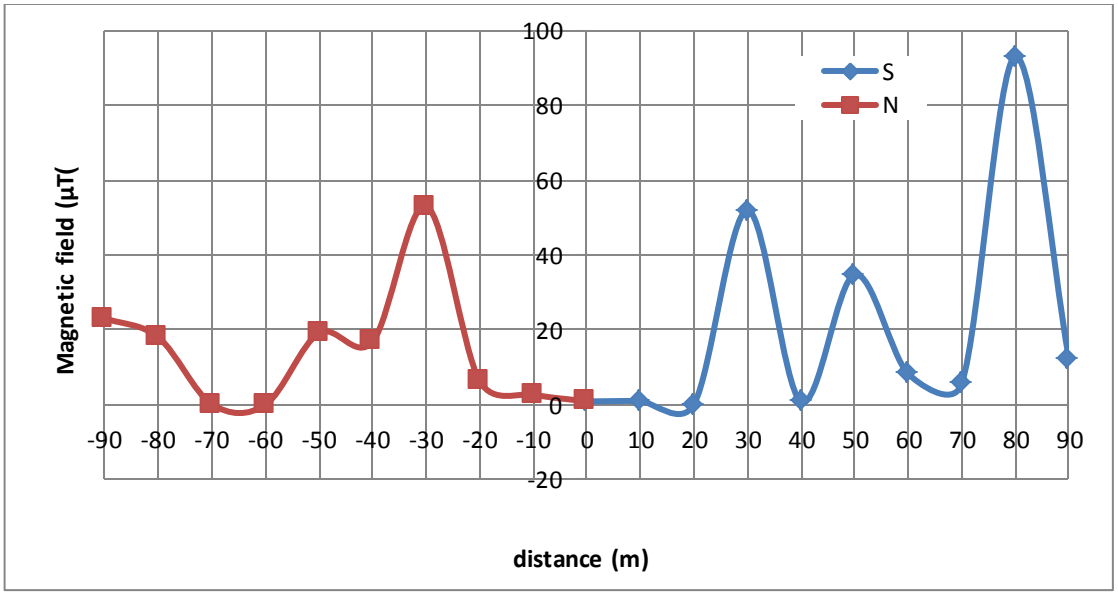

Fig 5.5 Electromagnetic field measured in North-South direction (a)

Table (5.6) Electromagnetic field measured in North-South direction (b)

KV/m	North
0.022	0
0.27	10
0.61	20
1.26	30
1.56	40
2.8	50
1.7	60
1.8	70
1.9	80
3.03	90
KV/m	**South**
0.022	0
0.093	10-
0.015	20-
1.75	30-
0.062	40-
3.12	50-
0.92	60-
2.49	70-
2.69	80-
1.1	90-

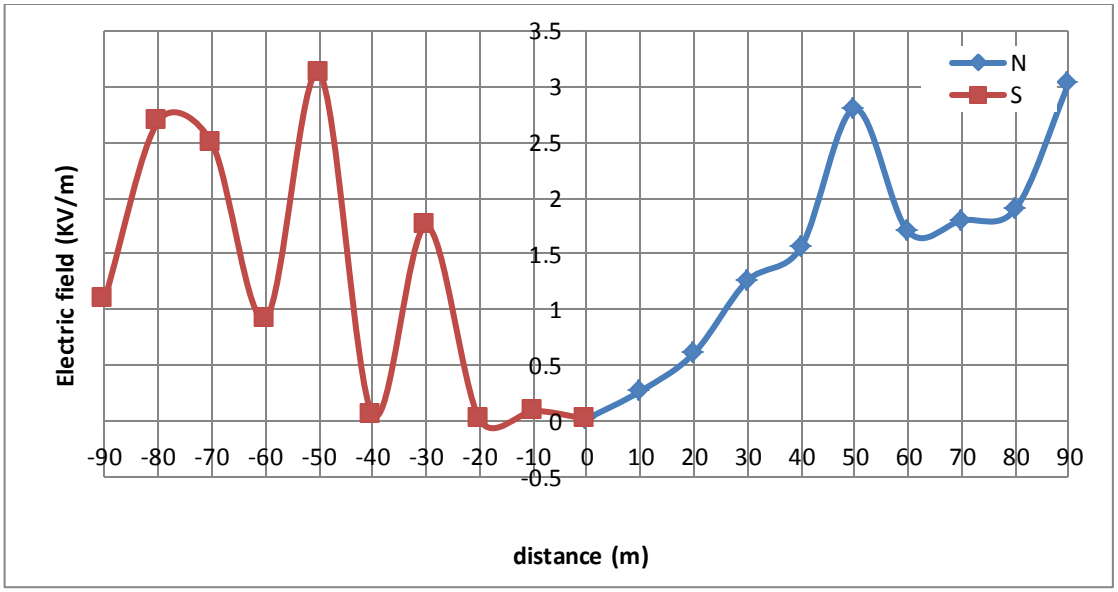

Fig 5.6 Electromagnetic field measured in North-South direction (b)

The electromagnetic field under the 400 kV transmission line also was tested at both sides of the tower base as shown in Fig (5.7a-5.8b) and b. Each distance of profile is 90m for each direction (from East to West). As can be seen from figures that there are some oscillations were achieved, and might be due to the soil resistivity at horizontal line is non-uniform.

Table (5.7) Electromagnetic field measured in East – West direction (a)

µT	**East**
0.89	0
1.09	10
5	20
2.53	30
5.67	40
0.892	50
0.339	60
0.276	70
0.0635	80
0.628	90
µT	**West**
0.89	0
1.105	10-
4.58	20-
3.64	30-
1.57	40-
0.955	50-
0.276	60-
0.276	70-
0.439	80-
0.540	90-

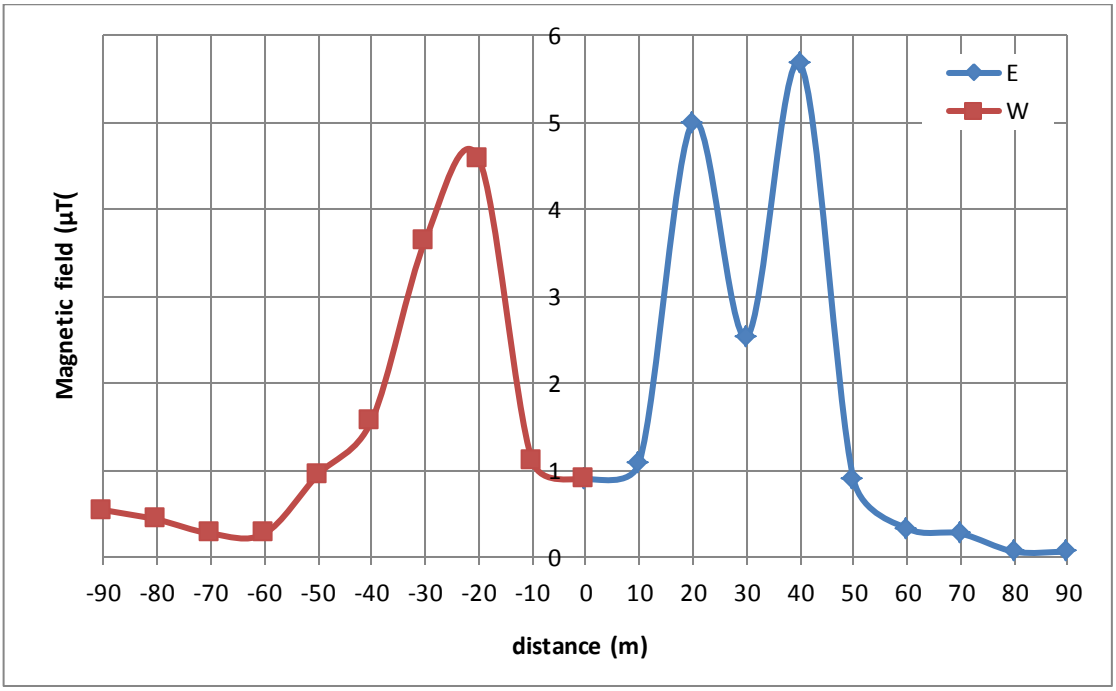

Fig 5.7 Electromagnetic field measured in East – West direction (a)

Table (5.8) Electromagnetic field measured in East – West direction (b)

KV/m	East
0.022	0
0.103	10
0.38	20
0.25	30
0.25	40
0.077	50
0.26	60
0.036	70
0.052	80
0.062	90
KV/m	**West**
0.022	0
0.081	10-
0.26	20-
0.41	30-
0.15	40-
0.093	50-
0.024	60-
0.031	70-
0.058	80-
0.066	90-

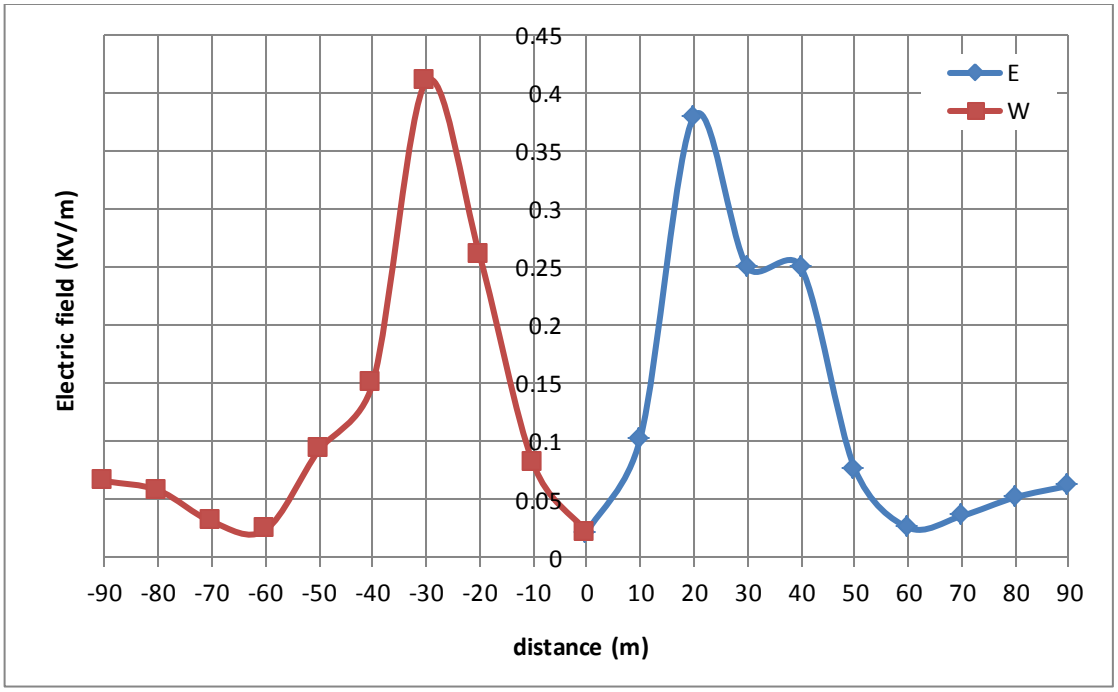

Fig 5.8 Electromagnetic field measured in East – West direction (b)

5.2- Comparison between measured with simulated results:

The comparison between measured and simulation using mat lab was conducted as shown in Fig (5.9). it is can be seen clearly that there is very good agreement between computed and measured values, and the small differences due to the weather conductions do not take into account by computer simulation.

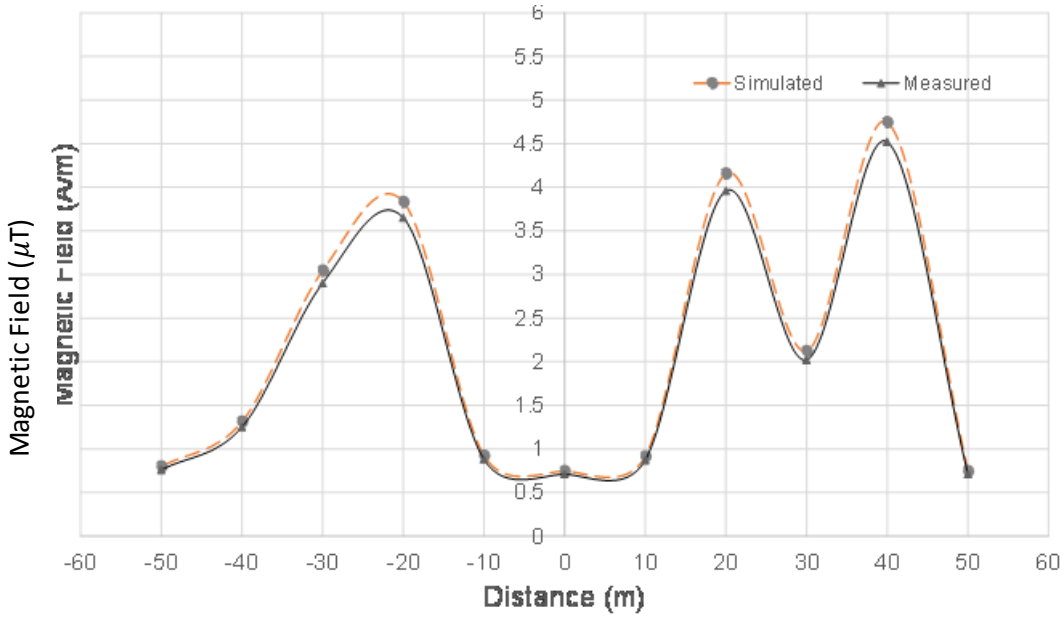

Fig 5.9 Comparison between measured with simulated results

Chapter six

Conclusions and Future Work

6.1- Conclusions:

In this thesis the effect of the electric and magnetic field under and surrounding of the 400 kV transmission line is practically conducted. It was compared between simulation mat lab and practical measurements under the transmission line 400kv in the west and east direction, and the load current during the experiment was 200A, and through this comparison, agreement was found between simulation mat lab and the practical results, where both proved the values of the magnetic field within the permissible limit in the World Health Organization. The results were also compared with the computer using Mat lab and only one measured result is selected for this comparison. According to the results obtained in this test field, it was agree with the WHO requirements, which are presented in Table (4.4). As for the comparison between the practical side of the computer, there is agreement due to the computer does not take into account several factors surrounding the transmission line such as temperature, air and humidity.

From investigations on lab animals it is evident that cellular, physiological and behavioral changes in human being are caused by powerful ELF electric fields. Although not all the results can be scaled to human beings but these studies gives us a warning that we should try to avoid unnecessary interactions with strong electric fields as much as possible.

From table (4.1),(4.2) it can be seen that the concentration of radon in the first region is approximately (Bq/m 3463.26) In the second area about (Bq/m 3083.04) The data showed that the radon level in the first region compared to the second zone. As a result, the level of radon concentration and respiration rate in the soil of high-pressure wires is relatively high than the empty soil because of the presence of high-pressure wires and their electromagnetic radiation.

6.2-Future Work:

The following suggestions are proposed for future work:

i) Further experimental investigations on the electromagnetic and electric fields using different types of instruments surrounding the high voltage transmission lines.

ii) Experimental studies could be conducted at different locations of the field test site near the 400kv transmission lines and comparing it with computer simulations.

iii) More experimental investigations could be performed to measure the concentration of radioactive radon in the soil close to the power transmission lines using the nuclear impact detectors

References

1. Grandolfo M. Michaelson S M, Rindi A eds. Biological effects and dosimetry of static and ELF electromagnetic fields. New York and London: Pleunm Press, 1985.
2. Grandolfo M, Vecchia P. Existing safety standards for high voltage transmission lines. In: Franceschetti G, Gandhi 0 P, Grandolfo M eds. Electromagnetic biointeraction: mechanisms, safety standards, protection guides, New York and London: Plenum Press, 1989.
3. Daniel Greenan, "Calculation of the Magnetic field level in vicinity of a 400kv Transmission Line". Dublin Institute of Technology (D.I.T), 2012.
4. Dib Djalel and Mordjaoui Mourad, "Study of the Influence High-voltage power Lines on Environment and Human Health". Journal of Electrical and Electronic Engineering, February 20, 2014.
5. NMK Abdel-Gawad. "An Investigation into field Management under power Transmission Lines using Delta Configurations". The open Environmental Engineering Journal. 2009.
6. Adel Z, El Dein. "Mitigation of Magnetic field under Egyptian 500kv Overhead Transmission Lins", 7th International Multi-Conference on systems, Signals, and Devices. 2010.
7. Taktak, F., Tiryakioğlu, İ., & Yilmaz, İ. (2005). Gps'de Kullanilan Elektromanyetik Dalgalarin Insan Sağliğina Etkilerinin Irdelenmesi.
8. WHO`S International EMF Project. (WHO 2007).
9. Daniel Greenan, "Calculation of the Magnetic field level in vicinity of a 400kv Transmission Line". Dublin Institute of Technology (D.I.T), 2012.
10. William H hayt, Jr (Late Emeritus professor purdue University, Indiana, USA), John A Buck, (Georgia Institute of Technology, Georgia, USA), adapted by M Jaleel Akhtar (Department of Electrical Engineering Indian Institute of Technology (IIT) Kanpur, India), Engineering Electromagnetics, Eighth Edition, 2014.

11. Deno, D.W.; and Zaffanella, L. 1982. Field effects of overhead transmission lines and stations. Chap. 8. In: Transmission Line Reference Book: 345 KV and Above. Second ed. (Ed: LaForest, J.J.). Electric Power Research Institute, Palo Alto, CA, 329-419.
12. IEEE. 2002. National Electrical Safety Code. 2002 ed. Institute of Electrical and Electronics Engineers, Inc., New York, NY. 287 Pages.
13. IEEE. 1994. IEEE Standard procedures for measurement of Power frequency Eclectic and Magnetic fields from AC Power Lines. ANSI/IEEE Std. 644-1994, New York, NY.
14. IEC Standards:
    1- IEC 60228: Conductors of insulated cables.
    2- IEC 61089: Round wire concentric-lay overhead electrical stranded conductors.
    3- IEC 60888: Zinc-coated steel wires for stranded conductors.
    4- IEC 60889: Hard-drawn aluminum wire for overhead line conductors.
    5- IEC 61232: Aluminum-clad steel wires for electrical purposes.
    6- IEC 61597: Overhead electrical conductors - Calculation methods for stranded bare conductors.
15. Overend, P.R. and Smith, S., Impulse Time Method of Sag Measurement.
16. Grainger, J. J., & Stevenson, W. D. (1994). Power system analysis. McGraw-Hill. Chicago Style (17th ed.) Citation. Grainger, John J., and William D. Stevenson.
17. أسس الفيزياء الإشعاعية – تم الإطلاع على الموقع يوم 2018/11/22م.
18. غاز الرادون، د. محمد بن ابراهيم الجار الله، جامعة الملك فهد للبترول والمعادن عمادة البحث العلمي الطبعة الأولى، سنة 2009م.
19. Tanner, A. B., the Natural Radiation Environment, University of Chicago press, Chicago, 1964.

20. Tanner A. B. (1964). Radon migration in the ground: review. The Natural Radiation Environ ment. University of Chicago, 161-190.
21. Karamdoust N.A., (1989), Parametric in Visitations and Various applications of SSNTDS in the environmental and basic fields. ph D thesis, school of physics and space Research, the University of Brimming ham.
22. Stranden E., Kolstad A. K. and Lind B., (1984), Radon exhalation: Moisture and temperature dependence, Health phys., 47-3.
23. Ingersol, J.G., "A survey of Radionuclide contents and Radon Emanation Rats in Building Materials Used in the United States, Lawrence Berkeley Laboratory, LBL-11771, May 1981".
24. Paper Radon Exhalation rate from various Building materials Ching-Jiam chen, pao – shan Weng, and Tiehchi Institute of Nuclear science, National Tsing Hua University, Hsinchu, 300, R.O.C.
25. رسالة ماجستير بعنوان قياس مستوى غاز الرادون بالمنازل بمنطقة الحرشة بمدينة الزاوية، أ. نجاة علي شهبون، الأكاديمية الليبية، طرابلس، 2008م.
26. Mcpherson R. B., (1980), Environmental Radon and radon daughter dosimeter in the respiratory tract. Health phys., 39, 929-936.
27. Environmental protection agency of USA ,(1986),acitizen , s guide to radon , what it is and do about it . published with the department of Health and human services , OPA-86-005 (August)
28. Shahbon N., Ali M. S. and Elorabi, S.F. M.Sc.. thesis, The academy of graduate study, Libya.
29. London, S.J., et al., Exposure to residential electric and magnetic fields and risk of childhood leukemia, American Journal of Epidemiology, 131 (9), 923–937, November (1992).
30. Dawalibi, F. P. Selby, A. : Electromagnetic Fields of Energized Conductors, IEEE Transactions on Power Delivery 8 No. 3 PP.1275–1284 (1993).

Appendix

```
%-------------------------------------------------------------------%
-------%Straight wire Magnetic Field and Electrical field produced by
400Kv system%----------
----------%By Mawloud Albakoush%-----------------------------------
%-------------------------------------------------------------------%

clc
close all
clear all
%-------------------------------------------------------------------%
---%Wire is along the X-axis%-----------------------------------------
%-------------------------------------------------------------------%
Nx=100;
Nz=100 ;
Ny=100 ;
N=100;  % length of the wire
Xw=(floor(-N/2):floor(N/2));  % X-coordinates of the wire
Yw=zeros(N+1,1); % Y-coordinates of the wire
Zw=zeros(N+1,1); % Z-coordinates of the wire
I=500;   % current
u0=1;  % permeability
xp(1:Nx)=-(Nx-1)/2:(Nx-1)/2 ;
yp(1:Ny)=-(Ny-1)/2:(Ny-1)/2   ;
zp(1:Nz)=-(Nz-1)/2:(Nz-1)/2 ;
X(1:Nx,1:Ny,1:Nz)=0;
Y(1:Nx,1:Ny,1:Nz)=0 ;
Z(1:Nx,1:Ny,1:Nz)=0;
```

```
for i=1:Nx
    X(i,:,:)=xp(i  ‹(
end
for i=1:Ny
    Y(:,i,:)=yp(i  ‹(
end
for i=1:Nz
    Z(:,:,i)=zp(i‹(
end

----------------------------------------------------------------------%
----------------------------------------------------------------------%
for a=1:Nx
for b=1:Ny
for c=1:Nz

    ----------------------------------------------------------------------%
----------------------------------------------------------------------%
for i=1:N-1
Rx(i)=X(a,b,c)-(0.5*(Xw(i)+Xw(i+1‹(((
Ry(i)=(Y(a,b,c)-(0.5*(Yw(i)+Yw(i+1‹((((
Rz(i)=(Z(a,b,c)-(0.5*(Zw(i)+Zw(i+1‹((((
dlx(i)=Xw(i+1)-Xw(i‹(
dly(i)=Yw(i+1)-Yw(i‹(
dlz(i)=Zw(i+1)-Zw(i‹(
end
Rx(N)=(X(a,b,c)-0.5*(Xw(N)+1‹((
Ry(N)=(Y(a,b,c)-(0.5*(Yw(N)+1‹(((
Rz(N)=(Z(a,b,c)-(0.5*(Zw(N)+1‹(((
```

```
dlx(N)=-Xw(N)+1;
dly(N)=-Yw(N)+1;
dlz(N)=-Zw(N)+1;
----------------------------------------------------------------------%
----------------------------------------------------------------------%
for i=1:N
Xcross(i)=(dly(i).*Rz(i))-(dlz(i).*Ry(i;((
Ycross(i)=(dlz(i).*Rx(i))-(dlx(i).*Rz(i;((
Zcross(i)=(dlx(i).*Ry(i))-(dly(i).*Rx(i;((
R(i)=sqrt(Rx(i).^2+Ry(i).^2+Rz(i).^2;(
end
----------------------------------------------------------------------%
----------------------------------------------------------------------%
Bx1=(I*u0./(4*pi*(R.^3))).*Xcross;
By1=(I*u0./(4*pi*(R.^3))).*Ycross;
Bz1=(I*u0./(4*pi*(R.^3))).*Zcross;
----------------------------------------------------------------------%
----------------------------------------------------------------------%
BX(a,b,c)=0;      % Initialize  sum magnetic  field  to be zero first
BY(a,b,c)=0;
BZ(a,b,c)=0;
----------------------------------------------------------------------%
----------------------------------------------------------------------%
for i=1:N   % loop over all current elements  along LINE
   BX(a,b,c)=BX(a,b,c)+Bx1(i;(
   BY(a,b,c)=BY(a,b,c)+By1(i;(
   BZ(a,b,c)=BZ(a,b,c)+Bz1(i;(
end
----------------------------------------------------------------------%
```

```
end
end
end
----------%visualizing the result----------
figure(1(
quiver3(X,Y,Z,BX,BY,BZ,2؛(
hold on
line([-5 5],[0 0], [0 0],'linewidth',3,'color','r؛('
 axis([-100 100 -100 100([
Xlabel('X-axis','fontsize',14(
Ylabel('Y-axis','fontsize',14(
Zlabel('Z-axis','fontsize',14(
title('B-field of a current wire along X-axis','fontsize',14(
h=gca ؛
set(h,'FontSize',14(
fh = figure(1 ؛(
set(fh, 'color', 'white ؛('
figure(2(
quiver(Y((Nx-1)/2,:,:),Z((Nx-1)/2,:,:),BY((Nx-1)/2,:,:),BZ((Nx-
1)/2,:,:),2؛(
hold on
G1=plot(0,0,'.','markersize',6؛(
set(G1,'MarkerEdgeColor','r('
axis([ -100 100 -100 100([
Xlabel('Y-axis','fontsize',14(
Ylabel('Z-axis','fontsize',14(
title('B-field YZ plane','fontsize',14(
h=gca ؛
set(h,'FontSize',14(
```

```
h = get(gca, 'ylabel‹('
fh = figure(2 ‹(
set(fh, 'color', 'white ‹('
----------%
%----------%
---%TRANSMISSION LINE is in the X-Y plane and Magnetic Field is
Evaluated%----------
----------%at every point in the Y-Z plane(X=0%----------(
%----------%
Nz=51; % No. of grids in Z-axis
Ny=51; % No. of grids in Y-axis
N=25; % No of grids in the coil ( X-Y plane(
Ra=10; % Radius of the coil in the X-Y plane
I=500; % current in the coil
u0=1; % for simplicity, u0 is taken as 1 (permitivity(
phi=-pi/2:2*pi/(N-1):3*pi/2; % For describing a circle (coil(
Xc=Ra*cos(phi); % X-coordinates of the coil
Yc=Ra*sin(phi); % Y-coordinates of the coil
yp(1:51)=-25:1:25; % Y-coordinates of the plane
zp(1:51)=0:1:50;% Z-coordinates of the plane
Y(1:Ny,1:Nz)=0; % This array is for 1-d to 2-d conversion of coordinates
Z(1:Ny,1:Nz)=0‹
for i=1:Ny
   Y(i,:)=yp(i); % all y-coordinates value in 2-d form
end
for i=1:Nz
   Z(:,i)=zp(i);% all z-coordinates value in 2-d form
end
 %%SUB-FIEL FOR FIGURS
```

```
clc
clear all

E=zeros(3,50؛(
E_0=8.85e-21؛
ii=1؛
for i=2:0.1:7
   tmp_mat=zeros(3,1؛(
    tmp_mat=cal(i)./(2*pi*E_0*i؛(

    E(1:3,ii)=tmp_mat؛
    ii=ii+1؛
end
axes1 = axes('YGrid','on...،'
'    XTick',[2 2.1 2.2 2.3 2.4 2.5 2.6 2.7 2.8 2.9 3 3.1 3.2 3.3 3.4 3.5 3.6
3.7 3.8 3.9 4 4.1 4.2 4.3 4.4 4.5 4.6 4.7 4.8 4.9 5 5.1 5.2 5.3 5.4 5.5 5.6
5.7 5.8 5.9 5.99999999999999  6.09999999999999  6.19999999999999
6.29999999999999  6.39999999999999  6.49999999999999
6.59999999999999  6.69999999999999  6.79999999999999
6.89999999999999  6.99999999999999  7...،[
'    XGrid','on؛('
hold(axes1,'all؛('
plot(2:0.1:7,E(1,:),'Marker','*','Color',[1 0 0؛([
xlabel('Variation  of radius [m؛('[
ylabel('GRADIENT-  [kv/cm؛('[
title('Figure  One؛('
%%%%%%%%%%%%%%%%%%%%%%%%%%%%%%%%%%%%%%%%%%%%%%
%%%%%%
figure
```

```
axes1 = axes('YGrid','on...،'
'    XTick',[2 2.1 2.2 2.3 2.4 2.5 2.6 2.7 2.8 2.9 3 3.1 3.2 3.3 3.4 3.5 3.6
3.7 3.8 3.9 4 4.1 4.2 4.3 4.4 4.5 4.6 4.7 4.8 4.9 5 5.1 5.2 5.3 5.4 5.5 5.6
5.7 5.8 5.9 5.99999999999999  6.09999999999999  6.19999999999999
6.29999999999999  6.39999999999999  6.49999999999999
6.59999999999999  6.69999999999999  6.79999999999999
6.89999999999999  6.99999999999999  7...،[
'    XGrid','on؛('
hold(axes1,'all؛('
plot(2:0.1:7,E(2,:),'Marker','*','Color',[0 1 0؛([
xlabel('Variation  of radius [m؛('[
ylabel('GRADIENT-  [kv/cm؛('[
title('Figure  Two؛('
%%%%%%%%%%%%%%%%%%%%%%%%%%%%%%%%%%%
%%%%%%%
figure
axes1 = axes('YGrid','on...،'
'    XTick',[2 2.1 2.2 2.3 2.4 2.5 2.6 2.7 2.8 2.9 3 3.1 3.2 3.3 3.4 3.5 3.6
3.7 3.8 3.9 4 4.1 4.2 4.3 4.4 4.5 4.6 4.7 4.8 4.9 5 5.1 5.2 5.3 5.4 5.5 5.6
5.7 5.8 5.9 5.99999999999999  6.09999999999999  6.19999999999999
6.29999999999999  6.39999999999999  6.49999999999999
6.59999999999999  6.69999999999999  6.79999999999999
6.89999999999999  6.99999999999999  7...،[
'    XGrid','on؛('
hold(axes1,'all؛('
plot(2:0.1:7,E(3,:),'Marker','*','Color',[0 0 1؛([
xlabel('Variation  of radius [m؛('[
ylabel('GRADIENT-  [kv/cm؛('[
title('Figure  Three؛('
```